

8

Rosemary Island Excavations

JO MCDONALD, WENDY REYNEN, ZANE BLUNT, KANE DITCHFIELD,
CARLY MONKS, MATTHIAS LEOPOLD, JOE DORTCH



Figure 8.1. The Rosemary Island excavation locations showing survey areas.

Five landscapes in three sample areas (Areas 1, 4 and 5) were targeted with eight test excavations on Rosemary Island (Figure 8.1).

These locations were assessed to have good archaeological potential, they included a range of different art site types and geomorphic conditions and were associated with locales with varying water permanency on Rosemary Island. These were:

1. the calcareous sand flats at the north of the island, below several rock art sites on the rocky gabbro slopes in Sample Area 1 (two test squares: RIA01-426618 (which was sterile) and RIA01-619706);
2. the central valley at a semi-permanent waterhole with rock art (RIA05-885878) and two squares amongst a stone feature complex further upstream and upslope

Three of the squares recovered no cultural remains (Figure 8.1). Wadjuru Pool (DPLH 978) was previously excavated by archaeologist Elizabeth Bradshaw (1995). Her earlier excavation (WPEB) and the current one (WP01-912361) at DPLH 978, and the Rosemary 8 excavations at DPLH 11773 (RIA04-335582 and RIA04-253614) were the subject of Megan Berry's PhD thesis (Berry 2018). Elizabeth Bradshaw's early work also included the extensive collection from numerous recent dunes around the island: these have not been analysed in detail. Sites RI117, RI118 and RI119 were all previously registered as DPLH 968. Our excavation targets were focused on the western side of the island, on gabbro substrate (or the associated sandy matrix which has accumulated in the Holocene and overlying older alluvium).

(RIA05-023799 and RIA05-016764) which yielded no artefacts;

3. the Rosemary 08 site complex (RIA04-335582) - the island's largest rock art and stone feature complex with a cluster of stone structures interpreted as house bases (see McDonald and Berry 2016) and close to a now dry waterhole (RIA04-253614) surrounded by a midden (redesignated as RIA-043);
4. the sand dunes close to the southern edge of the island adjacent to Wadjuru Pool, a seasonal rock pool with numerous grinding patches and an extensive surface midden and artefact scatter (WP-912361).

The project's work during the last season, particularly on the eastern side of the island, has identified several other locations where further research would be usefully focused. This includes an extensive quarry site with stone features along the high eastern ridgeline of the island (Area 3); the interior valley with several archaic faces and circular stone features; and the north-western beaches hosting rock art and stone features near an identified spring (still seeping, and as reported by locals) accompanied by a freshwater spring which is now submerged by sea.

The aim of the excavations reported here was to contextualise the rock art sequence and characterise the occupation deposit on this outer island of the archipelago and to determine whether occupation (and rock art production) continued here after islandisation.

Face Palm Valley – Sample Area 1

Two excavations were completed in Sample Area 1 (Figure 8.2) in July/August 2016. Both excavations were preceded by a GPR (ground penetrating radar) survey to determine the likely depth of deposit and its archaeological potential. One excavation square was located in the floor of the valley below one of the larger rock art assemblages (MLP-RI100) which was is not associated with any identified water sources. This excavation square yielded no cultural remains. The other square was located on the broad, flat area below the nose of this central ridgeline (again not associated with any identified water source, although notably a historic well has been sunk to the north, near a palm tree). A tall white (Holocene) sand

dune fronts Chookie Bay to the north. This flat plain was covered in buffel and spinifex grasses.

The dune was previously recorded as a midden and artefact scatter. The site was documented by Elizabeth Bradshaw in 1993 as having a moderate density of artefacts and shell, including large cores and 20 grinding surfaces. The midden was mainly composed of *Chiton Acanthopleura* sp. (99%) with a number of fragments of 'large water carrying shell species', including *Syrinx araus* and *Melo amphoroa* (Site File DPLH 968).

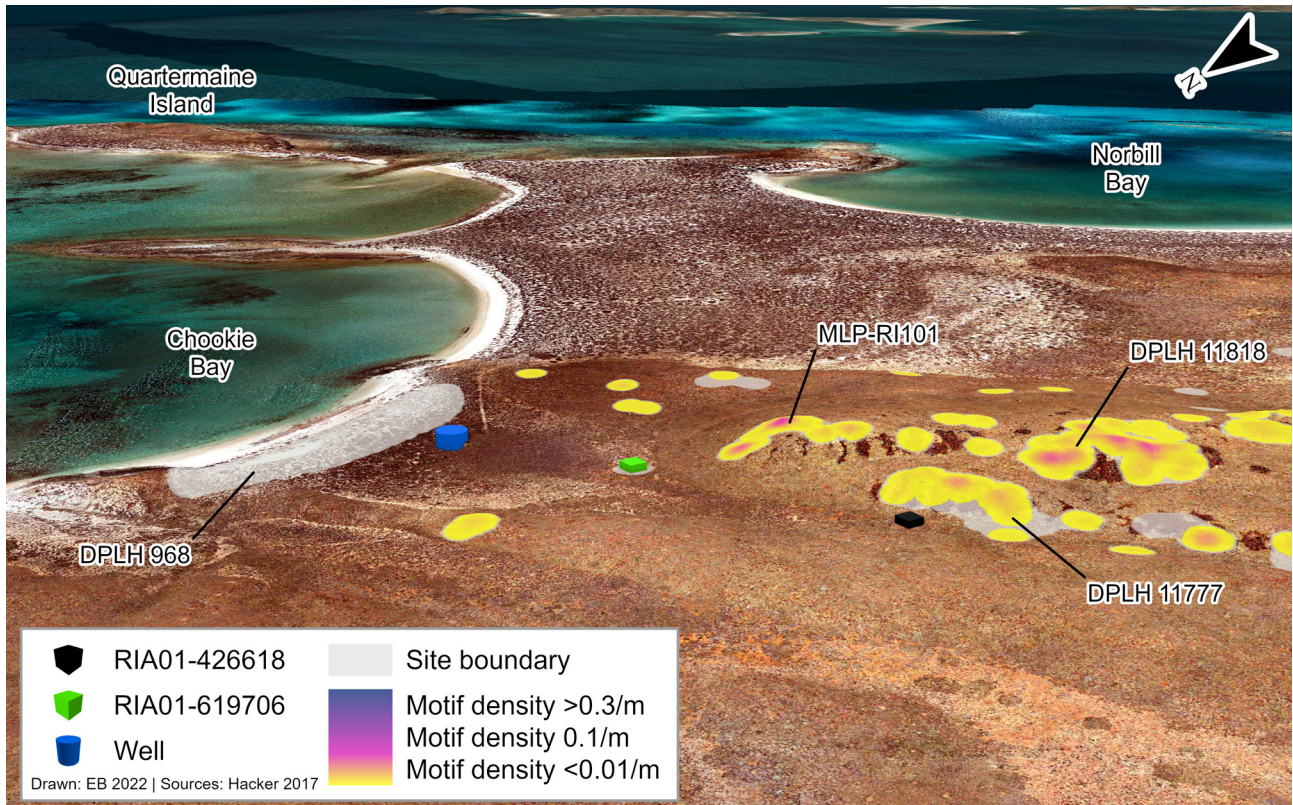


Figure 8.2. Landscape view of Area 1 excavations showing location of excavation squares relative to recorded rock art assemblage (coded for motif density).

Square RIA01-426618

This square was excavated in the valley below site MLP-RI100 and is characterised by a high proportion of older looking motifs (CS1), including the two archaic faces. GPR indicated that there was an area approximately 10 m from the edge of the boulder field with a

reasonable depth of deposit, and the square was placed in this vicinity. No cultural material was seen on the surface of this location, and the spinifex and buffel grass growth across this valley was of medium density.

Stratigraphy

Excavation in the 1.0 m x 1.0 m square proceeded in 13 XUs dug in 2–4 cm depths (Table 8.1). The lowest stratigraphic unit (XU10–13) was reached in the south-east quadrant (Figure 8.3 and Figure 8.4). Four stratigraphic (pedogenic) units were encountered (Figure 8.5):

SU1 – A thin veneer of fine red (5YR 3/3) gravelly silty deposit comprised the Ao layer. pH 6.5;

SU2 – Red brown (7.5YR 5/2) fine-grained friable deposit with rocky inclusions. Ant nest and insect/bioturbation throughout most of the square (though not visible in all sections). pH 6.5;

SU3 – Very rocky, pebble-sized rocks and blocks interlocking in the same red brown (7.5YR 5/2) fine-grained friable deposit as unit II. pH 6;

SU4 – Redder (7.5YR 5/3), more compact and clayey deposit (similar colour and texture to SU3) chaotically bedded with calcium carbonate clumps. pH 6.

No cultural material (specifically stone artefacts or economic shellfish) was recovered from this excavation, which removed c. 350 kg of deposit and 100 kg of rocky matrix (Table 8.1). Land snails were encountered throughout the sequence.

UNIT	DEPTH BELOW SURFACE (CM)	DEPOSIT EXCAVATED (KG)	WEIGHT ROCKS DISCARDED (KG)	PH	MUNSELL
XU01	2.9	38.9	1.1	6.5	5YR 3/3
XU02	5.6	41.1	1	6	7.5YR 2.5/3
XU03	7.7	37.2	3	6.5	7.5YR 2.5/3
XU04	10.6	45	4.2	6	7.5YR 2.5/2
XU05	13.6	45.8	4.5	6.5	7.5YR 2.5/2
XU06	17.0	44.4	4.5	6.5	7.5YR 2.5/2
XU07	20.1	50.9	11.5	6	7.5YR 2.5/2
XU08	22.5	30.5	2	6.5	7.5YR 2.5/2
XU09	24.1	30.9	5.2	6.5	7.5YR 2.5/3
XU10_SE	34.5	23	30.5	6	7.5YR 2.5/2
XU11_SE	39.4	24.6	15.4	6	7.5YR 2.5/2
XU12_SE	43.6	23	11.2	6	7.5YR 2.5/3
XU13_SE	46.5	20.8	12	6	7.5YR 2.5/3
<i>Total</i>		<i>456.1</i>	<i>106.1</i>		

Table 8.1. Square 426618: excavation units' average depth and weights for deposit.



Figure 8.3. Landscape context for Square 426618. The engraved boulder slope is visible (left), as is the more open valley context to the west (right).



Figure 8.4. Square 426618 at the commencement of excavation (left) and completion of XU13 (right).

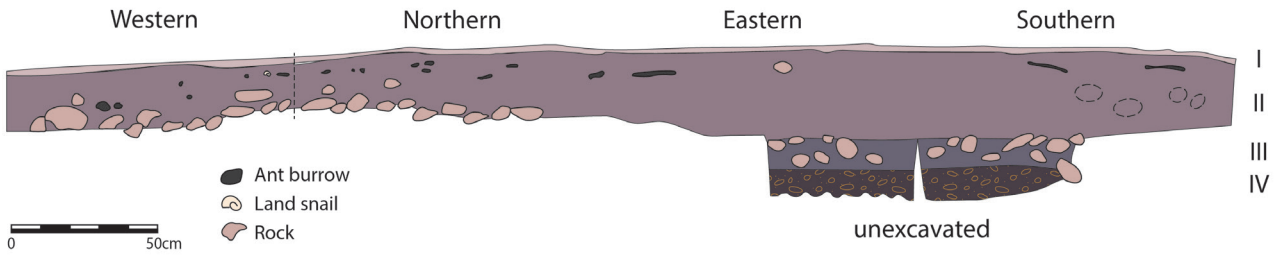


Figure 8.5. Square 426618 stratigraphic section drawings (all four baulks).

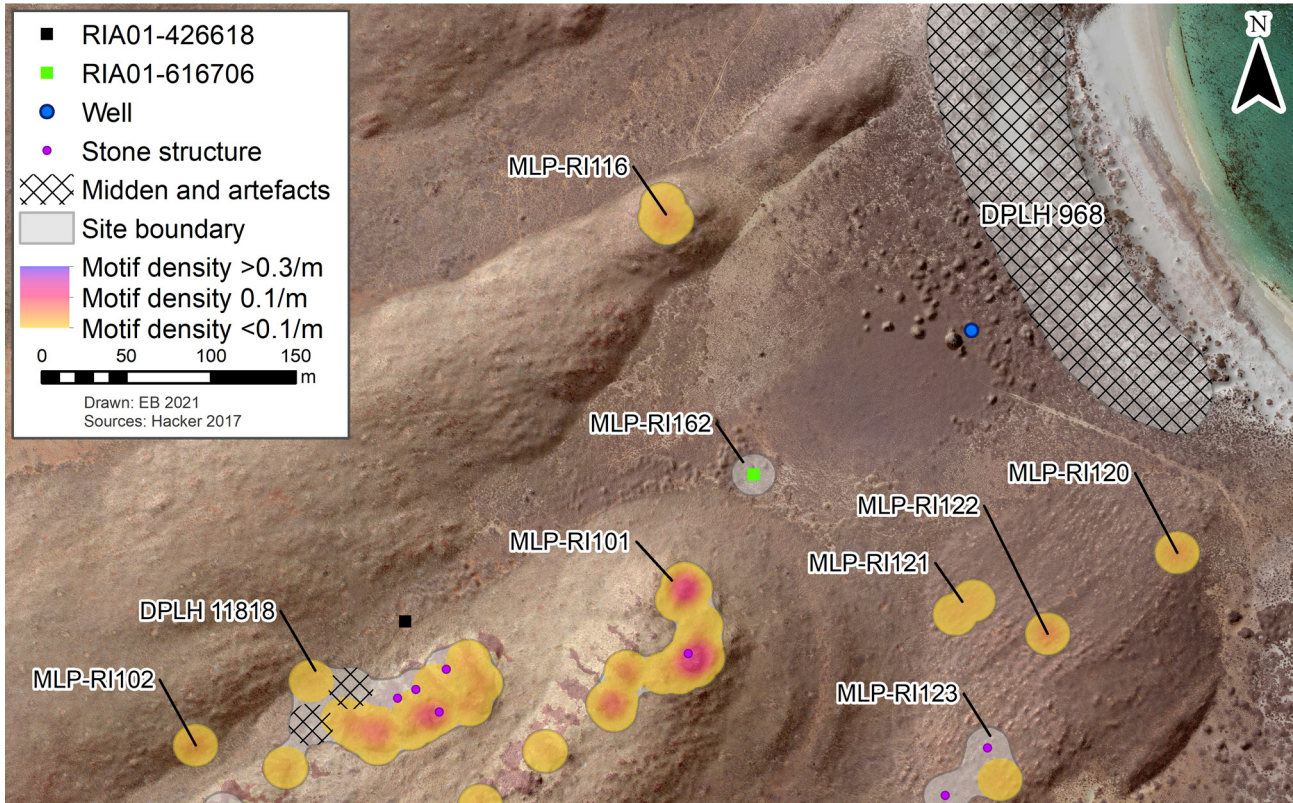


Figure 8.6. Detail of Rosemary Island Area 1 excavations, showing location of excavation squares relative to recorded rock art assemblage coded for motif density.

Square RIA01-619706

This excavation was located at the foot of the northern toeslope of the rocky ridgeline that formed Area 1. The square was positioned towards the back of the low infilled plain, 400 m behind the 5m-high white sand dune, which has formed since islandisation (Figure 8.2 and Figure 8.7). This square was not associated with any obvious water sources and/or landscape features, and there were no rock art panels or stone features in the immediate vicinity (Figure 8.2).

Square 619706 measured 1.0 m x 1.0 m and was excavated in 24 2–4 cm excavation units (XUs) to a depth of c. 65 cm (Figure 8.7). Below XU15 there was a decline in artefacts and shell density, with the sample initially reduced to a 1.0 m x 0.5 m sample. However, when a higher number of artefacts were encountered below this level, the other half of the square was excavated to complete the sample: i.e. XUs 16–24 are designated to

north and south subsamples. At the base of the square the deposit became cemented and the excavation ceased. The deposit comprised five stratigraphic units beneath a thin veneer of loose windblown sand (Figure 8.8). All material was sieved on-site using the standard nest of 4 mm and 2 mm sieve meshes.

A total of 983 kg of deposit was excavated, this yielding a little over 2 kg of cultural material: mostly shellfish, followed closely by stone artefacts (Figure 8.9). A very small amount of bone was recovered, this mainly fish and some small land animals. Shell material was distributed throughout this excavated sequence.



Figure 8.7. Landscape context of Square 619706 (left of top) at the toeslope of the main ridgeline of Area 1; and (bottom) looking towards the foredune (in background), note the exotic date palm (arrowed) planted near a historic well.



Figure 8.8. Square 619706 (left) at the commencement of excavation and (right) at the end of XU13.

Stratigraphy and dating

The excavation revealed five stratigraphic units:

SU1 – friable but firm, dark brown (7.5YR 3/3) sandy, silty soil with a thin veneer of Ao (red sandy silt) at surface. Buffel grass (*Cenchrus ciliaris*) roots contribute to friability of this unit, particularly on the south side of the square. Neutral at the surface (pH 7), increasing to highly alkaline in

XU2 (pH 10);

SU2 – increasingly compact sandy sediment, dark brown (7.5YR 3/4) carbonate rich, with small marine shell fragments;

SU3 – slightly redder (5YR 4/4), finer and firmer than SU2; decreasing marine shell fragments and increasingly clayey;

SU4 – calcrete rich rubble layer (pH 9), with finer darker red (5YR 4/4) sediment sitting above basal layer;

SU5 – concreted gravelly basal floor. Not excavated.

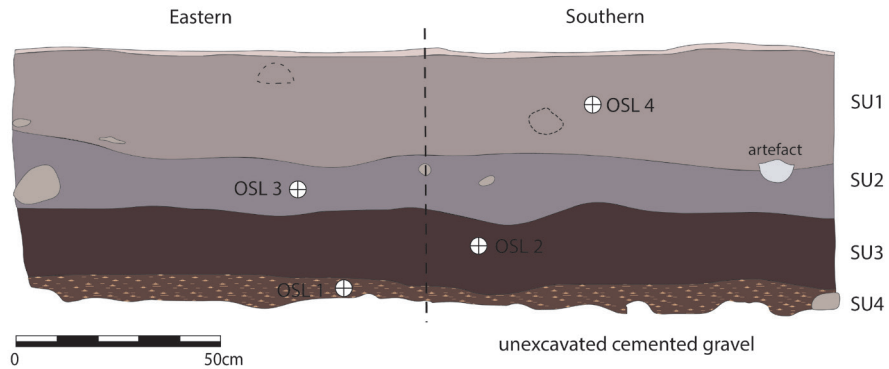


Figure 8.9. Square 619706 east and south baulks showing stratigraphy and the location of the OSL tube placement.

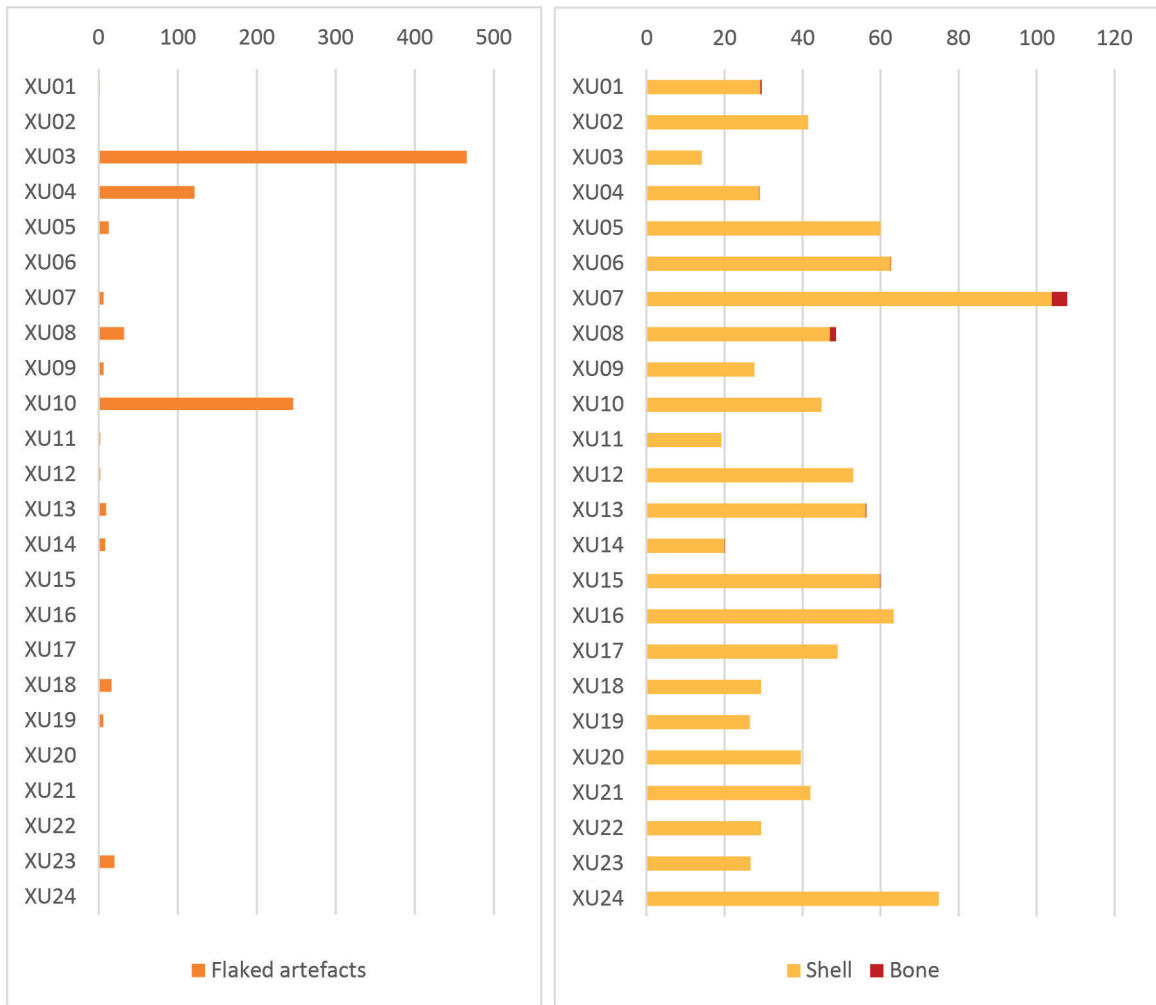


Figure 8.10. Square 619706: (left) vertical distribution of stone and (right) shell and bone per XU. Artefacts by count; shell weights in grams.

Four OSL tubes were collected at the completion of excavation. These were processed by the OSL Lab at Sheffield University (see Supplementary Information appendices). Two chiton samples were also submitted to

Waikato for radiocarbon determinations (Table 8.2). These age determinations demonstrate that this deposit has accrued relatively rapidly since islandisation (Figure 8.11).

LAB CODE	SAMPLE TYPE	XU	SU	AU	DEPTH BELOW SURFACE (CM)	% MODERN CARBON	CONVENTIONAL RADIOCARBON AGE (YRS BP 1σ ERROR)	CALIBRATED AGE RANGE	MEAN CALIBRATED AGE
Wk46111	Chiton	2		1	5	81.8 ± 0.2	1612 ± 16	1213–1030	1122 ± 92
OSL4	Sediment		1	1	13	NA	NA	1400–1240	1320 ± 80
Wk46112	Chiton	12		2	29	59.9 ± 0.1	4122 ± 16	4208–3983	4096 ± 113
OSL3	Sediment		2	2	35	NA	NA	3800–3460	3630 ± 170
OSL2	Sediment		3	3	49	NA	NA	4580–4180	4380 ± 200
OSL1	Sediment		4	3	58	NA	NA	5380–4920	5150 ± 230

Table 8.2. Square 619706: OSL and radiocarbon determinations.

ANALYTICAL UNIT	EXCAVATION UNITS	STRATIGRAPHIC UNITS	AGE
1	1–9	1	Last Millennium
2	10–19	2	Mid-Holocene
3	20–24	3/4	Islandisation

Table 8.3. Square 619706: correlation of excavation units, stratigraphy and age.

Bayesian analysis

Bayesian analysis for Square 619706 used a sequence depositional model (Bronk Ramsey 2008, 2009a), based on the analytical units listed in association with OSL and radiocarbon dates (see Table 8.3). The dates were entered into the model in order of their depth and ordered by a series of phases, which represent three major analytical units (Table 8.4). These analytical units were established based on archaeological assemblage

patterning and site stratigraphy. In Bayesian analysis, phases assume that age determinations are uniformly distributed with no order (Bronk Ramsey 1998). This is appropriate for this site since we cannot assume a lack of intra-strata movement but, given the overall agreement between dates, we can be confident there is little inter-strata movement.

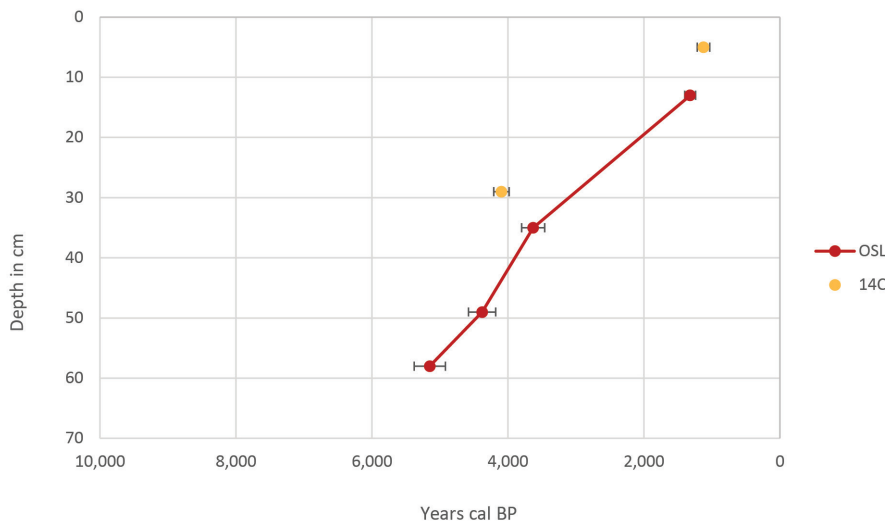


Figure 8.11. Square 619706: depth-age curve based on age determinations and depth below surface.

Phases are separated by boundaries that represent the chronological 'beginning' and 'end' of each analytical unit. Since there is no evidence for discontinuities in deposition here, continuous boundaries, representing unbroken transitions from one analytical unit to the next, were used (see Bronk Ramsey 2009a). The 'deposit surface' boundary was constrained with a uniform distribution between 0 and 400 cal. BP to prevent the model from producing dates into the future. To assess the likelihood of any of the dates being an outlier, a General t-type Outlier Model was inset into the sequence model (Bronk Ramsey 2009b). All dates were assigned a prior

outlier probability of 0.05. This was also supported by an Agreement Index which indicates the 'goodness-of-fit' for individual dates and, more generally, the whole model using a 60% threshold value (Bronk Ramsey 1998). The model was calibrated using Marine20 (Heaton et al. 2020) with a 109 ± 25 marine reservoir value (Veth et al. 2017). Modelled dates were rounded following normal conventions (Stuiver and Polach 1977).

The Bayesian analysis (Table 8.4 and Figure 8.12) estimates that this Face Palm Valley location was first occupied at 6,030–4,790 cal. BP and was occupied throughout the Holocene until the last millennium. The

surface boundary was constrained to be essentially modern. This sequence is well supported, as each date has <5% chance of being an outlier ($A_{\text{model}} = 99.8$; $A_{\text{overall}} = 98.7$) and all dates return high agreement index results.

NAME	68.2%		95.4%		SUM. STATISTICS			INDICES	
	FROM	TO	FROM	TO	μ	σ	M	AI	OP
Boundary: Deposit Surface	400	150	400	10	220	110	220	100	
Phase: Last Millennium									
Wk46111	950	800	1,030	730	880	80	880	101	96.3
OSL4	1,400	1,240	1,480	1,150	1,320	80	1,320	101.1	96.3
Boundary: Mid-Holocene / Last Millennium	3,850	1,390	3,850	1,350	2,830	770	3,040		
Phase: Mid-Holocene									
Wk46112	3,910	3,740	3,990	3,650	3,830	90	3,830	101.3	96.3
OSL3	3,840	3,520	3,970	3,330	3,660	160	3,670	101.8	96.1
Boundary: Islandisation/Mid-Holocene	4,290	3,820	4,620	3,730	4,130	240	4,090		
Phase: Islandisation									
OSL2	4,640	4,250	4,840	4,060	4,460	200	4,450	99.4	95.8
OSL1	5,290	4,790	5,540	4,540	5,040	250	5,040	92.8	95.1
Boundary: Deposit Base	6,030	4,790	9,360	4,490	5,760	900	5,500		

Table 8.4. Bayesian analysis results for Square 619706 in Face Palm Valley.

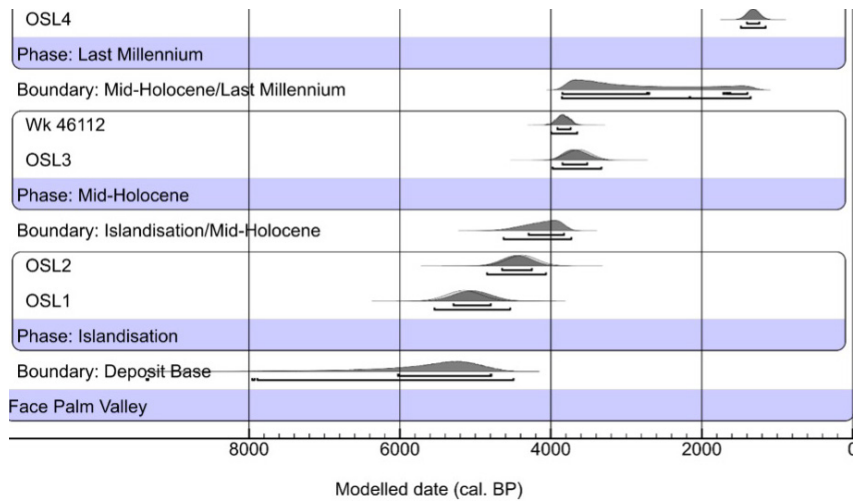


Figure 8.12. Square 619706 Bayesian analysis.

The excavated assemblage

A total of 983 kg of deposit was excavated, yielding a little under 2 kg of cultural material: mostly shell, followed closely by stone artefacts (Table 8.5). Cultural material persists in low densities throughout, with slight peaks in lithics (XU3, XU10) and shell (XU7).

Shell

While over one kilogram of shell was recovered here, only 227 g was identifiable to species. There was high fragmentation on this open site, and generally low midden deposition rates (i.e. despite the relatively alkaline deposit and good preservation environment). There was a high proportion of windblown marine sediment in this matrix.

Three analytical units were determined based on the Bayesian analysis and changing shell compositions. While the deposit appears to have built up relatively quickly in the Mid-Late Holocene, there is evidence of changing habitation use throughout time: from rocky

species platforms in the site's earliest occupation period to mixed-resource zones in the Mid-Holocene and then to sandy beach species in the most recent past (Figure 8.13). This is most clearly demonstrated by the presence of oyster in lowest XUs switching to *Melo* (baler shell) in the most recent periods (Figure 8.14). Baler more likely indicates non-economic shellfish – i.e. for holding water / cooking rather than representing food remains – but there is a notable decrease in Rock Oyster and other rocky platform species in this upper unit. Very small quantities of *Terebralia* are found in all analytical units, indicating that occupation here post-dates the Early Holocene mangrove forest phase of occupation documented along much of the western coast of Rosemary Island, but also of interest given the absence of mangroves around the island today.

UNIT	DEPOSIT EXCAVATED (KG)	ROCKS DISCARDED (KG)	PH	MUNSELL	STONE ARTEFACTS	SHELL	BONE	TOTAL WEIGHT
XU01	34.1	1.3	7.5	7.5YR 3/3	1.5	29.23	0.3	31
XU02	38.4	0.1	10		0.4	41.41		41.8
XU03	39.7	1.1	9.5		465.1	14.15		479.3
XU04	42.8	3			0	28.91	0.08	29
XU05	40.9	1			11.5	59.95		71.5
XU06	41.2	1.2			0.2	62.64	0.01	62.9
XU07	40	1			3.5	103.94	3.92	111.4
XU08	36.2	1.2			31.6	47	1.56	80.2
XU09	34.9				5.8	27.67		33.5
XU10	33.4	1.2	9		244.9	44.87		289.8
XU11	31.9	2.3			1.8	19.2		21
XU12	44.8		8.5		1.9	53		54.9
XU13	50	4.8			9.2	56.24	0.12	65.6
XU14	47.8	1	8		7.7	20.03	0.04	27.8
XU15	51.6	1	9	7.5YR 3/4	0.2	59.91	0.03	60.1
XU16 N+S	41.4	1.7			0.3	63.35		63.7
XU17 N+S	40.8	1.6			0.3	48.971		49.3
XU18 N+S	45.6	1.7	8.5		15.9	29.36		45.3
XU19 N+S	43.6	2	8	5YR 4/4	5.3	26.49		31.8
XU20 N+S	40.1	2.5	8.5		0	39.56		39.6
XU21 N+S	42.7	2.8	9		0	42.04		42
XU22 N+S	44.2	8.2			0	29.37		29.4
XU23 N+S	29.1	8.1			19.5	26.65		46.2
XU24 N+S	47.4	15			0	74.95		75
Total	982.6	63.4			826.7	1,048.90	6.06	1,881.70

Table 8.5. Square 619706: excavation weights for deposit and sediment characteristics.

HABITAT	SPECIES	AU1 XUS 1-9	AU2 XUS 10-19	AU3 XUS 20-24	TOTAL (G)
Mangrove	<i>Terebralia palustris</i>	0.35	3.02	0.49	3.86
Rocky	<i>Patella</i> sp.	6.1	14.32	1.85	22.27
Rocky	<i>Acanthopleura</i> sp.	8.77	5.48	0.59	14.84
Rocky	<i>Trochid</i>	0.88	19.31	23.64	43.83
Sandy	<i>Dentalium</i>	0.03	2.10	0.05	2.18
Sandy	<i>Melo amphora</i>	119.88	12.55	0.00	132.43
Sandy	<i>Syrinx aruanus</i>	0.00	6.88	0.00	6.88
	Total weights (g)	136.01	63.66	26.62	226.29
	Age range	0.4–1.2 ka	4.1–3.0 ka	5.5–4.1 ka	

Table 8.6. Square 619706: identified shell species and analytical units.

Eleven *Dentalium* (tusk shell) beads were found, mostly in AU2 (n = 8) and one each in AU1 and in AU3. Most of these have been analysed by Wade Goldwyer (2018: Table 22). All *Dentalium* pieces here are beads, which were likely to have been lost while being worn on-site. None of the breakage patterns / edge-wear recorded suggests that these beads were manufactured in this location (Goldwyer 2018). No beads have been directly dated. Based on the age estimates for AU2, most

beads are estimated to have been lost at this location between 4,000 and 3,000 years ago. The bead from XU1 is longer in size than the earlier examples and is fresher looking and more robust. This bead appears to have been lost here more recently (between 1,200 and 400 years ago).

Table 8.7. Square 619706: *Dentalium* beads (lengths in mm; weights in grams). ID 1–7 from Goldwyer 2018: p. 152; ID A–D recovered during later sorting.

ID	XU	DEPTH	PORTION	LENGTH	BP THICKNESS	BP W1	BREAK POINT W2	WEIGHT	EDGE STATE	EDGE SMOOTH
A	01	0-5	Medial	11				0.14	Straight	1
B	12	29-31	Medial	3.1				0.05	Concave	1
1	13	32-35	Medial	2.9		0.4	2.5	0.08	Concave	1
2	14	35-37	Medial	4.1		0.3	3.0	0.07	Jagged	1
3	14	35-37	Medial	3.5		0.2	2.3	0.07	Jagged	1
C	15	38-41	Medial	9.1				0.08	Concave	1
4	16	41-44	Medial	6.3		0.3	2.5	0.07	Concave	1
5	16	41-44	Posterior	6.75		0.3	2.4	0.07	Concave	1
6	17	44-46	Anterior	8.75	2.7	0.3	2.7	0.08	Concave	1
7	20	52-54	Medial	3.8		0.3	2.7	0.05	Jagged	1
D	21	55-57	Medial	3.5				0.07	Straight	1

Figure 8.13. Square 619706: changing resource focus during the site's occupation in AUs (weights in grams).

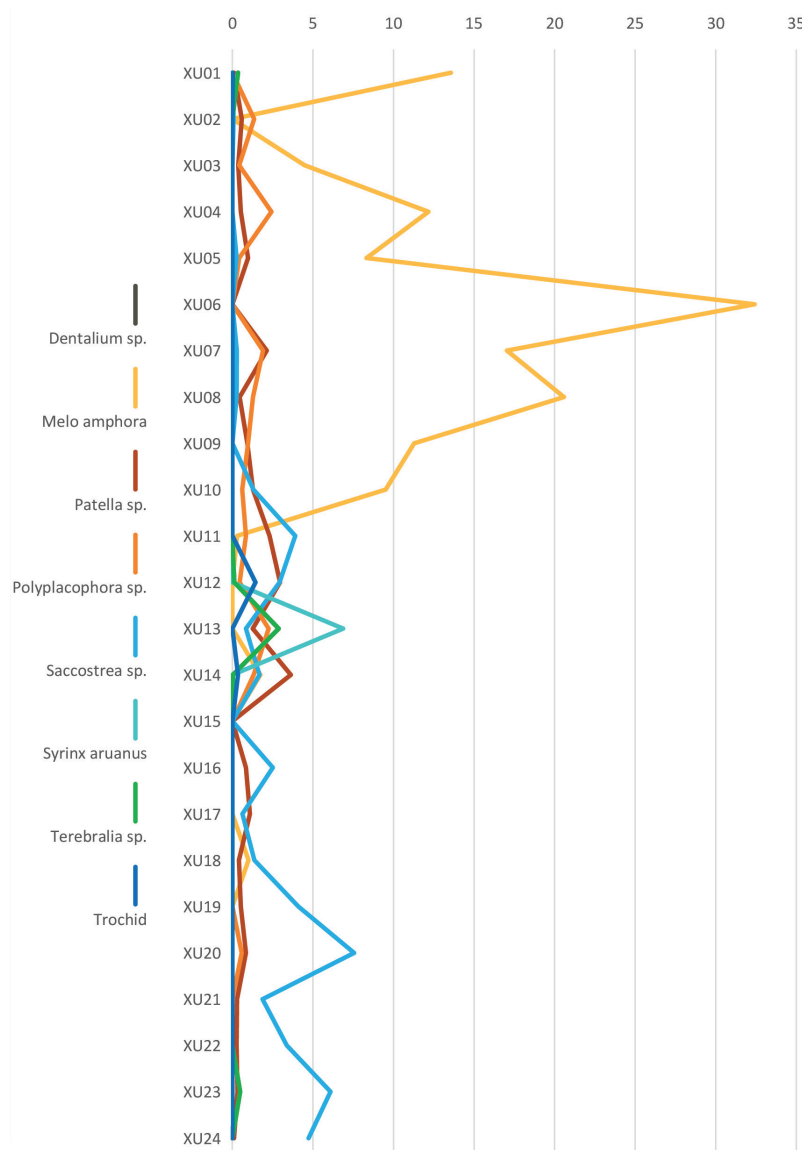


Figure 8.14. Square 619706: changing shellfish species preferences with depth.

Stone artefacts

Square 619706's stone artefact assemblage weighs 826.7 g. This relatively small assemblage has 29 artefacts >10 mm and 35 <10 mm artefacts. Artefact density in the 1 m x 1 m square is 98.5 artefact/m³. The small size of the stone assemblage makes it difficult to make meaningful

temporal comparisons between occupation phases. Nonetheless, the stone assemblage was characterised within the three analytical units outlined above.

Assemblage composition

Lithologies were identified on 12 representative stone artefacts from Square 619706 using a pXRF (Figure 8.15; see Chapter 2). The stone assemblage was predominantly made on Rosemary Island volcanoclastic siltstone (Figure 8.15 and Table 8.8). Silicified rock, fine and medium-grained gabbro, fine-grained volcanic material, quartz and fine-grained sedimentary artefacts were also recorded. Sources for both gabbro and volcanoclastic siltstone are widely distributed across the island, but also located nearby (see Figure 6.2 in Chapter 6). Groups visiting the site used material sourced from nearby locations on Rosemary Island, although it would appear that they also transported dacite artefacts to this location from elsewhere. A quartz source is located on

the north-eastern extension of the island (Quartermaine Island; see Figure 6.2), associated with basalt geology. Sources for the fine-grained sedimentary and silicified material are likely to derive from the mixed geological unit outcropping on the north-east corner of the island and the two smaller islands which are accessible at low tide.

Almost all artefacts (except one fine-grained volcanic flake and one silicified flake) were discarded at the site within the last c. 4,000 years (AU1 and AU2, see Figure 8.17). Two small (<10 mm) quartz artefacts were discarded during AU1. Stone artefact density at Face Palm Valley is lowest immediately post-islandisation and increases from the Late Holocene (Figure 8.16).

MATERIAL AU	QUARTZ	%F	RI GABBRO	%F	VOLCANICLASTIC SILTSTONE	%F	SILICIFIED	%F	TOTAL
1	2	6.3	2	6.3	21	65.6	7	21.9	32
2	-	-	1	3.3	17	56.7	12	40.0	30
3	-	-	-	-	-	-	1	2	2
Total	2	3.1	3	4.7	38	59.4	20	29.7	64

Table 8.8. Square 619706: 4 mm and 2 mm stone artefact assemblage showing material frequency by AU. The assemblage also includes one fine-grained volcanic flake from XU23 (100%f) and one fine-grained sedimentary flake from XU3 (25%f).

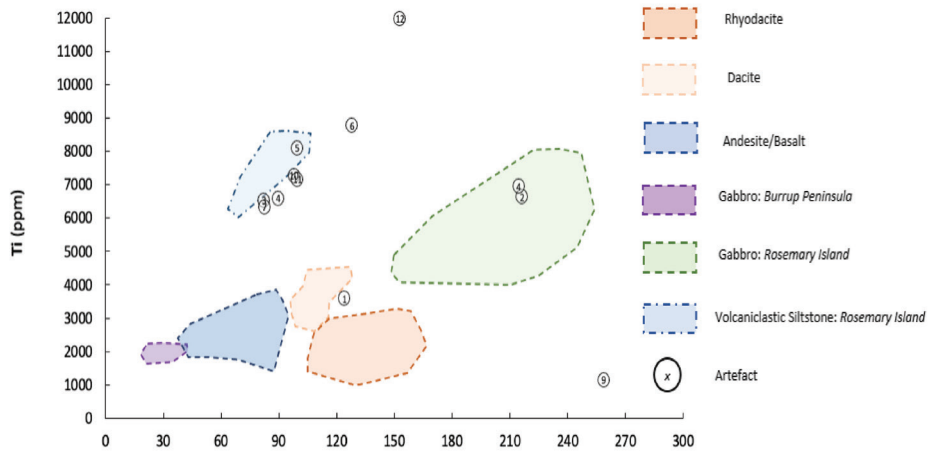


Figure 8.15. Artefacts from this site overlaid on the regional pXRF mapping of the different raw materials sampled from across Rosemary Island (see Chapter 2).

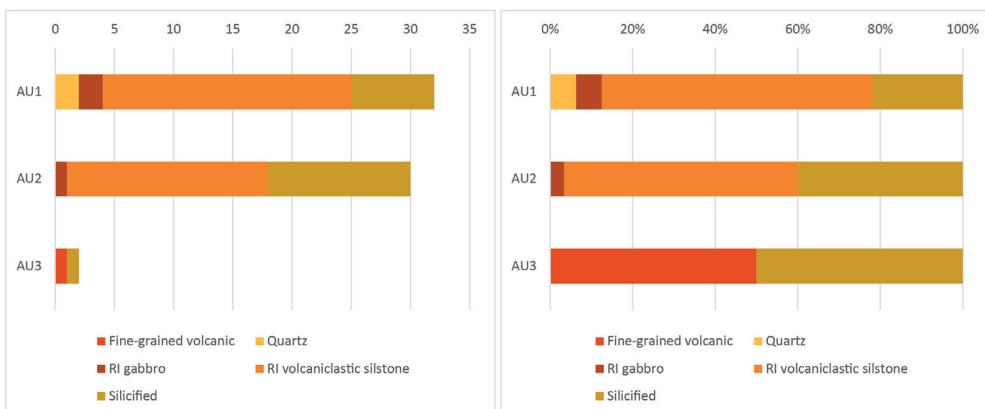


Figure 8.16. Square 619706: proportions of raw materials within AUs.

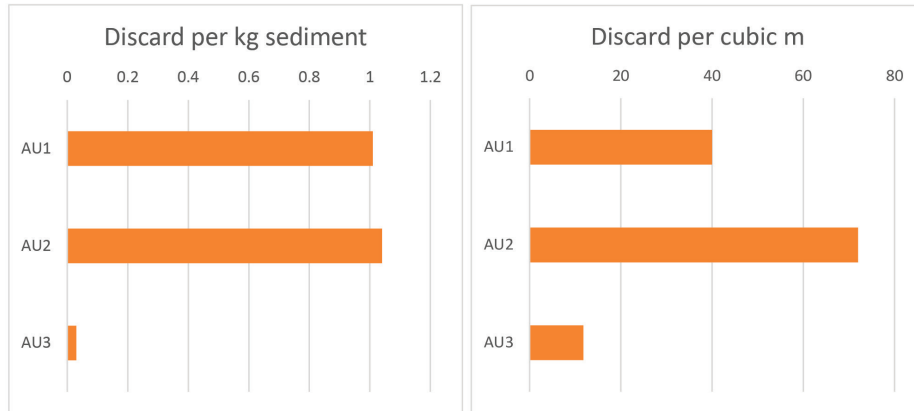


Figure 8.17. Square 619706: artefact density per kilogram sediment and per cubic metre per AU.

The artefact assemblage (n = 29) consists of flakes, broken flakes and two cores, and no formal tools were identified (Table 8.9). The cores are made on medium-sized volcanoclastic siltstone cobbles (see Table 8.9) and were discarded during the Late Holocene (AU1 and AU2). A single tool, made on a fine-grained sedimentary flake (619706-XU03-LA003) with microscopic evidence for use along its edge, was discarded during the last millennium (see Figure 8.18).

The microdebitage assemblage (n = 35) consists of

<1 cm flakes and flake fragments made on volcanoclastic siltstone (n = 22), silicified material (n = 11) and quartz (n = 2). Microdebitage occurs throughout the deposit, although the larger and smaller debitage categories do not always correlate. While two pieces of quartz microdebitage were found in XU2, no larger quartz artefacts were recovered in AU1. This suggests that people transported preferred materials around the landscape, or that our small sample did not capture all depositional activity in this location.

Assemblage reduction

Although the sample of complete flakes is small (Table 8.10), the Scar Density Index (SDI) gives some indication of the reduction state of the cores from which these flakes were removed. The high SDI value on the fine-grained volcanic flake (Figure 8.18) indicates that it derives from a more intensively reduced core than flakes made from other nodules. Generally, however, the SDI suggests that overall nodule reduction was non-intensive (Table 8.10). Indeed, no flakes exhibit multidirectional

dorsal scars (i.e. these cores were not rotated prior to flake removal). Except for one silicified flake with a flaked platform, all complete flakes exhibit flat platforms. Platform preparation, however, was noted on a volcanoclastic siltstone flake and two gabbro flakes. These same three flakes have remnant cortex on their dorsal surfaces, indicating they are in a preliminary stage of reduction. Cortex was only present on one third (n = 10, 34.5%) of the assemblage (>10 mm).

ARTEFACT TYPE	BROKEN FLAKE		COMPLETE FLAKE		CORE/CORE FRAGMENT		TOOL		TOTAL		NAS:MNA RATIO
	N	%	N	%	N	%	N	%	N	%	
Fine-grained volcanic			1	100					1	3.4	1.0
RI gabbro	1	3.3	2	66.6					3	10.3	1.2
RI volcanoclastic siltstone	8	50	6	37.5	2	12.5			16	55.2	1.9
Silicified	7	87.5	1	12.5					8	27.6	3.2
Fine-grained sedimentary							1	100	1	3.4	1.0
<i>Total</i>	<i>16</i>	<i>55.2</i>	<i>10</i>	<i>34.5</i>	<i>2</i>	<i>6.9</i>	<i>1</i>	<i>3.4</i>	<i>29</i>	<i>100</i>	

Table 8.9. Square 619706: stone assemblage composition by frequency and proportion. Artefacts <10 mm not included here.

MATERIAL	N	μ	SD
Fine-grained volcanic	1	2.48	-
RI gabbro	2	1.05	0.47
Volcanoclastic siltstone	6	1.18	0.35
Silicified	1	1.52	-
Fine-grained sedimentary	1	0.83	-

Table 8.10. Square 619706: Scar Density Index (SDI) for complete flakes (excluding flakes <10 mm).



Figure 8.18. (Left) Fine-grained volcanic flake from AU3 (619706-XU23-LA030); (right) Rosemary Island volcaniclastic siltstone cobble core from AU1 (619706-XU03-LA002). Scales are 10 mm.

Flakes are relatively small, with a mean maximum dimension of 34.6 mm. The complete flakes discarded at the site vary widely in size, from 19.2 mm (maximum dimension, fine-grained sedimentary flake) to 60.6 mm (a fine-grained volcanic flake). Most flakes are longer than they are wide but are not typically elongated (Table

8.12), i.e. more than twice as long as they are wide. No differences in flake attributes were noted on volcaniclastic siltstone flakes between AU1 and AU2.

MATERIAL	WEIGHT (G)			SURFACE AREA (MM ²)	
	N	μ	SD	μ	SD
Fine-grained volcanic	1	19.5	-	1,678.6	-
RI gabbro	2	5.0	2.2	717.0	136.6
Volcaniclastic siltstone	6	8.4	11.5	1,089.2	949.7
Silicified	1	2.5	-	429	-
Fine-grained sedimentary	1	0.6	-	259.2	-

Table 8.11. Square 619706: weight and surface area for complete flakes (not including flakes <10 mm).

The two volcaniclastic siltstone cores (101.9 mm and 84.7 mm maximum dimension) discarded here have low SDI values (0.9 and 0.93) and are mostly cortical. Both cores represent non-intensively reduced 'test cores',

MATERIAL	N	μ	SD
Fine-grained volcanic	1	2.0	-
RI gabbro	2	1.3	0.2
Volcaniclastic siltstone	6	1.4	0.6
Silicified	1	1.8	-
Fine-grained sedimentary	1	0.7	-

Table 8.12. Square 619706: elongation ratio for complete flakes (not including flakes <10 mm).

where several flakes were removed from the broken face of a cobble before being discarded (Figure 8.18). These 'test cores' had been brought from their source on nearby outcrops for testing in this location.

Usewear and residue analysis

Two artefacts from the last millennium (AU1) were analysed for usewear and residue. Artefact XU03-LA003 is a polished fine-grained sedimentary flake that has a single shallow edge scar on the right dorsal margin (Figure 8.19). Residues found along the right ventral margin showed a wide variety of plant species morphologies. A black residue was extracted but could not be identified. The surrounding red viscous material is consistent with resin. Starch molecules and wood were also recovered from the artefact. The starch molecules are consistent with those commonly found in *Poaceae* sp., a large family of flowering grasses. Artefact XU03-LA003 tested negative for blood. Usewear and residue analysis suggests that artefact 619706-XU03-LA003 was used primarily to process siliceous

plant materials, most likely grasses that deposited the starch residue and created the polish that covers approximately 40% of the ventral surface. The resin on the right ventral margin was also likely deposited during this process. Post-depositional contamination cannot be ruled out given the resin-rich spinifex landscape.

Artefact XU08-LA004 is a dark grey volcanoclastic siltstone flake with macroscopic edge damage (Figure 8.20). No microscopic usewear was identified. The artefact was thus not tested for residues.

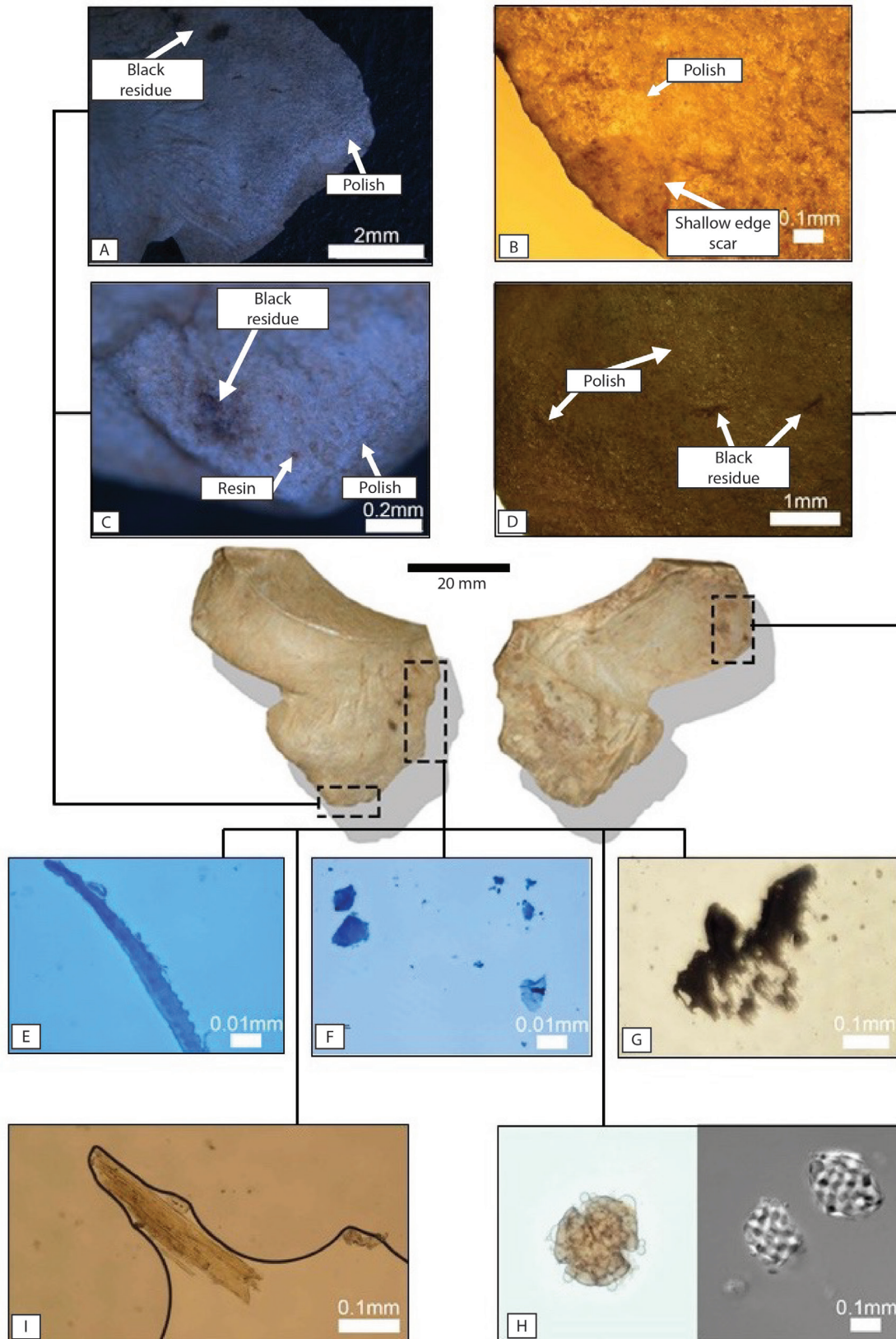


Figure 8.19. Square 619706 artefact XU03-LA003. Images A to D show the usewear and residues present. Plant residues vary widely and include an unidentified complete fibre (E), a typical small fibre scatter (F), non-diagnostic woody tissue (H) and a cluster of starch molecules consistent with *Poaceae* sp. (I; recovered starch shown on left, reference on right). Scale is 5 mm. Artefact XU08-LA004 is a dark grey volcanoclastic siltstone flake with macroscopic edge damage (Figure 8.20). No microscopic usewear was identified. The artefact was thus not tested for residues.



Figure 8.20. Square 619706 artefact XU08-LA004. Scale is 30 mm.

Discussion

Square 619706 has a very low-density mixed lithic material stone assemblage. The assemblage from this square suggests that this part of Rosemary Island was occupied by Aboriginal people sporadically from 5,000 years ago and that this use became more focused in the Late Holocene, and particularly in the last millennium (AU1).

Initial Mid-Holocene use of this location shows a focus on shell species that could have been collected from the nearby rock platforms at either end of the beach just to the north. This resource focus changes to a mixture of resource zones in the Mid–Late Holocene and then to predominantly sandy beach species in the most recent past (Figure 8.13). This is most clearly demonstrated by the early presence of oyster in the lowest AU, with a switch to *Melo* (baler shell) during the most recent periods (Figure 8.14). There is a distinctive decrease in Rock Oyster and other rocky platform species in this upper unit. At some time between 4,000 and 3,000 years ago, one of the site's occupants was wearing a *Dentalium* necklace. This broke and a small number of beads were left at this location.

Minute quantities of *Terebralia* are found in all analytical units, which is interesting given that there are no mangroves growing around Rosemary Island today. While occupation here post-dates the Early Holocene mangrove forest phase of occupation which occurs along the western coast of Rosemary Island, at the times that this location was being used mangroves were still growing around this island. Further investigation is required into when mangroves stopped growing on this outer part of the archipelago.

Despite the small artefact assemblage, lithic diversity is high. Most materials were acquired

from identified local sources on Rosemary Island. The fine-grained sedimentary tool, which has been used to process siliceous plant materials (probably grasses) and has evidence of resin on one face (see Figure 8.19), may have derived from the area with different geology in the north-east corner of Rosemary Island – or has been transported by Aboriginal people to the island in the last millennium, as part of a mobile toolkit. The diversity of materials selected and used by people visiting this plain reflects the range of locally available sources on the island and indicates multiple site visits by small groups over the last 5,000 years. Preferences for different source locations across the island appear to have shifted slightly through time.

The presence of quartz debris in the absence of larger quartz artefacts suggests that quartz nodules brought to this place were curated and removed from the site after knapping. Similarly, very few cores were found at Square 619706. It is possible that cores may simply have been discarded within other parts of the site as well as being taken with the site's occupants for use elsewhere. The microdebitage found is indicative of some on-site reduction and/or tool manufacture and maintenance. Overall, however, this small assemblage from a single 1 m x 1 m square does not suggest intensive on-site reduction or heavy repeated utilisation of a nearby source. Indeed, the two volcanoclastic siltstone cobble cores indicate 'casual' and non-intensive use of the most suitable, and closest, local tool-stone. Flake attributes also demonstrate mostly non-intensive nodule reduction, as would be expected within a landscape of abundantly available raw materials:

Rosemary Island Central Valley – Sample Area 5

A minor, westerly draining valley in the centre of the island was found to have an ephemeral pool (full after rain in August 2016, dry on all other occasions). One excavation square (RIA05-885878) was placed immediately adjacent to the pool (Figure 8.21) in an area surrounded by panels of art in this an extensive rock art site complex now named Site RIA-005. Within this site

there is also extensive modification and movement of stone to create a series of structures. These structures are mostly found within the boulder slopes above the blocks with engraved panels. A further two squares (RIA05-023799 and RIA05-016764) were excavated amongst the structures (see Figure 8.21 below).

Square RIA05-016764

The excavation was located amongst the stone structures on top of the ridge above the main valley.

Stratigraphy

Excavation in the 0.5 m x 0.5 m square proceeded in seven XUs dug in 1–4 cm depths (Table 8.13). The lowest stratigraphic unit (XU07) was reached in the south-east quadrant (Figure 8.22). Two stratigraphic (pedogenic) units were encountered (Figure 8.22):

SU1 – dark brown (7.5YR 3/4) gravelly silty deposit including the Ao layer. Deposit compacted by insect activity. pH 6;

SU2 – very dark brown becoming finer and redder at base (7YR 3/3 to 7.5YR 2.5/3); fine-grained increasingly friable deposit with rocky inclusions. pH 6.5.

No cultural material (i.e. stone artefacts, charcoal or economic shellfish) was recovered from this excavation, which removed c. 48 kg of deposit, including 14.7 kg of rocky matrix (Table 8.13). The excavation was photographed throughout, but at the conclusion of the excavation was backfilled without a section being drawn.

UNIT	DEPTH BELOW SURFACE (CM)	DEPOSIT EXCAVATED (KG)	WEIGHT ROCKS DISCARDED (KG)
XU01	1	5.2	
XU02	2	5.1	
XU03	5	5.5	1.2
XU04	2	6.1	1.6
XU05	6	9.4	6.5
XU06	5	6.4	1
XU07	11	10.2	4.4
<i>Total</i>	<i>32</i>	<i>47.9</i>	<i>14.7</i>

Table 8.13. Square 016764: excavation units' average depth and weights for deposit.

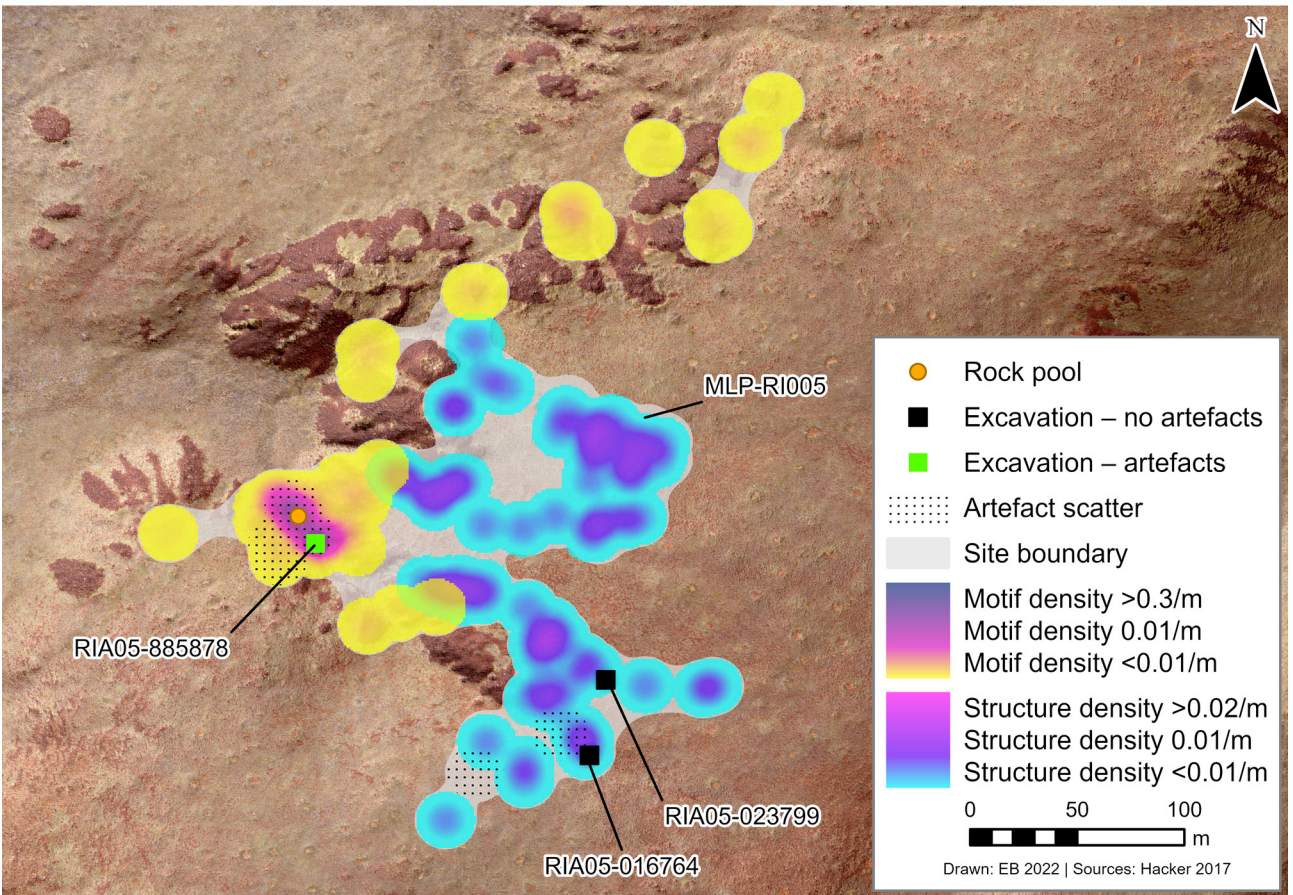
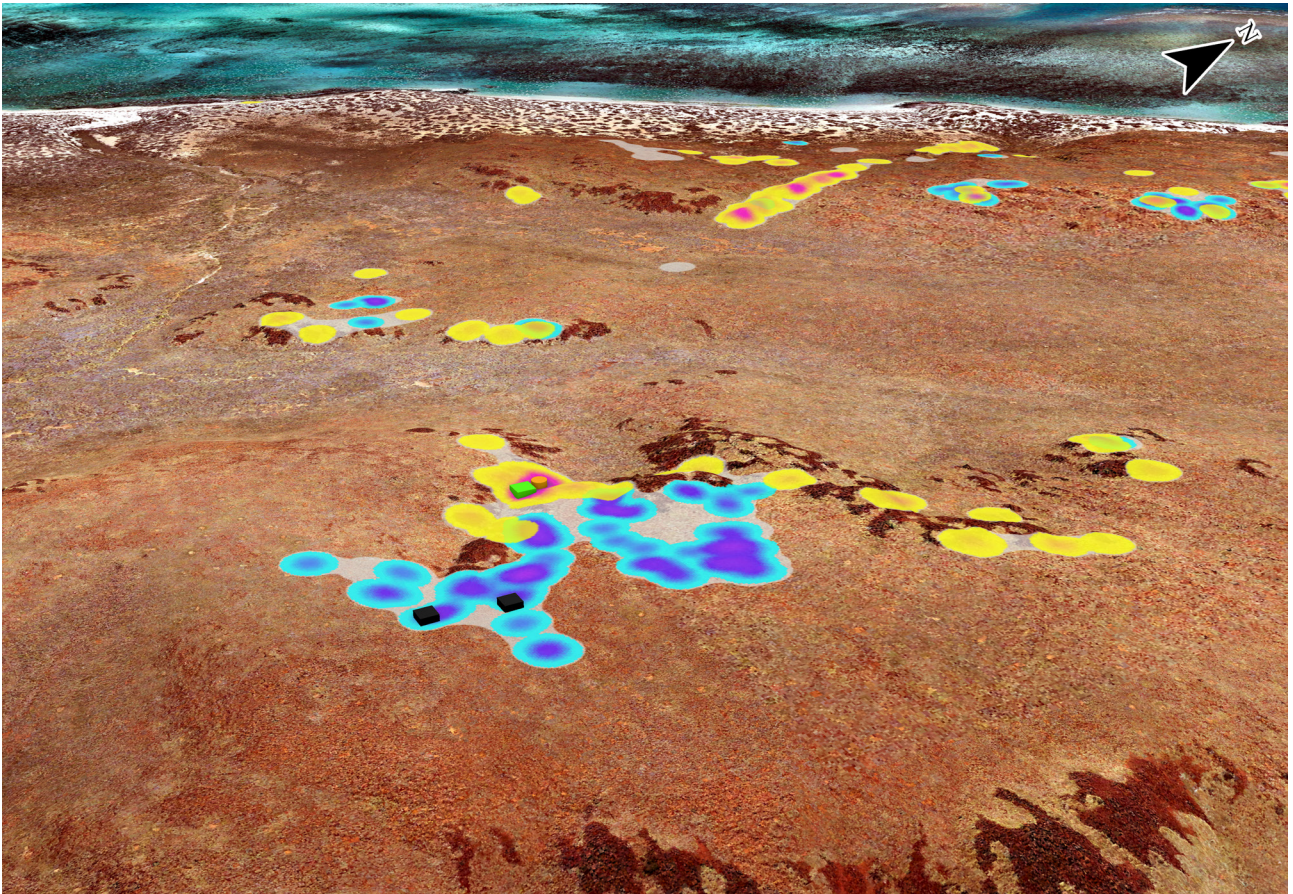


Figure 8.21. Rosemary Island Sample Area 5 excavations, showing excavation squares relative to the recorded rock art assemblage coded for motif density.



Figure 8.22. Square 016764 at (left) the commencement of excavation, and (right) completion of XU07.

Square RIA05-023799

This test excavation was in the flat floor area within another stone structure on top of the ridge above the main central valley.

Stratigraphy

Excavation in the 0.5 m x 0.5 m square proceeded in seven XUs dug in 2–4 cm depths (Table 8.14). The lowest level was reached only in the north-west quadrant (in XU07). Two broad stratigraphic (pedogenic) units were encountered (Figure 8.23):

SU1 – dark brown (7.5YR 3/4) gravelly silty deposit, including a shallow Ao layer. Spinifex roots throughout north-west quadrant. pH 6.5;

SU2 – dark brown (7.5YR 3/4 to 5YR 3/4) fine-grained friable deposit with rocky inclusions. pH 6.5.

No cultural material (i.e. stone artefacts, charcoal or economic shellfish) was recovered from this excavation, which removed c. 76 kg of deposit of which 45 kg was rocky matrix (Table 8.14). The excavation was photographed throughout, but at the conclusion of the excavation was backfilled without a section being drawn.

UNIT	DEPTH BELOW SURFACE (CM)	DEPOSIT EXCAVATED (KG)	WEIGHT ROCKS DISCARDED (KG)
XU01	3.5	5.6	
XU02	5.5	8.8	3.8
XU03	3	9.8	4.4
XU04	7	11.4	8
XU05	4	18	12.8
XU06	5	12.8	9
XU07	3.5	9.4	7
Total	31.5	75.8	45

Table 8.14. Square 023799: excavation units' average depth and weights for deposit.



Figure 8.23. Square 023799 at (left) the commencement of excavation, and (right) completion of XU07.

Square RIA05-885878

Excavation in this 1.0 m x 0.5 m square proceeded in two (50 cm x 50 cm) quadrants (A and B) with 13 XUs dug in 2–4 cm depths initially (A). The second, shallower

square (B) was excavated in eight XUs according to the stratigraphy encountered in the first quadrant.



Figure 8.24. Stringing up Square 885878A, August 2016. View to the west from the creekline.

Stratigraphy and dating

Three stratigraphic units were encountered (Figure 8.26). Within the profile, colour intensifies and becomes generally redder with depth. Compaction also increased with depth. The upper two SUs have a significantly less rocky matrix.

SU1 – a thin crust of fine red (7.5YR 3/3) silty sediment comprises the Ao layer. pH 8.5;

SU2 – red brown (5YR 3/4) friable sediment, with ant

nest / bioturbation areas present across most of the square (not visible in all sections). pH 6;

SU3 – very rocky, chaotically bedded mixed-sized rocks and blocks interlocked. Shell fragments visible in several sections, amongst the redder deposit (5YR 3/4) becoming more clayey just above bedrock.



Figure 8.25. Square 885878A: (left) charcoal encountered in XU3 and (right) excavation completed in square A; end of XU13.

UNIT	DEPTH BELOW SURFACE (CM)	DEPOSIT EXCAVATED (KG)	ROCKS DISCARDED (KG)	PH	MUNSELL
XU01	1.8	14.4	2.1	8.5	7.5YR 3/3
XU02	3.6	9.5	1.9	9	7.5YR 3/3 - 5YR 3/4
XU03	5.1	13	4.4	9	7.5YR 3/3 - 5YR 3/4
XU04	8.0	23.8	16	9	7.5YR 3/3 - 5YR 3/4
XU05	12.8	38.6	29.4	9	7.5YR 3/3 - 5YR 3/4
XU06	15.8	27.2	21.1	9	5YR 3/4
XU07	19.8	24.2	15.5	9	5YR 3/4
XU08	21.3	36	27.4	8.5	5YR 3/4
XU09	23.3	9.8	7.2	9	5YR 3/4
XU10	27.1	18	13.4	8	5YR 3/4
XU11	29.1	11.2	9.2	7.5	5YR 3/4
XU12	33.3	13.2	8.6	7.5	5YR 3/4
XU13		0	No data		
Wall clean		11.2	5.4		
<i>Total</i>		<i>258.5</i>	<i>161.6</i>		

Table 8.15. Square 885878: excavation units, weights for deposit and sediment characteristics.

Four dates were returned from this excavation square. A hearth encountered in XU3 was dated to between 272 and 232 calibrated years ago, while a chiton shell in the same XU (but slightly lower in the sequence) was dated to 908–753 calibrated years ago.

Terebralia from XU4 and XU10 were dated to the Early Holocene, indicating that the lowest stratigraphic unit accumulated over a roughly 400-year period just before 8,000 BP (Table 8.16).

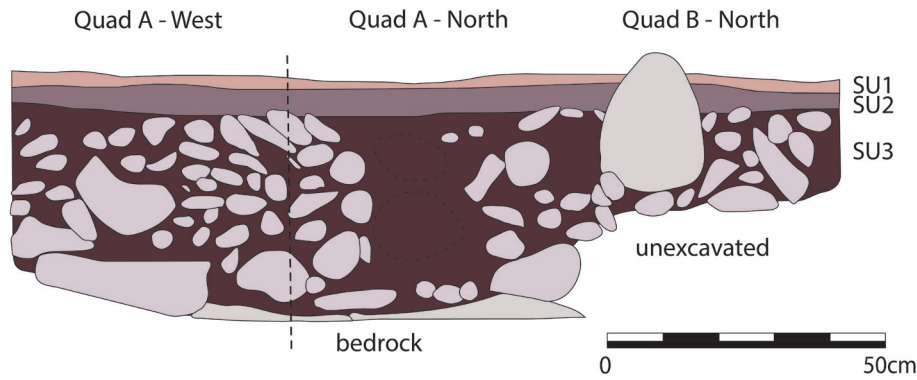


Figure 8.26. Square 885878 stratigraphic section drawings (western and northern baulks).

LAB CODE	SAMPLE TYPE	XU	SU	DEPTH BELOW SURFACE (CM)	% MODERN CARBON	CONVENTIONAL RADIOCARBON AGE (YRS BP 1σ ERROR)	CALIBRATED AGE RANGE	MEAN CALIBRATED AGE
Wk46113	Charcoal	3	2	3–5	98.0 ± 0.2	160 ± 15	272–232	152 ± 120
Wk46114	Chiton	3	2	5	84.6 ± 0.1	1,345 ± 14	908–753	831 ± 77
Wk46115	<i>Terebralia</i>	4	3	7	38.5 ± 0.1	7,674 ± 18	8,157–7,991	8,074 ± 83
Wk46116	<i>Terebralia</i>	10	3	28	36.6 ± 0.1	8,081 ± 18	8,555–8,395	8,475 ± 80

Table 8.16. Square 885878 radiocarbon dates returned on charcoal and shellfish.

Bayesian analysis

The Bayesian analysis used a sequence deposition model (Table 8.17) following the same structure and model parameters as the Face Palm Valley model. Here a sequential model was used (unlike the continuous model used for Face Palm Valley) since there is one clear chronological discontinuity in the dated sequence for Square 885878 (see Bronk Ramsey 2009a). The Central Valley charcoal dates were calibrated using SHCal20 (Hogg et al. 2020). This model estimates that, based on

the 885878 sequence, Central Valley was first occupied between 9,630 and 8,180 cal. BP and until 7,930–6,130 cal. BP, at which time there was a chronological discontinuity. Occupation restarted again after 1,580–560 cal. BP and continued into the more recent past. This sequence is well supported by the outlier analyses, as each date has <3% chance of being an outlier and all dates return high agreement index results ($A_{model} = 101.1$; $A_{overall} = 99.4$).

NAME	68.2%		95.4%		SUM. STATISTICS			INDICES	
	FROM	TO	FROM	TO	μ	σ	M	AI	OP
Boundary: Deposit Surface	70	1	90	0	50	30	50	100	
Phase: Last Millennium									
Wk46113	260	70	270	10	150	80	120	97.5	96.2
Wk46114	680	560	750	500	620	80	620	100	95.4
Boundary: Base of Last Millennium	1,580	560	4,580	490	1,540	1,190	1,080		
Boundary: Top of Early Holocene	7,930	6,130	7,990	2,710	6,420	1,560	7,030		
Phase: Early Holocene									
Wk46115	7,920	7,780	7,980	7,690	7,840	80	7,850	100.9	95.8
Wk46116	8,330	8,190	8,400	8,100	8,250	80	8,260	99.7	95.8
Boundary: Deposit Base	9,630	8,180	13,280	8,050	9,530	1,590	8,920		

Table 8.17. Square 885878 Bayesian analysis.

The excavated assemblage

Based on the stratigraphy, the dates and the Bayesian analysis, the assemblage was divided into two analytical units:

- Analytical Unit 1: Last Millennium XUs 1–3
- Analytical Unit 2: Early Holocene XUs 4–13

The excavated assemblage is predominantly stone artefacts (1.4 kg) and shellfish (1.1 kg; Figure 8.28). There was a reasonable amount (28.5 g) of mostly unidentifiable bone fragments (Table 8.18). Shell is found throughout the sequence, as are bone fragments, although the weights of these are significantly greater

during the earlier occupation. Artefacts are also found mostly in the earlier XUs (Figure 8.28). Artefact discard

suggests a peak in occupation in XU10, which is dated to between 8,555 and 8,395 calibrated years ago.

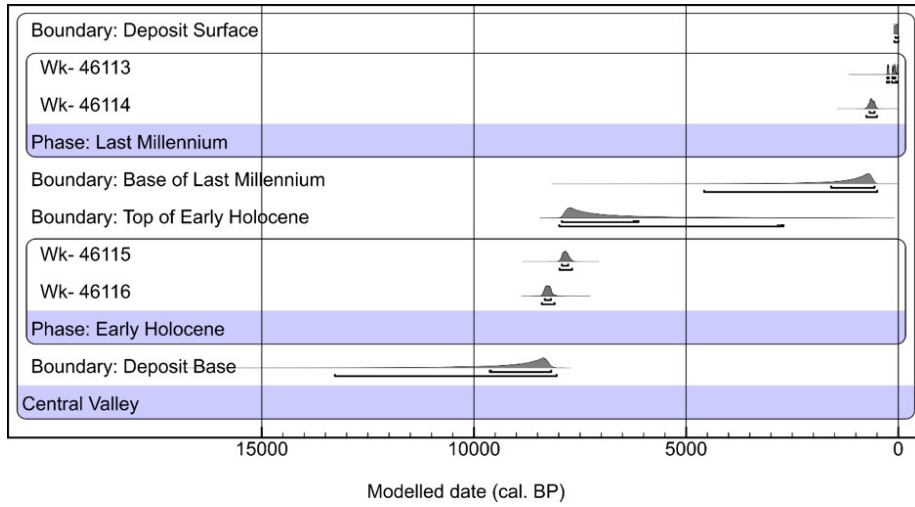


Figure 8.27. Square 885878 Bayesian analysis results.

UNIT	AU	FLAKED ARTEFACTS (G)	SHELL (G)	BONE (G)	TOTAL WEIGHT
XU01	1	0.34	8.52	7.22	16.08
XU02	1	0.18	6.89	3.79	10.86
XU03	1	1.53	5.54	1.44	8.51
XU04	2	38.36	25.151	2.59	66.101
XU05	2	13.19	24.471	0.031	37.692
XU06	2	45.12	55.35	0.2	100.67
XU07	2	14.78	68.84	1.3	84.92
XU08	2	0.53	138.56	0.03	139.12
XU09	2	8.9	170.36	0.87	180.13
XU10	2	908.95	259.75	5.18	1173.88
XU11	2	0.48	124.33	0.53	125.34
XU12	2	61.61	117.06	2.02	180.69
XU13	2	308.35	107.161	3.32	418.831
<i>Total</i>		<i>1,402.32</i>	<i>1,111.98</i>	<i>28.52</i>	<i>2,542.82</i>

Table 8.18. Square 885878 excavated assemblage.

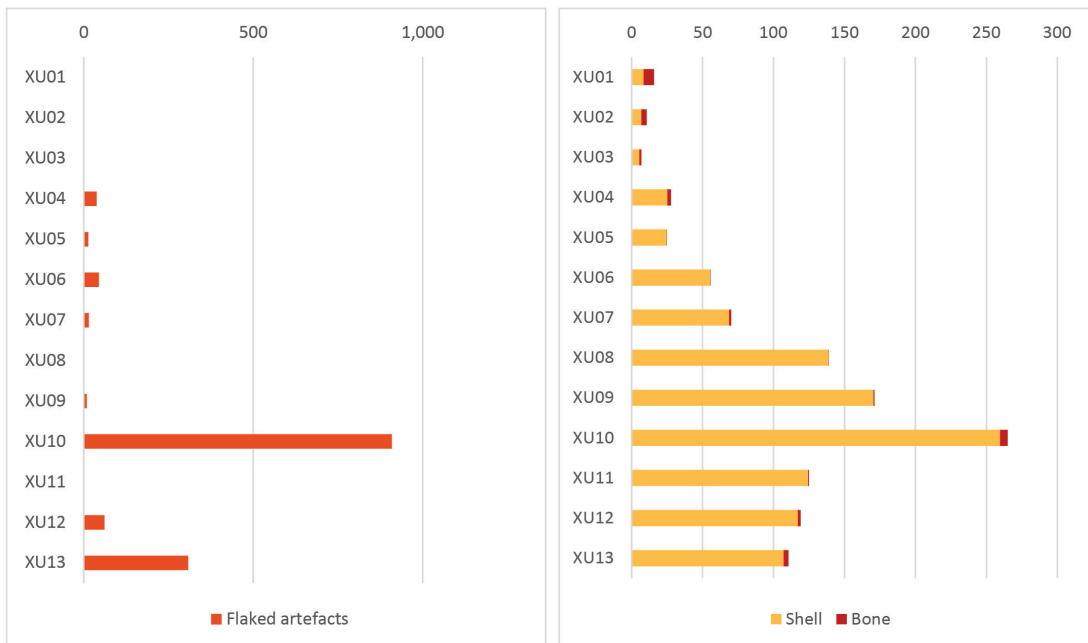


Figure 8.28. Square 885878: proportions of stone artefacts, shell and bone (weights in grams).

Shellfish remains

The vast majority of the economic shell species (by weight) was found in AU2; these are predominantly (92%) the mangrove species *Terebralia* (Table 8.19). Only c. 8 grams of shellfish was found in AU1, from a mixture

of rocky platform and sandy habitats (Figure 8.29). Baler shell (*Melo amphora*) was found in both analytical units, and its presence potentially indicates the use of shell for collecting/storing potable water.

HABITAT	SPECIES	AU1 XUS 1-3	AU2 XUS 4-13	TOTAL (G)
Mangrove mudflats	<i>Terebralia palustris</i>		887.59	887.59
Mangrove mudflats	<i>Terebralia semistriata</i>		0.82	0.82
Rocky	<i>Acanthopleura</i> sp.	2.06	1.04	3.1
Rocky	<i>Saccostrea</i> sp.		2.54	2.54
Sandy	<i>Melo amphora</i>	5.87	61.39	67.26
		7.93	953.38	

Table 8.19. Square 885878; shellfish species found in the two analytical units. Weight in grams.

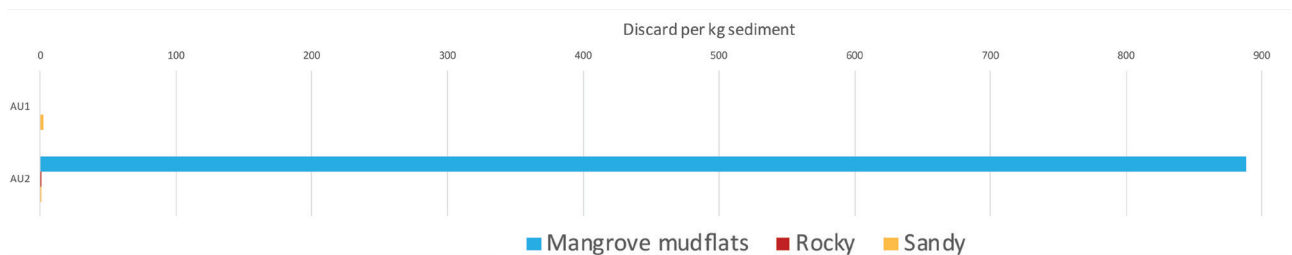


Figure 8.29. Square 885878; proportions of shellfish species found in the two analytical units.

In situ rock with motif

One piece of natural rock with three abraded parallel lines was uncovered in XU12 (Figure 8.30). This angular block with calcium carbonate encrustation was found during excavation with the motif located on the surface facing downwards. At some point this rock was likely embedded nearby around the waterhole/creek bed where there is a relatively continuous thick calcium carbonate drape

(Figure 8.30). This rock has been dislodged from that location and moved to its current location in the deposit. This amorphous geometric motif can be dated by association to older than 8,555–8,395 calibrated years ago, although this is a minimum age that indicates when this blocky fragment was dislodged from the creekline and became incorporated in the occupation deposit.



Figure 8.30. Square 885878 with rock found in situ (in XU12) with parallel scratched lines.

The calcium carbonate may be able to be used for refining this chronology, although this too is likely to not necessarily indicate when this motif was created. The carbonate may determine when this rock became

dislodged from being embedded in the creekline, and the carbonate may be much older than the rock art. Further analysis is required to determine whether the scratched motif continues beneath the encrustation.



Figure 8.31. View of the creek bed near Square 885878 showing the calcium carbonate encrustation and rock art panels in the vicinity.

Stone artefacts

The stone artefact assemblage was analysed by Zane Blunt (2019). This assemblage consists of 144 artefacts, weighing 3,501.5 g. Almost half of these artefacts (n = 60)

are microdebitage (<10 mm maximum dimension). The stone assemblage was characterised within the two identified analytical units (AUs).

Assemblage composition

Lithic materials were identified using a combination of pXRF and visual inspection by geologist John Fairweather, who determined that the assemblage is entirely composed of local gabbro which varies in grain size and colour (Table 8.20 and Figure 8.32). Fairweather’s (2019) geological mapping of Rosemary

Island indicates that gabbro is the surface bedrock in the Central Valley, and that this manifests as the blocks upon which there are engraved panels as well as the material utilised for the stone artefacts. Most artefacts were discarded in AU1.

AU	GABBRO	%F
1	35	24.3
2	109	75.7
Total	144	100.0

Table 8.20. Square 885878: stone artefact assemblage showing material frequency per AU.

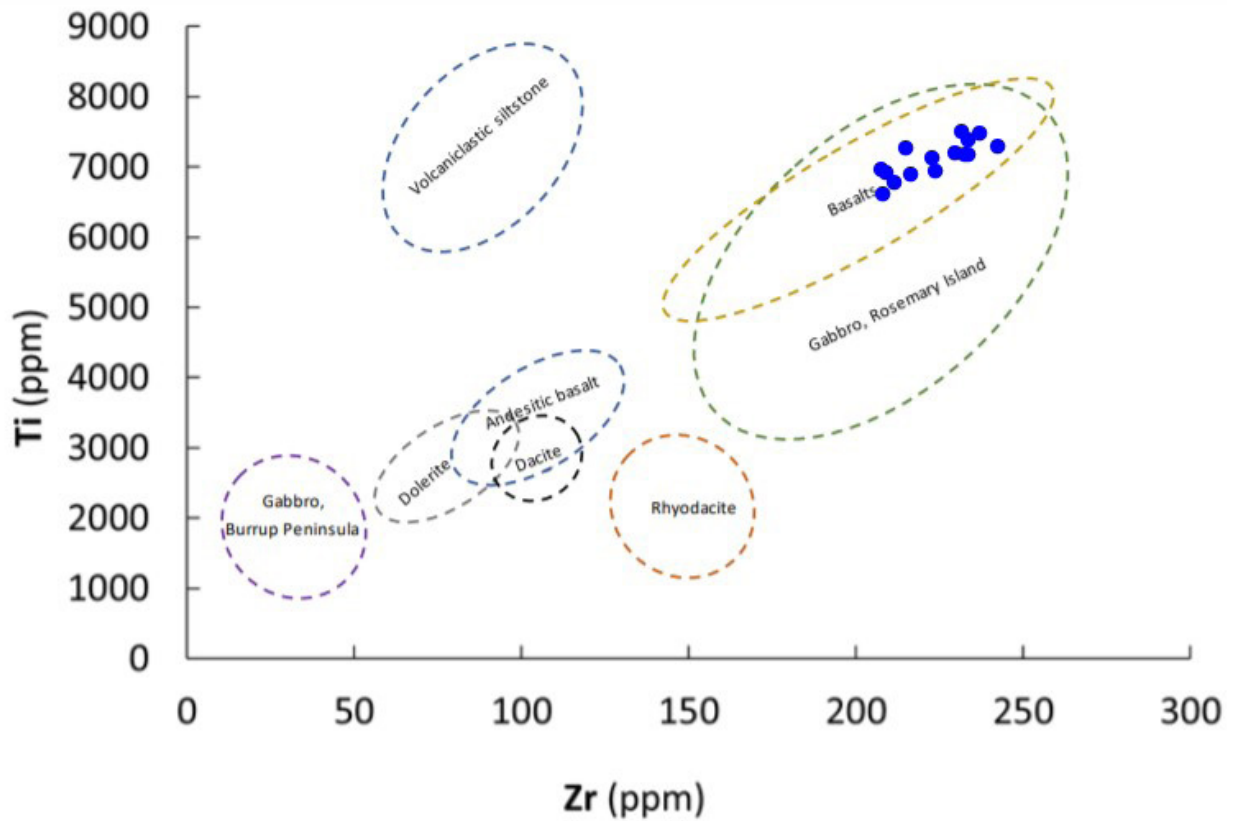


Figure 8.32. Square 885878: artefact pXRF results (shown in blue) showing Rosemary Island raw material type clusters based on titanium and zirconium (from Fairweather 2019: Figure 33).

Artefact density per kilogram sediment (Figure 8.33) indicates that the site was visited more often during the Early Holocene (AU2) than in the last millennium (AU1). However, discard per cubic metre shows the opposite

pattern. This contrast most likely relates to a greater proportion of rocky matrix in the lower deposit which has skewed the density per kilogram sediment data for this square.

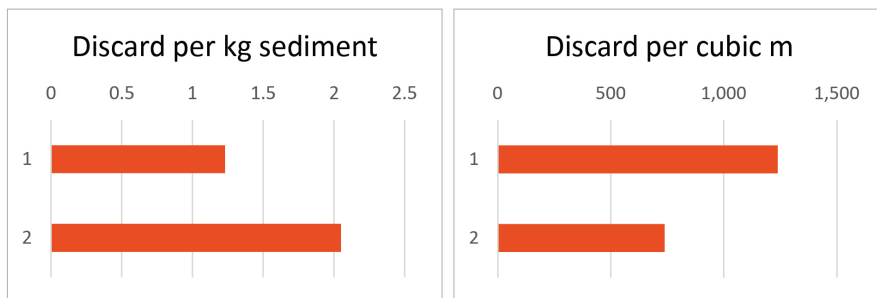


Figure 8.33. Square 885878: artefact density per kilogram sediment and per cubic metre for each AU.



Figure 8.34. Square 885878: grain size and colour variation in Rosemary Island gabbro artefacts. Scale is 50 mm.

Tools dominate the 885878 lithic assemblage (Table 8.21). Most tools are made on complete flakes and proximal flake fragments. As with other Rosemary Island excavated assemblages, cores comprise a very low proportion of this assemblage: only four cores were recovered from AU2.

The 885878 microdebitage comprises 60 flakes <1 mm maximum dimension. Microdebitage is proportionally more common during the Early Holocene occupation phase (AU1: 15%, AU2: 55%), most likely reflecting more stone tool manufacture taking place during this time.

ARTEFACT TYPE MATERIAL	BROKEN FLAKE		COMPLETE FLAKE		CORE/CORE FRAGMENT		TOOL		TOTAL		NAS TO MNA RATIO
	N	%	N	%	N	%	N	%	N	%	
Gabbro	11	13.1	11	13.1	4	4.8	58	69	84	100	1.7

Table 8.21. Square 885878: stone assemblage composition by frequency and proportion. Artefacts <10 mm are not included.

Assemblage reduction

Complete gabbro flakes and tools have very few dorsal flake scars ($\mu = 1.1 \pm 1$), indicating that gabbro nodules were non-intensively reduced on-site. A comparatively higher number of flakes and tools have remnant cortex on their dorsal surfaces ($n = 17, 47.2\%$) when compared to other Rosemary Island stone assemblages. This likely reflects the proximity of this assemblage to its lithic source. All but nine flakes are less than 3 cm in maximum dimension, and most flakes discarded at the site are small and light (Table 8.22). Most flakes are longer than they are wide (elongation ratio $\mu = 1.3 \pm 0.75$) but no blades (elongated flakes) were recorded.

The four cores discarded at RIA-005 vary widely in size (weight $\mu = 783.5 \pm 785.8$) and reduction intensity (SDI $\mu = 1.89 \pm 1.74$). The largest core (XU05-LA001, AU2) weighs nearly two kilograms (1,879.3 g) but this was non-intensively reduced (SDI: 1.2): six flakes were removed from a single platform. This core also has calcium carbonate encrustation, suggesting that it too has been sourced from the rock pool nearby (Figure 8.35). Only three flake scars were removed from a much

smaller (331.4 g) and non-rotated core (SDI: 0.69). In contrast, a third core (807.9 g), which was also discarded during the earliest phase of site use (XU10-LA001, AU2), was rotated twice to remove a total of 20 flakes (Figure 8.35). Its high SDI value (4.46) demonstrates that this nodule was intensively reduced at the point of discard. Despite the relatively minimal reduction of all but one core, no cores have more than 30% cortex. This indicates that cortex is not necessarily a good indicator of reduction intensity at this site and is more likely to relate either to cortex on the original source material or more intensive initial testing of lithic materials at the source before transport to this location.

Two cores have possible evidence for subsequent use in the form of polish and striations. However, it is difficult to ascertain whether this is related to use since usewear on platforms can often be attributed to the percussion and buffing processes of platform preparation (Hayes et al. 2014: 87). The cores from the lower layers also were encrusted with calcium carbonate (Figure 8.36).

Tool selection and use

The 58 tools discarded at RIA-005 mostly contain macroscopic and/or microscopic evidence for use along their edges and surfaces. Tool size and shape varies

widely, and many broken flakes were selected for tool use ($n = 33, 56.9\%$).

Usewear and residue analysis

All >10 mm flakes from RIA05-885878 were inspected for usewear and 18 artefacts were sampled for residues based on microscopic inspection.

Usewear was identified on a large proportion of the tool assemblage (Table 8.23), with polish dominating

the usewear types (Table 8.23). Although more tools were discarded during the earlier occupation phase, proportionally similar percentages of artefacts in each assemblage were discarded during the two phases (Table 8.23 and Figure 8.33).

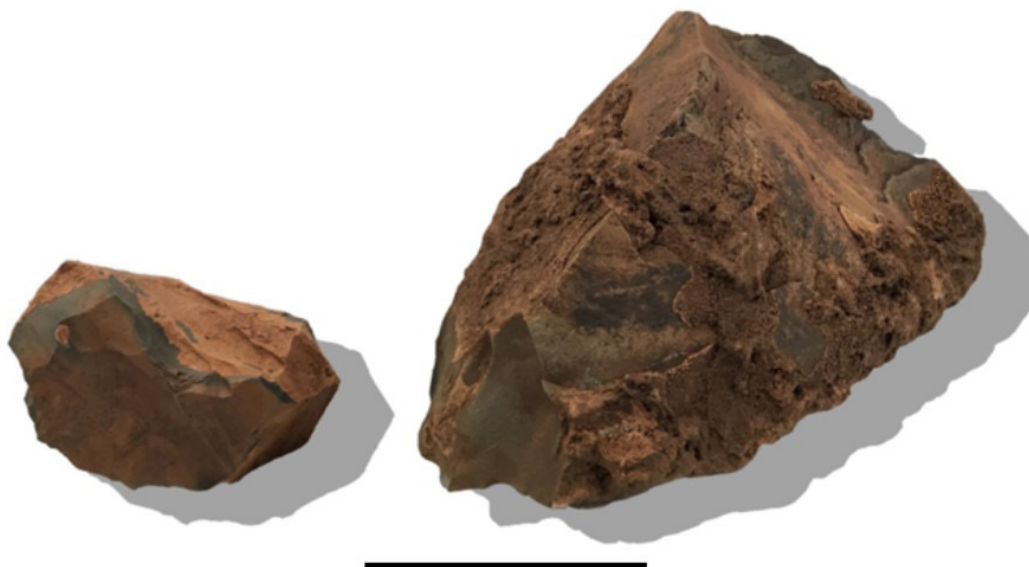


Figure 8.35. Square 885878: (left) small multiplatform core (885878-XU10-LA001) and (right) large single platform core (885878-XU05-LA001) discarded in AU2. Scale is 10 cm.

	USEWEAR		NO USEWEAR	
	N	%	N	%
AU1	20	64.5	11	35.5
AU2	38	77.6	11	22.4
<i>Total</i>	<i>58</i>	<i>72.5</i>	<i>22</i>	<i>27.5</i>

Table 8.23. Square 885878: stone artefacts with evidence for use.

		MACROSCOPIC EDGE WEAR		POLISH		SHALLOW EDGE SCARRING		STRIATIONS		EDGE ROUNDING	
		N	%	N	%	N	%	N	%	N	%
AU1	Y	10	32.3	14	45.2	3	9.7	4	12.9	1	3.2
	N	21	67.7	17	54.8	28	90.3	27	87.1	30	96.8
AU2	Y	22	44.9	27	55.1	5	10.2	7	14.3	4	8.2
	N	27	55.1	22	44.9	44	89.8	42	85.7	45	91.2
<i>Total</i>		<i>80</i>		<i>80</i>		<i>80</i>		<i>80</i>		<i>80</i>	

Table 8.24. Square 885878: presence and absence of usewear types identified on 80 >10 mm flakes.

	TESTED		NOT TESTED		PLANT FIBRES	POSITIVE BLOOD TESTS
	N	%	N	%		
AU1	5	16.1	26	83.9	15	0
AU2	13	24.5	41	75.5	121	1
<i>Total</i>	<i>18</i>	<i>21.4</i>	<i>67</i>	<i>79.7</i>	<i>136</i>	<i>1</i>

Table 8.25. Square 885878: proportion of artefacts tested for residues.

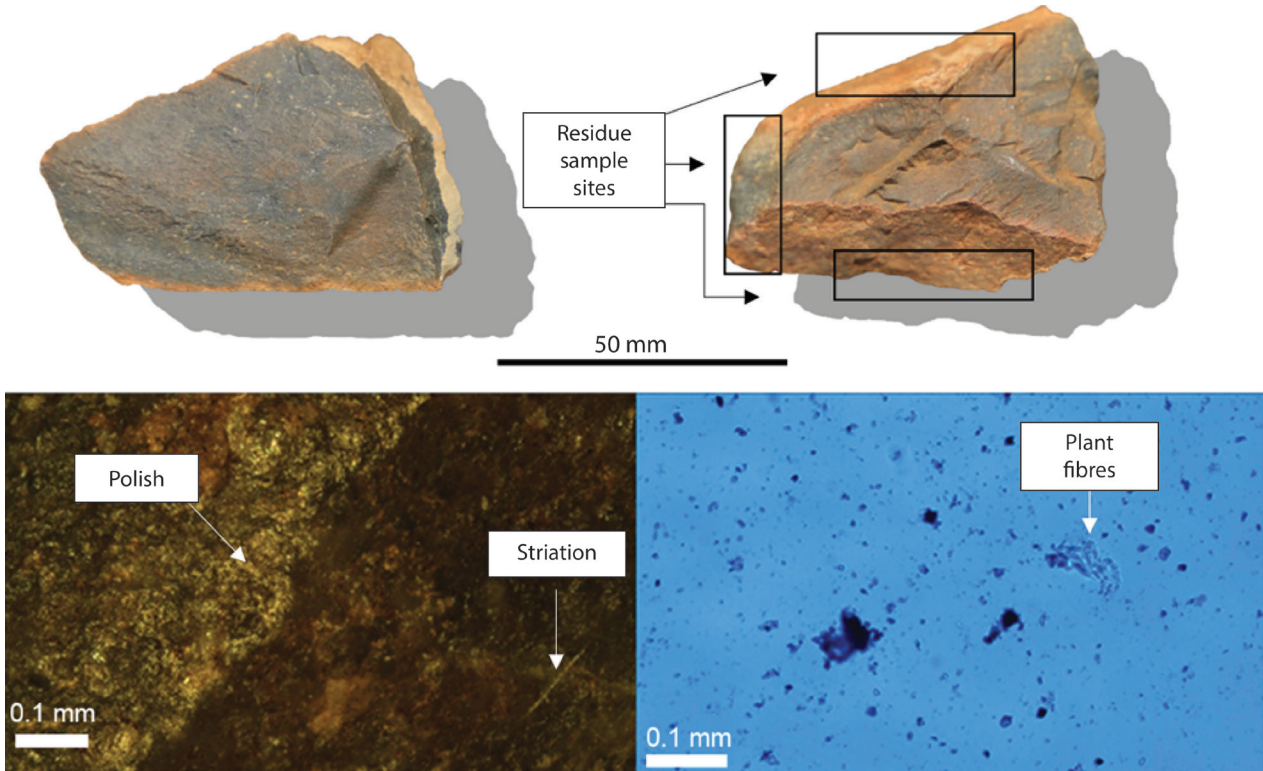


Figure 8.36. Square 885878 artefact XU04-LA001: (bottom left) example of polish, (top right) the sampled edges and (bottom right) the recovered plant fibres from these edges. Note that the darker objects are non-soluble minerals and the plant fibres are see-through blue. Scale is 50 mm.

Eighteen of the 80 flakes with usewear from 885878 were tested for plant fibres and blood. All were found to be positive for plant fibres and a single artefact tested positive for blood (Table 8.25 and Figure 8.37). The plant

fibres recovered show a wide variation in morphology and species (Figure 8.39); however, the fibre to artefact ratio demonstrates a decrease in the number of fibres present on the artefacts through time (Table 8.25 and Figure 8.34).

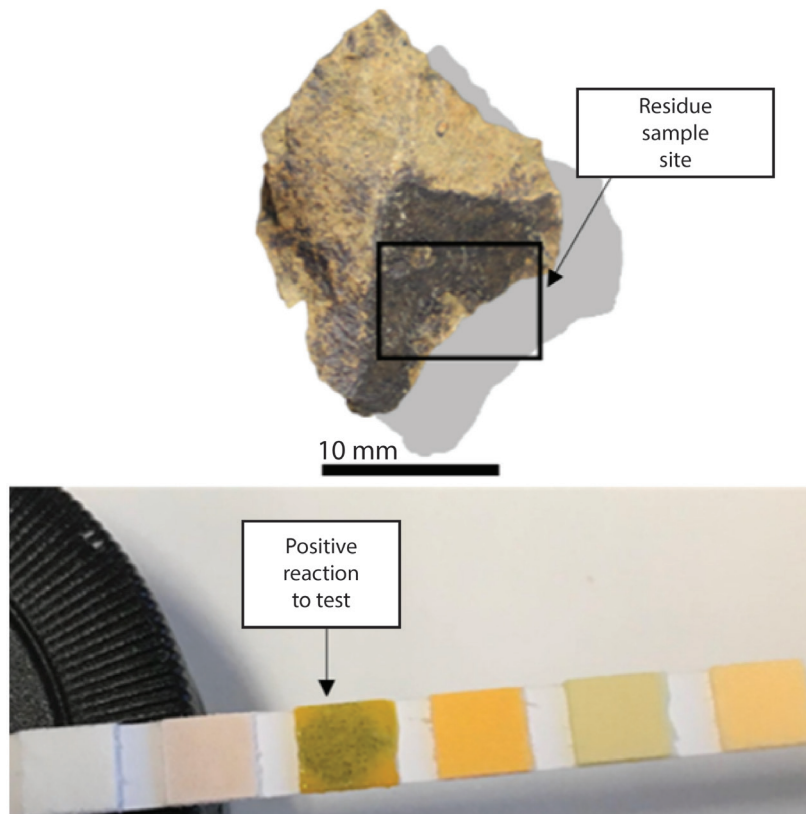


Figure 8.37. RIA05-885878 artefact XU10-LA001, showing (top) the residue sampling site and (bottom) the green reaction indicating a positive trace blood test. Scale is 10 mm.

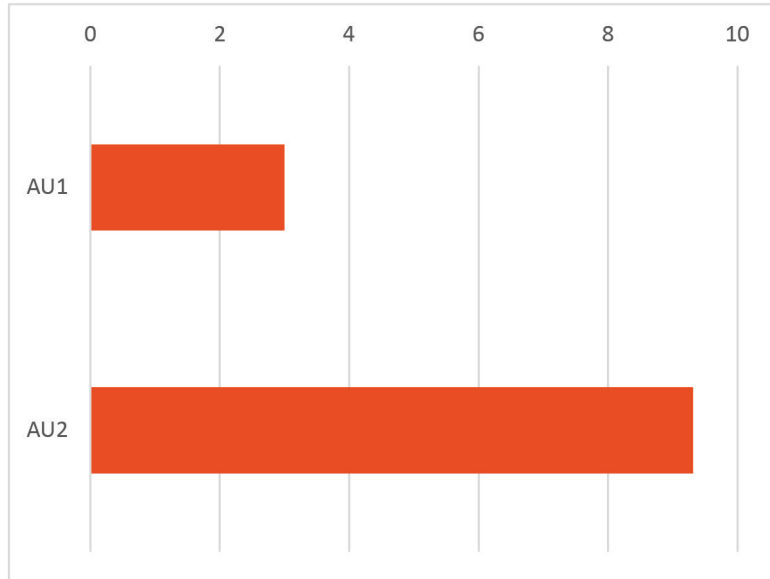


Figure 8.38. Square 885878: fibre to artefact ratio showing the decline through time.

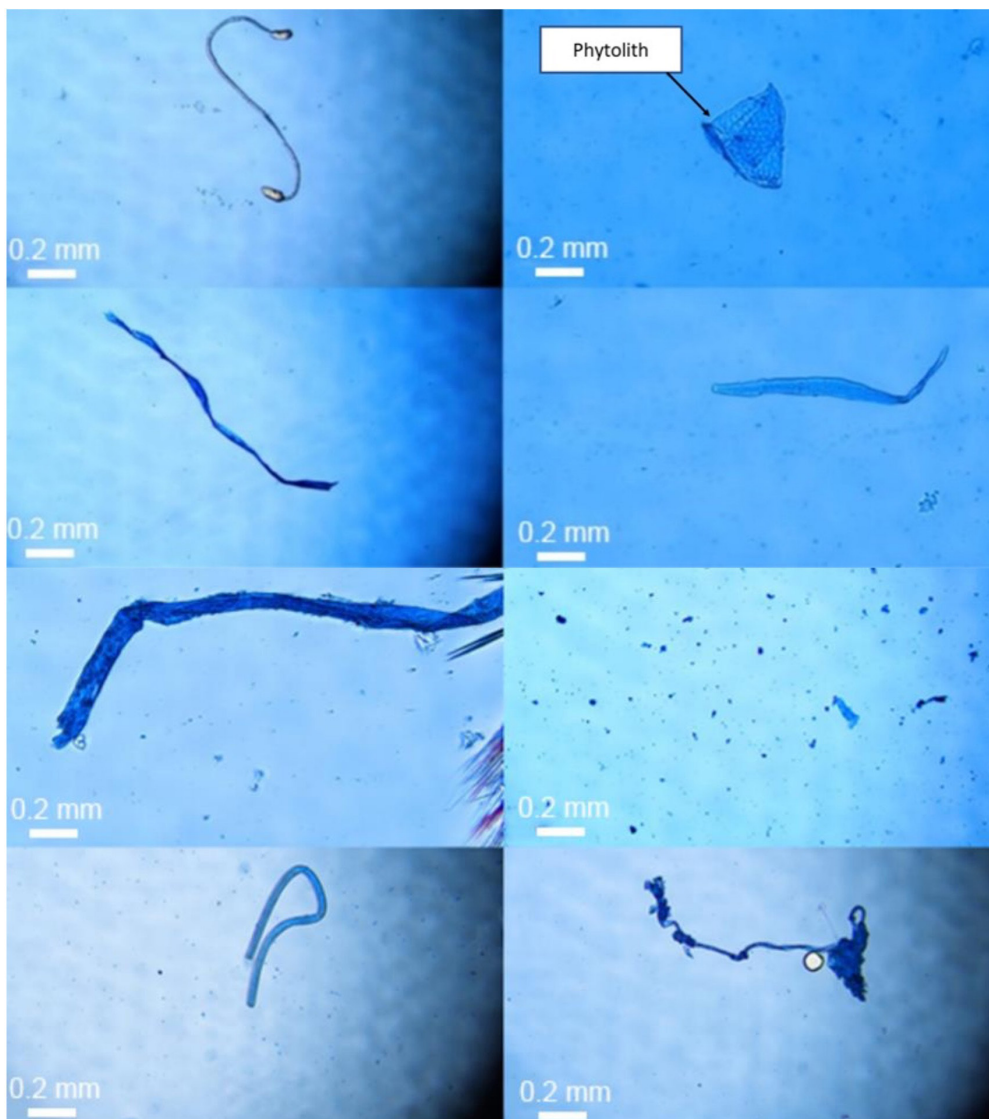


Figure 8.39. Square 885878: variation in recovered plant fibre morphology and species. Note the possible phytolith in the top right.

Discussion

The RIA05-885878 assemblage reveals that Aboriginal people began using this site around 8,500 years ago. At this time, the coastline had almost reached what is now Rosemary Island, which was still attached to the coastal landmass. People consumed small quantities of shellfish brought from mangrove forests located at least three kilometres distant (Semeniuk 1993) and quarried local gabbro to manufacture stone tools.

Stone artefact densities infer that occupation intensity was relatively more intensive and/or frequent in the last millennium compared to the Early Holocene occupation period, with the density per cubic metre suggesting comparatively higher stone artefact discard during the last 1,000 years.

Usewear and residue analysis shows that plant processing was an important activity for the earliest Aboriginal people occupying this site. Without a local reference collection, we cannot identify exactly what plants have been processed with these stone tools. However, the variability found in the tools indicates that plant processing activities involved multiple plant species. Phytoliths (that occur in high concentrations in fruits,

leaves and silicon-rich grasses; Shakoor et al. 2014: 11) have also been identified on several artefacts. Plants were an important resource that were processed here during the Early Holocene. One artefact tested positive to blood. This may have been from processing animal flesh, although no cellulose was identified amongst the residues. This blood residue may also have resulted from the person using the tool having cut themselves.

When people returned to the site in the last millennium, they continued to use locally sourced gabbro to produce their stone tool kit and to use these stone tools to process plant material. The variety of plants processed decreased in this period and plants were processed with less intensity. This matches the decreasing presence of shellfish in the upper layers and supports an interpretation of groups only using this inland waterhole on a seasonal basis in the most recent past. More ephemeral site visits during this recent period is supported by decreasing lithic manufacture/use, less shellfish consumed, and less art produced at this time (see the discussion about contrast state conditions at this site, in Chapter 7).

Rosemary 8 and Wadjuru Pool – Sample Area 4

Three test excavations were undertaken in Area 4 (Figure 8.40). Two of these were excavated on the site initially known as Rosemary 8 (DPLH 11773; Berry 2018) and the other was excavated at Wadjuru Pool. Since our systematic recording has

been completed, Square 253614 has been reassigned to Site MLP-RI043) in keeping with the approach whereby all heritage items within a 25 m radius of each other are designated a site.

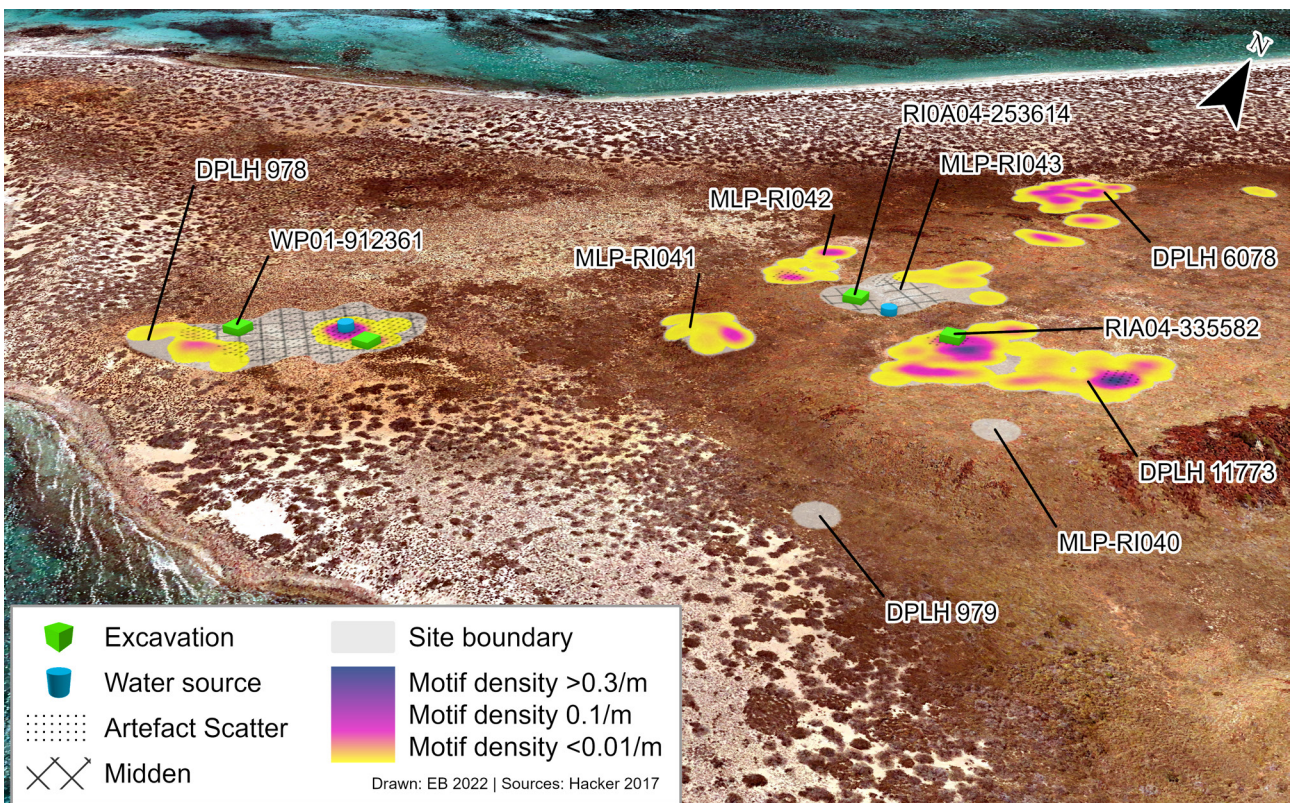


Figure 8.40. Location of all three test squares in Sample Area 4, shown with the recorded engraved motifs.

Rosemary Island 8

Rosemary Island 8 (also referred to as RM8 and DPLH 11773) was initially recorded by Virilli and Dix in 1979 (DPLH site records). Their early site record noted engravings, 12 grinding patches and 35 standing stones. Although their original record of the archaeology is an underestimation, their locational information and photographs indicate that this is the same site. Complex habitation evidence includes grinding patches on the flat gabbro platforms and a dense *Terebralia* sp. shell midden with lithic material scattered across the site. Our site designation process has identified that the two squares excavated here are separate sites (i.e. there is a 25+ m

gap in archaeological evidence between the two sites). Rosemary Island 8 measures c. 140 m N–S by 155 m E–W (Figure 8.41). A 50 cm x 50 cm square – 335582 (RM8 335E) – was excavated here by Meg Berry and Jacqueline Matthews (Berry 2018) within a circular stone feature on Platform 1 (Figure 8.41). These excavations were initially sorted and analysed by Meg Berry (2018). The lithics have been re-analysed by Wendy Reynen to ensure continuity of lithic description for the current analyses. We rely on, and reproduce here, the shellfish sorting results from Berry's (2018) analysis.

Rock art and stone features

Our current investigation of the site has recorded an extensive engraving site complex across six horizontal platforms with several circular stone features and many

standing stones (see McDonald and Berry 2016). A total of 438 panels were recorded across the six platforms, and a total of 643 motifs were recorded by the project.

MOTIF CLASS	TOTAL MOTIF COUNT	% FREQUENCY
Anthropomorphic	80	12.4
Geometric	250	38.9
Other	91	14.2
Tracks	139	21.6
Zoomorphic	83	12.9
<i>Total</i>	<i>643</i>	<i>100</i>

Table 8.26. Site DPLH 11773 motif classes.

Square RIA04-335582

A 50 cm x 50 cm test excavation (RIA04-335582) was placed within a circular clearing/enclosure (recorded as RIA04-2018-EF001-02 in the CRAR+M database: see Berry 2018: Figure 9.50). This stone structure is located amongst engravings at the southern end of the most westerly flat bedrock platform (Platform 1) where there is also extensive evidence of grinding (Figure 8.42) and an extensive stone artefact scatter, which continues into the surrounding spinifex. A standing stone is propped

near the westerly entrance to the structure. The surface cultural manifestation within the structure included stone artefacts and weathered *Terebralia* shells. The deposit within the stone structure is trapped within a shallow depression on the bedrock surface (Figure 8.43). The structure's stone walls lie directly on the platform surface and are only partially encased in deposit at a slightly downslope pocket at the structure's (western) margin.

Stratigraphy and dating

This test square involved removing the thin veneer of deposit (c. 10 cm deep) in three 2–5 cm XUs. Surface material was collected separately. The deposit comprises a compact reddish grey sediment and calcium carbonate

concretions surrounding shells and artefacts, fusing many together (Figure 8.43). This single stratigraphic unit is analysed as a single analytical unit.

XU	DEPTH BELOW SURFACE (CM)	EXCAVATED WEIGHT (KG)	ROCKS DISCARDED (KG)
1	4	7	3.5
2	8	33.2	14
3	10	3	2
Total		43.2	19.5

Table 8.27. Square RIA04-335582: cultural material weights. The XU1 stone artefact weight includes surface artefacts from the square. Figure 8.41. DPLH 11773 with Square 335582 and RIA-043 with Square 253614 showing density of rock art, stone structures and other features.



Figure 8.42. Square 335582 within the stone structure #4 on Platform 1 during excavation (drone footage Nik Callow).

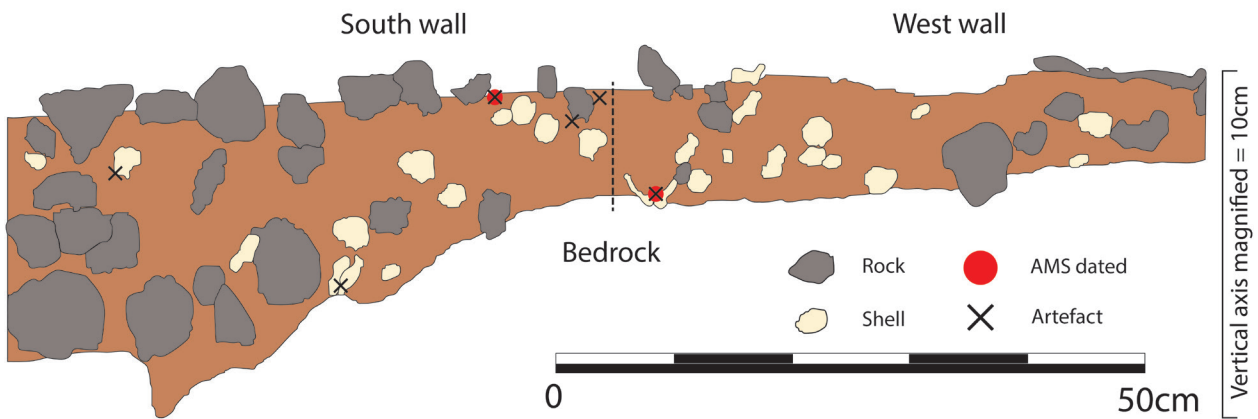


Figure 8.43. Square 335582 (left) at the completion of excavation showing the southern baulk and (right) stratigraphic section of the southern and western baulks (from Berry 2018).

Two radiocarbon determinations were made on *Terebralia* sp. and *Melo amphora* samples (Table 8.28). These determinations reveal a shallow Early Holocene

occupation between 8,000 and 7,000 calibrated years ago.

This dry-stone constructed stone feature has

been built on a horizontal bedrock platform. The dated structure is one of four similar structures, though this is the most clearly defined. These dates are interpreted as an age estimate for the use of the stone feature and therefore a minimum age for its construction. The simi-

larities between this and the nearby midden excavation sequences indicate that this landscape was first occupied intensively just before c. 8,000 calibrated years ago.

LAB CODE	SAMPLE TYPE	% MODERN CARBON (PMC 1 σ ERROR)	CONVENTIONAL RADIOCARBON AGE (YRS BP 1 σ ERROR)	CALIBRATED AGE RANGE (95.4%) (CAL. BP)	MEAN CALIBRATED AGE (CAL. BP \pm 2 σ ERROR)	DEPTH BELOW SURFACE
OZR811	<i>Terebralia</i> sp.	38.52 \pm 0.15	7,665 \pm 35	8,161–7,962	8,063 \pm 108	2 cm
OZR812	<i>Melo amphora</i>	42.35 \pm 0.17	6,900 \pm 35	7,434–7,262	7,355 \pm 88	6 cm

Table 8.28. Square 335582 radiocarbon determinations (from ANSTO).

Bayesian analysis

A sequence depositional was used (Bronk Ramsey 2008, 2009a) to model the Rosemary 8 chrono-stratigraphy (Table 8.24). Dates were ordered as a single phase given the single stratum and the likelihood of intra-strata movement given the depth/age inversion. Boundaries which represent the chronological 'beginning' and 'end' of the deposit were inserted, and to assess the likelihood of any date being an outlier (Bronk Ramsey 2009b).

Bayesian analysis models that this stone structure on Platform 1 was occupied from 8,470–7,730 cal. BP until 7,210–6,560 cal. BP (Table 8.29 and Figure 8.44). This sequence is well supported by the outlier analyses. Each date has <3% chance of being an outlier and all dates return high agreement index results ($A_{model} = 101.1$; $A_{overall} = 99.4$).

NAME	68.2%		95.4%		SUM. STATISTICS			INDICES	
	FROM	TO	FROM	TO	μ	σ	M	AI	OP
Boundary: Deposit Surface	7,210	6,460	7,260	4,990	6,590	570	6,800		
Phase: Rosemary 8									
OZR811	7,910	7,740	7,980	7,640	7,810	100	7,810	97.8	95.1
OZR812	7,220	7,040	7,300	6,930	7,120	110	7,120	99.7	95.4
OZR810	7,540	7,390	7,590	7,300	7,450	80	7,450	101	96.1
Boundary: Deposit Base	8,470	7,730	9,860	7,680	8,330	550	8,130		

Table 8.29. Bayesian analysis results for Square 335582.

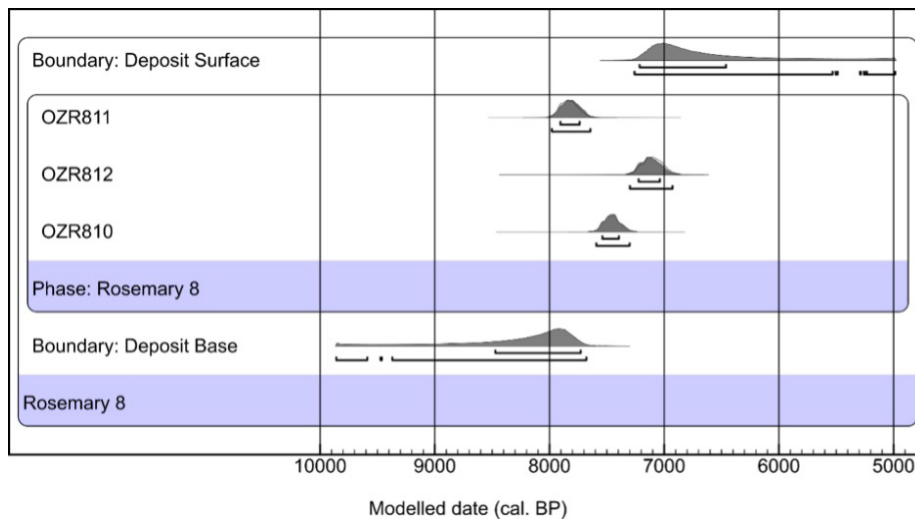


Figure 8.44. Square 335582 Bayesian analysis results.

The excavated assemblage

The excavated assemblage is predominantly (4.9 kg) shellfish (Table 8.30). Stone artefacts contribute a relatively small proportion (623.1 g) of the assemblage. There were a few (9.3 g) unidentifiable bone fragments. Many artefacts and shell were fused together with shell

by a calcium carbonate crust. This combined material weighed almost 1.6 kg. Because this carbonate matrix could not be easily separated from the cultural material, its presence is noted – but the analysed weights exclude this material.

XU	AU	SHELL	STONE ARTEFACTS	BONE	ORGANICS	ENCRUSTED SHELL & STONE ARTEFACTS	TOTAL
1	1	1,032.4	474.5	6.3	0.8	242.2	1,699.70
2	1	3,884.8	116.1	2.9	-	1,302.2	5,305.90
3	1	40.0	32.5	-	-	23.3	95.80
Total		4,957.1	623.1	9.3	0.8	1,567.7	7,101.50

Table 8.30. Square 335582: cultural material weights (in grams). The XU1 stone artefact weight includes surface artefacts from the square.

Shellfish remains

Terebralia sp. dominates (98%) the 4.9 kg of excavated and identifiable shellfish remains. Small quantities of *Melo amphora*, *Saccostrea* sp., *Telescopium telescopium* and *Acthopleura gemmata* also occur within the assemblage (Table 8.31).

SHELLFISH SPECIES (5 MM)	TOTAL WEIGHT (G)	% OF ANALYSED SHELLFISH
<i>Terebralia</i> sp.	4,541.40	98.1%
<i>Telescopium telescopium</i>	19.80	0.1%
<i>Melo amphora</i>	58.60	1.2%
<i>Saccostrea</i> sp.	6.11	0.1%
<i>Acanthopleura gemmata</i>	4.89	0.1%
	4,630.80	100%

Table 8.31. Square 335582 identified shellfish species.

Stone artefacts

One hundred and forty-nine flaked stone artefacts were recorded at 335582 (Table 8.32). Only a small proportion of this assemblage (nine pieces) is microdebitage (<10 mm). Projected artefact density (i.e. of a 1 m x 1 m x 1 m square) is 6,320 artefact/m³. The stone assemblage was analysed as a single analytical unit.

Assemblage composition

Lithic material identifications at 335582 were determined through macroscopic and microscopic comparison of artefacts with those from other Rosemary Island sites that have been classified using pXRF (see Chapter 2). All artefacts discarded at 335582 were made on locally available gabbro, volcanoclastic siltstone and a silicified material (Table 8.32 and Figure 8.45). The contact between gabbro and volcanoclastic siltstone could be seen in a single flake (Figure 8.46), indicating that the surface sources of these different materials were not likely to be separated by any great distance.

RI GABBRO	%F	VOLCANICLASTIC SILTSTONE	%F	SILICIFIED	%F	TOTAL
56	37.6	74	49.7	19	12.8	149

Table 8.32. Square 335582: 4 mm and 2 mm stone artefact assemblage showing material frequency.

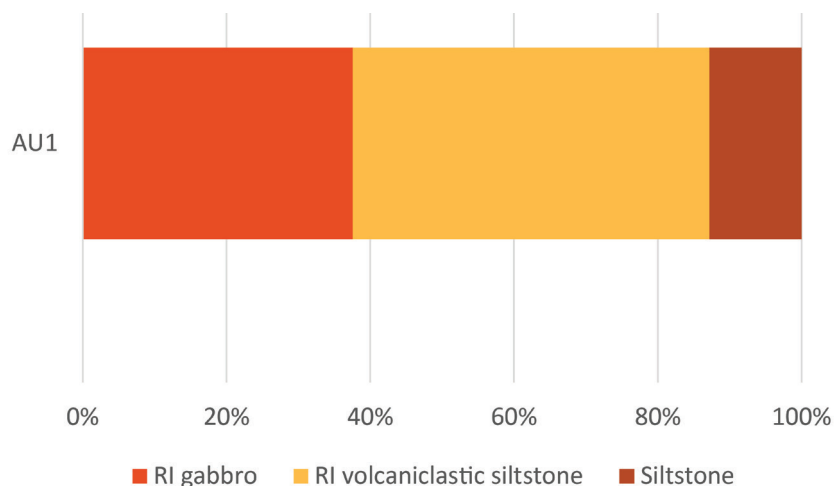


Figure 8.45. Square 335582: proportions of raw materials in analytical unit.



Figure 8.46. Square 335582 artefact XU01-LA090 showing contact of gabbro and volcanoclastic siltstone within the same artefact. Scale is 10 mm.

Most of this lithic assemblage comprises complete and broken flakes (Table 8.33). Three tools were recorded: one made on each of the site's lithic materials.

ARTEFACT TYPE MATERIAL	BROKEN FLAKE		COMPLETE FLAKE		TOOL		TOTAL		NAS TO MNA RATIO
	N	%	N	%	N	%	N	%	
Rl gabbro	35	62.5	20	35.7	1	1.8	56	40.0	1.7
Volcanoclastic siltstone	37	55.2	29	43.3	1	1.5	67	47.9	1.4
Silicified	10	58.8	6	35.3	1	5.9	17	12.1	2.0
<i>Total</i>	<i>82</i>	<i>58.6</i>	<i>56</i>	<i>40.0</i>	<i>3</i>	<i>2.1</i>	<i>140</i>	<i>100</i>	

Table 8.33. Square 335582: stone assemblage composition by frequency and proportion. Microdebitage (<10 mm) is excluded here.

Assemblage reduction

Although no cores were discarded at 335582, the flake assemblage provides some indication of reduction intensity. SDI values for gabbro and volcanoclastic siltstone are low (Table 8.34), indicating that these materials were non-intensively reduced. An absence of flaked platforms fits with this pattern. Although the average SDI value for silicified flakes is somewhat higher

than for other materials, large and overlapping standard deviation values indicate substantial overlap between all materials. Only nine flakes (16%) exhibit remnant cortex.

Most flakes discarded at the site are small: all but four artefacts have a maximum dimension <5 cm (Table 8.35). As appears typical for locally acquired materials on Rosemary Island, most flakes are squat in shape (Table 8.36).

MATERIAL	N	μ	SD
Rl gabbro	21	0.83	0.38
Volcanoclastic siltstone	29	0.98	0.38
Silicified	6	1.17	0.69

Table 8.34. Square 335582: Scar Density Index (SDI) for complete flakes (excluding flakes <10 mm)

MATERIAL	WEIGHT (G)			SURFACE AREA (MM ²)	
	N	μ	SD	μ	SD
Rl gabbro	21	2.8	4.8	454.8	412.4
Volcanoclastic siltstone	29	6.4	15.8	645.6	750.5
Silicified	6	7.8	13.6	708.5	734.2

Table 8.35. Square 335582: weight and surface area for complete flakes (not including flakes <10 mm).

MATERIAL	N	μ	SD
Rl gabbro	21	0.9	0.4
Volcanoclastic siltstone	29	1.2	0.5
Silicified	6	1.1	0.5

Table 8.36. Square 335582: elongation ratio for complete flakes (not including flakes <10 mm).

Tool selection and use

There are three tools discarded at Square 335582: a retouched volcaniclastic siltstone flake (SURFACE-LA001) and two used flakes made on a silicified material (XU01-LA060) and a medium-grained gabbro (XU02-LA103). The retouched complete flake is markedly larger

(47.7 g, 3,055.3 mm² surface area) than most flakes discarded at the site (Table 8.35). However, the utilised silicified flake is small (0.54 g), indicating variation in tool size preferences and most likely a variety of tasks being completed here.

Usewear and residue analysis

The three tools from Square 335582 were analysed for microscopic usewear and residues.

Artefact SURFACE-LA001 (Figure 8.47) has shallow edge scarring on both dorsal margins and the right ventral margin. A small amount of polish was also located along the right ventral margin where there is a black residue. Residues were extracted from two locations on the right

dorsal margin and one location from the right ventral margin. Analysis confirmed the presence of plant fibres; however, these were sparsely scattered (n = 10), very small (<0.05 mm), non-diagnostic and likely unrelated to use. The residue from the right dorsal margin tested positive for trace amounts of non-haemolysed blood.

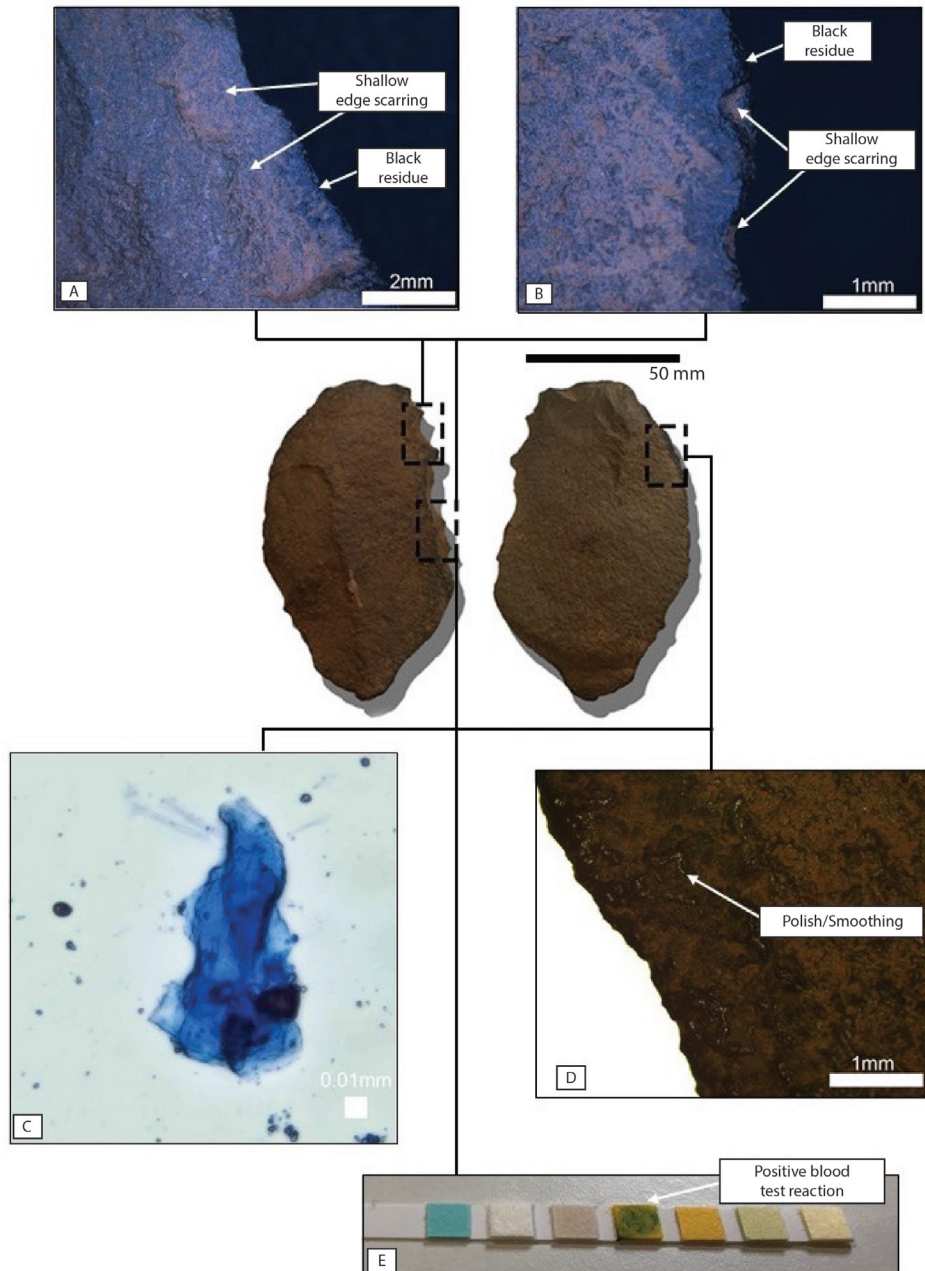


Figure 8.47. Square 335582 artefact Surface-LA001: shallow edge scarring and black residue on the right dorsal margin (A and B) and polish/smoothing of the residue on the right ventral margin (D). Typical small non-diagnostic plant residue (C) and a positive non-haemolysed blood test (E). Scale is 50 mm.

Usewear and residue analysis indicates that this SURFACE-LA001 artefact was used in two stages. First, it was used to process material that resulted in notable macroscopic edge damage and shallow edge scarring along the right dorsal margin. This type of usewear is broadly consistent with the processing of medium to hard material, such as animal bone (Claud et al. 2019). The artefact was then discarded for long enough for a dark residue to develop, overlaying the shallow edge scarring from previous use. It was then picked up again and used in a way that smoothed and polished the high points of the developed residue. Given that this artefact was retrieved from the surface of the square, this reuse could have occurred either in the terminal/ later stages of the main occupation at 335582, between 8,000 and 7,000 years ago, or later. While this interpretation is supported by the relative absence of plant fibres and presence of intact blood cells, definitive functional analysis requires material-specific experiments to be conducted.

Artefact XU01-LA060 is a small, dark-coloured silicified

fragment (Figure 8.48). Usewear analysis revealed shallow edge scarring along both the ventral and dorsal margins, light polish covering approximately 70% of the ventral surface, and light rounding of the high points on the dorsal surface.

Residues were extracted from two locations on the dorsal surface. Analysis confirmed the presence of plant fibres and silica on the artefact. One of the larger fibres is diagnostic and appears to be a phytolith (which occur in leaves, seeds and fruits, and the protective casings of grass seeds; Haynes 2017). The artefact tested negative for blood.

Usewear and residue analysis indicates that artefact XU01-LA060 was most likely used to process a variety of plant materials. Since polish is the dominant usewear and the artefact tested negative for blood, it is likely that it was primarily used to process plant material. The step terminations of the shallow edge scarring suggest that the artefact was also used on a harder material (Claud et al. 2019), indicating that this artefact was part of a multi-use toolkit.

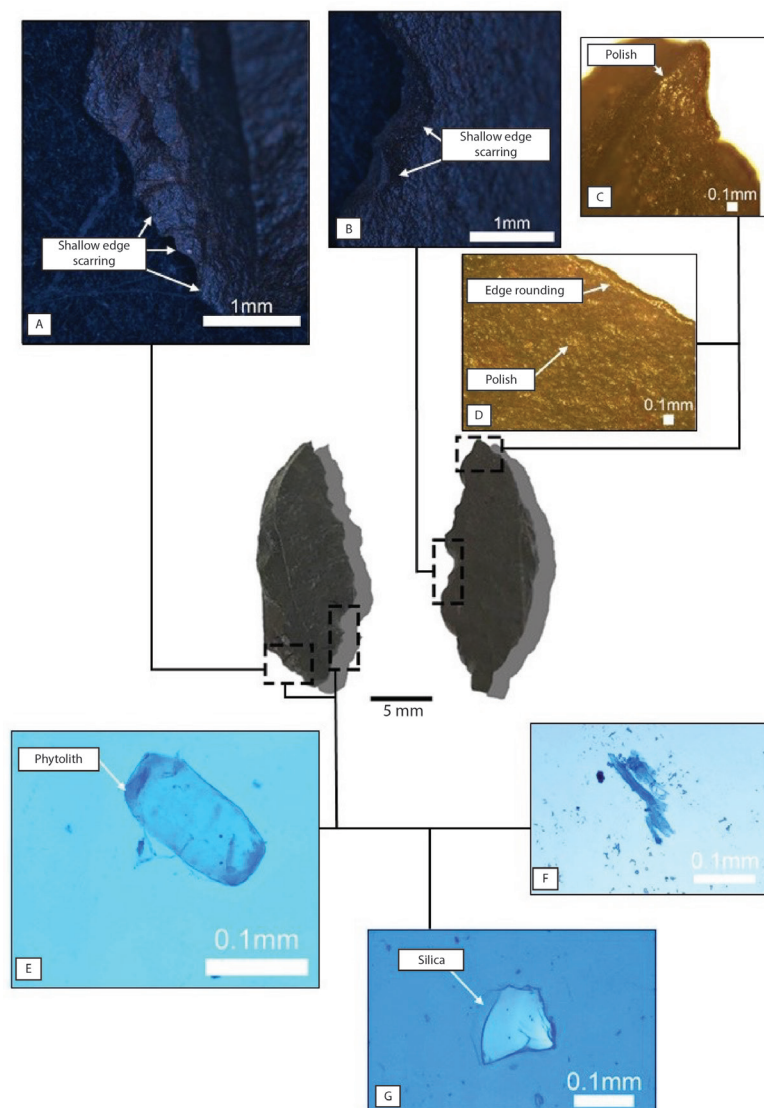


Figure 8.48. Artefact XU01-LA060. Shallow edge scarring on the left dorsal (A) and ventral (B) margins and polish and edge rounding on the ventral margin (C, D). Examples of residues are shown, including a phytolith (E), a larger non-diagnostic fibre (F) and a fragment of silica (G). Unlabelled scale is 5 mm.

Artefact XU02-LA103 is a medium-grained gabbro flake with desert varnish covering approximately 80% of the ventral surface and 15% of the dorsal surface (Figure 8.49). Usewear analysis revealed polish and striations, some of which are directional, and smoothing of high points of the varnish on both sides of the artefact. Residues were extracted from the left and right ventral margins. No plant fibres were recovered and the artefact tested negative for blood.

Analysis of artefact XU02-LA103 indicates that it was first used in a way that created traces of use on

the ventral surface. The artefact was then discarded for a long enough period to develop a layer of desert varnish which overlays the traces of use on the ventral surface. It is not possible to determine whether the usewear on the dorsal surface was created during the first or second stage of artefact use. The usewear on the ventral surface overlying desert varnish indicates clear additional phases of artefact use. The absence of blood and plant material on this artefact indicates either that it was used to process another type of material or that residues have not been preserved on the artefact.

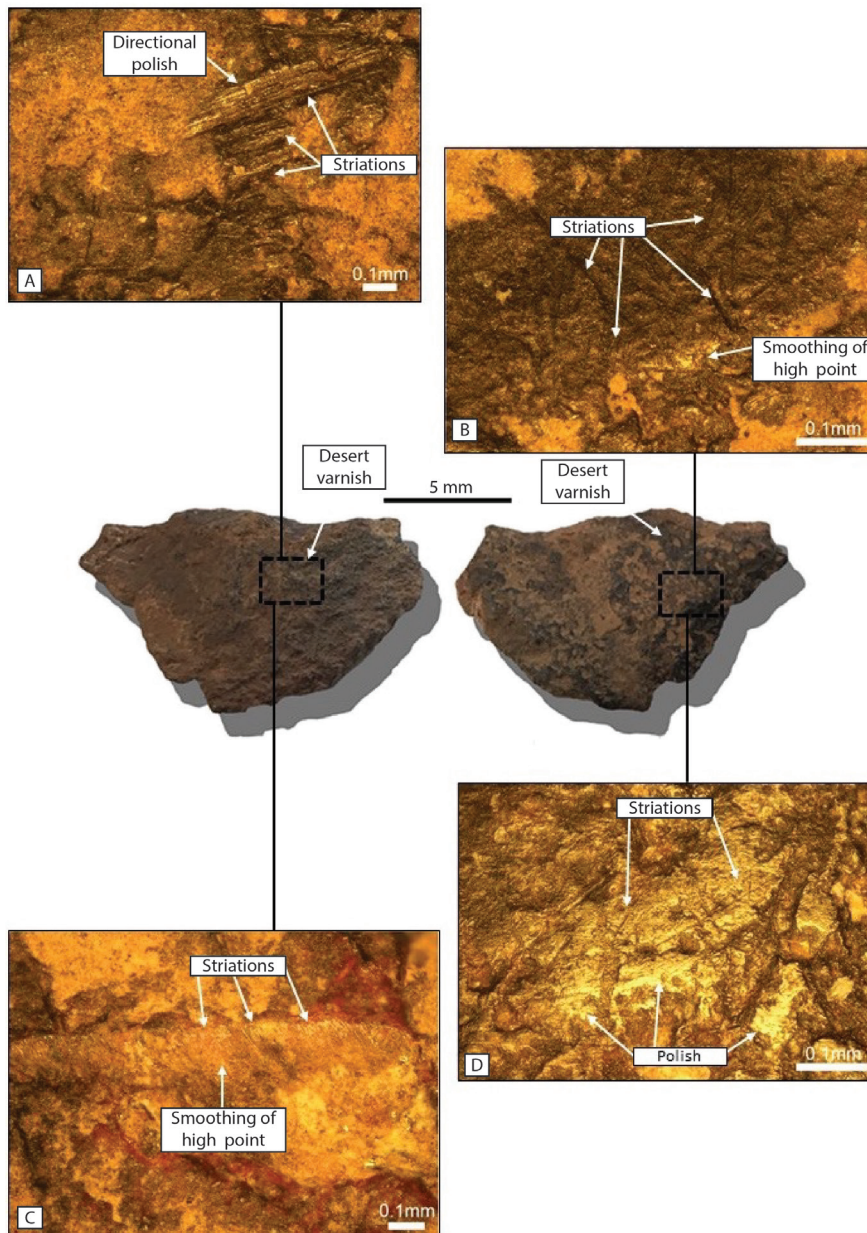


Figure 8.49. Artefact XU02-LA103 showing directional/non-directional polish (A, D), smoothing of high points (B, C) and striations. Scale is 5 mm.

Discussion

The stone assemblage located inside the stone structure at Rosemary 8 is locally sourced and associated with a predominantly mangrove shellfish assemblage which accumulated

between c. 8,000 and 7,300 cal. years BP. This occupational evidence correlates well with the midden material located downslope adjacent to a waterhole (now Site RIA-043).

Locally available stone was used expediently for stone tool manufacture. Microscopic analysis of three tools discarded at the site indicate that these were used to undertake various activities, including plant and animal processing.

The construction of these stone features during the Early Holocene has been argued as evidence for the demarcation and structuring of social space within a dramatically changing environment (McDonald and Berry 2016: see also Lourandos 1993; O'Connor 1999: 115–125 for similar arguments in the Late Holocene). Individuals and/or groups were accessing the nearby resource-rich mangrove stands and bringing their food back to the

Rosemary 8 landscape continuously over a 1,000-year period. Population pressure (Williams et al. 2015a) as the coastal plain was drowned by rising seas (Ward et al. 2013) may have influenced this development of more structured social organisation at the local level. The further modification of this landscape was achieved by the extensive engraving activity across the site complex as well as the construction of stone features on several other platforms across the site. At the eastern end of the site (Platform 6) this landscape modification was supplemented by the erection of almost 100 standing stones. The rock art at this site complex is discussed in more detail in Chapter 7.

Square RIA04-253614

To the northwest of the DPLH 11773 site complex are two low rises bisected by an ephemeral drainage line with a calcium carbonate encrusted pool (now largely dry). Both of these hillocks are densely covered by a *Terebralia* sp. midden and a scatter of stone artefacts concreted in place by calcium carbonate. The engravings, lithics and grinding patches on adjacent platforms of DPLH 11773 to the southwest are located more than 25 m from this

midden site, and hence this area has been designated a separate site number (see Figure 8.40).

One 50 cm x 50 cm test square (RIA04-253614) was located on the southern knoll of the *Terebralia* midden south of the drainage line and pool (Table 8.37 and Figure 8.50). This site was excavated by Meg Berry and assisted by Jaqueline Matthews (Berry 2018). The main details of this excavation are presented here.

Stratigraphy and dating

Two stratigraphic units were identified within Square 253614 (Figure 8.50):

SU1 (XUs 1-3) – light reddish grey (2.5YR 3/4) with gritty sand that increases in compaction with depth. At c. 16 cm below the surface there is a transition to

SU2 (XU4) – decomposing calcium carbonate concretion and rubble with few fragments of shell.

Due to extreme compaction through calcium carbonate encrustation, excavation ceased at c. 26.5 cm depth.

XU	DEPTH BELOW SURFACE (CM)	EXCAVATED WEIGHT (KG)
1	5.6	9.5
2	10.5	8.7
3	16.0	12.5
4	26.5	9.5
<i>Total</i>		<i>40.2</i>

Table 8.37. Square 253614: excavation weights for deposit.

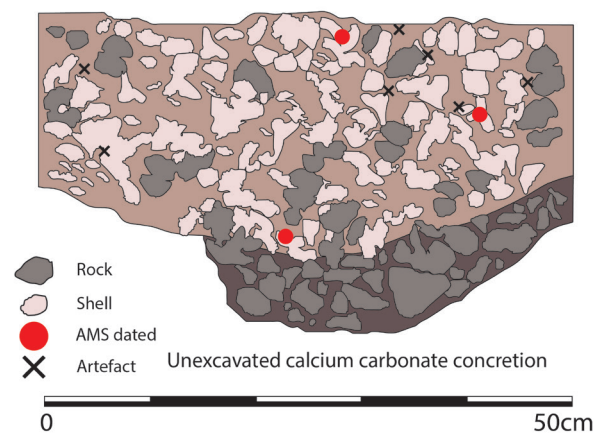


Figure 8.50. Square 253614 showing (left) profile of southern baulk and (right) stratigraphy (from Berry 2018: Figure 9.39).

Radiocarbon dating

A single *Terebralia* sp. specimen from each XU was AMS radiocarbon-dated (at Waikato Radiocarbon Laboratory or ANSTO Radiocarbon Laboratory). The sequence was

divided into three AUs based on dates, assemblage content and stratigraphy (Figure 8.50). AU3 represents the earliest pulse of midden accumulation. While

the upper two analytical units are very close in age, differences observed in stone artefact accumulation

suggest that it is worth distinguishing between these occupation-events.

LAB CODE	XU	AU	DEPTH (CM)	DATE ERROR (YRS BP 1σ ERROR)
Wk43057	1	1	2	6,880 20
OZ810	2	2	6.5	7,265 30
Wk43058	3	2	14	7,183 22
Wk43059	4	3	19	7,615 21

Table 8.38. Square 253614: radiocarbon determinations.

Bayesian analysis

A sequence depositional model was used (Bronk Ramsey 2008, 2009a) to model this midden’s chrono-stratigraphy (Table 8.39). Dates were ordered according to their depths interspersed by boundaries to represent the analytical units given the shallow deposit was in generally good stratigraphic order with little likelihood of intra-strata movement.

This model estimates that Square 253614 was first occupied at 8,070–7,680 cal. BP until 7,200–6,820 cal. BP. This sequence is well supported by the outlier analysis, with each date having <4% chance of being an

outlier, and all dates return high agreement index results ($A_{\text{model}} = 86.3$; $A_{\text{overall}} = 90.2$). Given how close these dates are in time, it may also be appropriate to model this as a single sequence without inserting boundaries. Regardless, this model would produce very similar results to those illustrated in Table 8.39 (i.e. the surface and base boundaries would return similar values). The entire accumulation of this midden occurred within a millennium between 6,970 and 7,900 cal. BP (median), with the main period of occupation (AU1 and AU2) accumulating in the latter half of this period.

NAME	68.2%		95.4%		SUM. STATISTICS		INDICES	
	FROM	TO	FROM	TO	μ	σ	M	AI OP
Boundary: Deposit Surface	7,200	6,820	7,290	6,040	6,870	330	6,970	
Wk43057	7,180	7,010	7,260	6,930	7,100	80	7,110	99.2 96.2
Boundary: AU1/AU2	7,430	7,200	7,480	7,050	7,280	110	7,300	
OZ810	7,450	7,330	7,510	7,270	7,390	60	7,390	86.6 96.4
Wk43058	7,490	7,370	7,550	7,320	7,430	60	7,430	92.4 96.2
Boundary: AU2/AU3	7,650	7,400	7,800	7,350	7,550	120	7,540	
Wk43059	7,830	7,680	7,910	7,610	7,760	80	7,760	98.4 96.3
Boundary: Deposit Base	8,070	7,680	8,820	7,590	8,000	330	7,900	

Table 8.39. Square 253614 Bayesian analysis results.

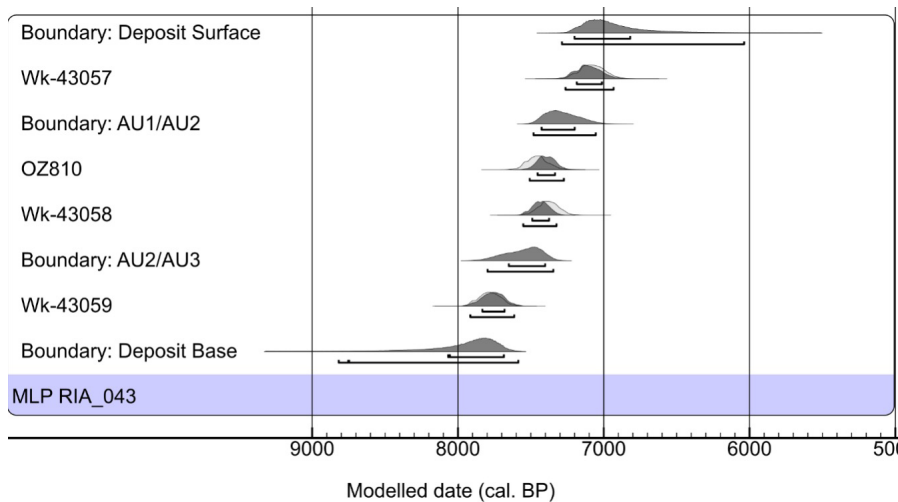


Figure 8.51. Square 253614: Bayesian modelling.

The excavated assemblage

Archaeological material consists of densely compacted shell (6.2 kg), stone artefacts (303.4 g), bone (5.6 g) and some surficial grasses, seeds and leaves (6.2 g) (Table

8.40). Bone is present only in XU1. Stone artefact weights are highest in XU1, and decline in weight and number with depth. Shell weights peak in AU2. The highly cemented

basal deposits mean that the lowest excavation unit is indicative only of the material at this level.

The sequence was divided into three AUs based on dates, assemblage content and stratigraphy. AU3 represents the earliest pulse of midden accumulation

around c. 8,000 years ago. While the upper two analytical units are very close in age, the difference in stone artefact accumulation suggests that it is worth distinguishing between these occupation-events, separated by c. 300 years.

AU	SU	XU	SHELL	STONE ARTEFACTS	BONE	ORGANICS	TOTAL
1	1	1	1,599.4	142.7	5.6	4.5	2,162.9
2	1	2	2,189.9	69.4	0	0.1	2,222.2
2	1	3	2,369.9	53.9	0	1.6	2,419.4
3	2	4	83.8	37.4	0	0.0	107.1
Total			6,243.0	303.4	5.6	6.2	6,911.6

Table 8.40. Square 253614: cultural material in each excavation unit and analytical unit. Weights in grams.

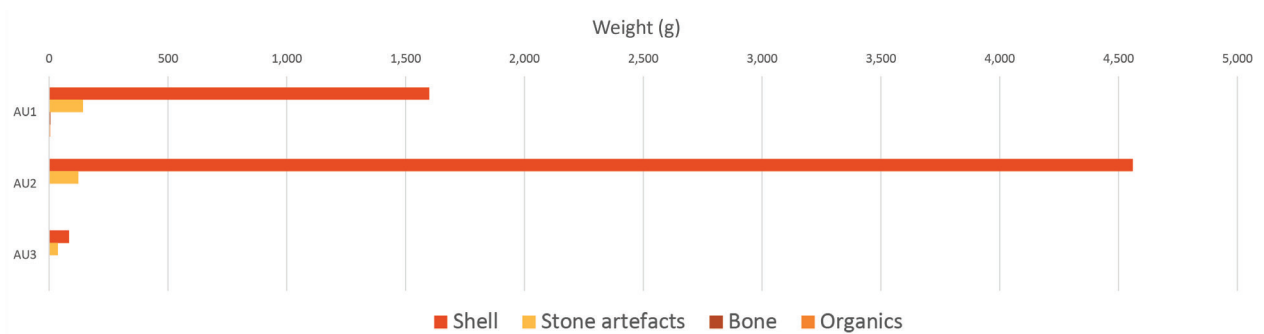


Figure 8.52. Square 253614: proportions of cultural material in each analytical unit.

Shellfish remains

The analysed shell midden is dominated (97.8%) by *Terebralia* sp. and this midden is made up almost entirely of mangrove habitat species throughout its occupation (Table 8.41). Shell breakage reflects food processing/ consumption rather than major post-discard taphonomic processes. *Syrinx aranus* (1.7%), *Melo amphora* (0.4%), *Saccostrea* sp. (0.1%) and a few limpets account for the

remainder of the assemblage. These minor species are only present within AU1 and AU2. A very small amount (2.8 g) of the mangrove-dwelling *Telescopium telescopium* was found in AU1. Small proportions of sandy intertidal shell species at c. 7,600 cal. years BP indicate larger sample sizes as well as transitional habitats at that time.

SPECIES (5 MM)	TOTAL WEIGHT (G)	%F ANALYSED SHELL	AU1	AU2	AU3
<i>Terebralia</i> sp.	5,440.2	97.8	X	X	X
<i>Telescopium</i>	2.8	0.1	X		
<i>Syrinx aranus</i>	95.3	1.7	X	X	
<i>Melo amphora</i>	19.8	0.4	X	X	
<i>Saccostrea</i> sp.	4.56	0.1	X	X	
<i>Patella</i> sp.	0.4	0.1	X	X	

Table 8.41. Square 253614: shellfish species in the three analytical units.

Stone artefacts

The 253614 stone artefact assemblage comprises 134 flaked stone artefacts (Table 8.42). Just under half of the artefact assemblage (n = 59, 44%) is microdebitage (<1 cm maximum dimension). Projected artefact density

(i.e. to a 1 m x 1 m x 1 m square) is 1,914 artefact/m³. The stone assemblage was characterised within the three analytical units outlined above, although it should be noted that these are all Early Holocene in age.

Assemblage composition

Material identifications at Square 253614 were determined through macroscopic and microscopic comparison of artefacts with those from other Rosemary Island sites that have been classified using pXRF. Most artefacts discarded

at Square 253614 were manufactured on Rosemary Island volcanoclastic siltstone, with smaller numbers of artefacts made on other locally occurring materials (quartzite, gabbro, silicified; Table 8.42 and Figure 8.53).

Most site visits occurred during the two most recent occupation phases (AU1 and AU2, Figure 8.54). Only three artefacts were discarded during the earliest phase (AU3). These were two volcaniclastic siltstone flakes and a small piece of silicified debris. While volcaniclastic siltstone is the dominant material used at the site

through all phases, artefacts made on the local gabbro become more commonly discarded through time (Table 8.42). The single broken quartzite flake was discarded at the site during the most recent phase of occupation. No silicified material occurs at the site during this time.

MATERIAL AU	QUARTZITE	%F	RI GABBRO	%F	VOLCANICLASTIC SILTSTONE	%F	SILICIFIED	%F	TOTAL
1	1	1.4	13	18.6	56	80.0			70
2			3	4.9	51	83.6	7	11.5	61
3					2	66.7	1	33.3	3
Total	1	0.7	16	11.9	109	81.3	8	6.0	134

Table 8.42. Square 253614: artefact assemblage showing material frequency by AU.

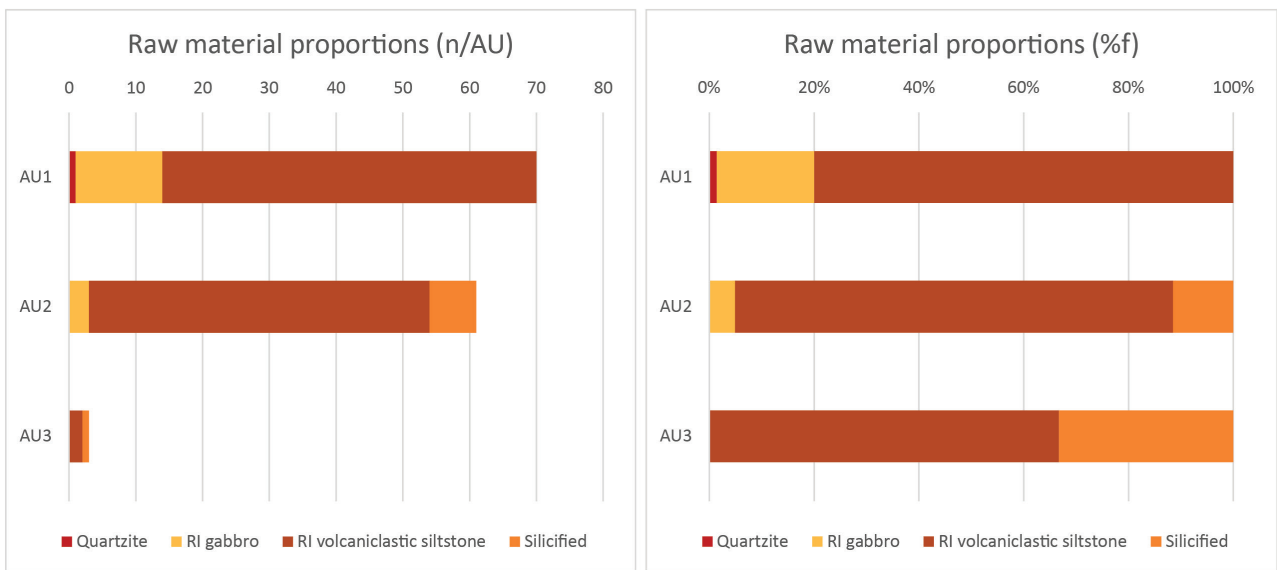


Figure 8.53. Square 253614: proportions of raw materials through the analytical units.

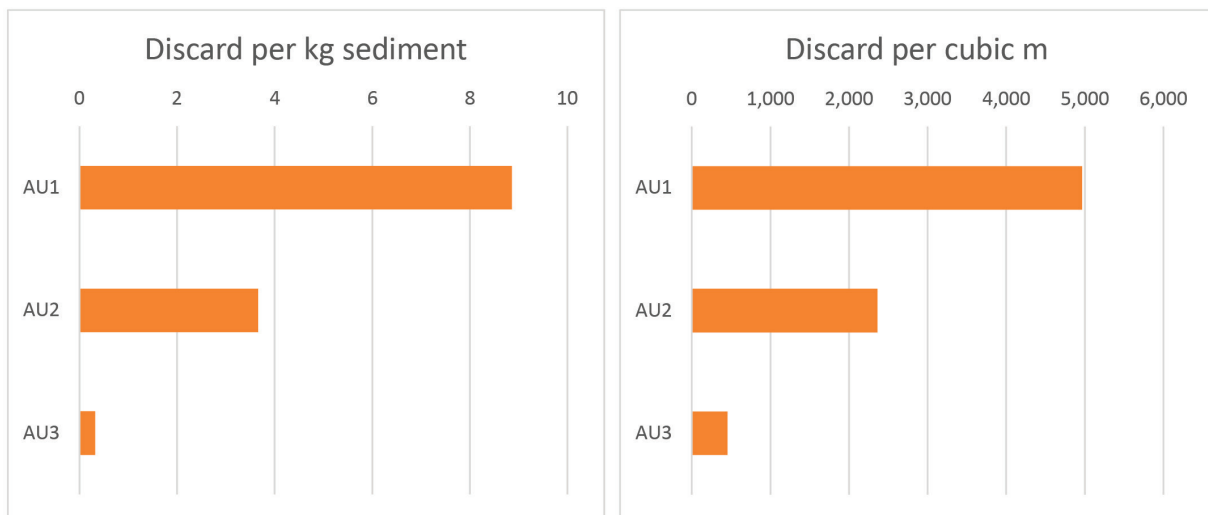


Figure 8.54. Square 253614: artefact density by AU.

Most of the stone assemblage is fragmented: more flakes are broken than complete (Table 8.43). Longitudinally broken flakes comprise the most common breakage type (n = 22, 56.4%), followed by transversely broken

flakes (n = 12, 30.8%). Together with the high proportion of debris at the site, this indicates that this was clearly a place where on-site nodule reduction was undertaken. Complete and broken flakes comprise the entirety of the

AU1 and AU3 assemblages, while a single volcaniclastic siltstone core fragment and two tools made on silicified

material were discarded during the middle occupation phase (AU2).

ARTEFACT TYPE MATERIAL	BROKEN FLAKE		COMPLETE FLAKE		CORE FRAGMENT		TOOL		TOTAL		NAS TO MNA RATIO
	N	%	N	%	N	%	N	%	N	%	
Quartzite	1	100.0	-	-	-	-	-	-	1	1.3	
RI gabbro	6	40.0	9	60.0	-	-	-	-	15	20.0	1.4
Volcaniclastic siltstone	28	52.8	24	45.3	1	1.9	-	-	53	70.7	1.5
Silicified	4	66.7	-	-	-	-	2	33.3	6	8.0	2.4
<i>Total</i>	<i>39</i>	<i>52.0</i>	<i>33</i>	<i>44.0</i>	<i>1</i>	<i>1.3</i>	<i>2</i>	<i>2.7</i>	<i>75</i>	<i>100</i>	

Table 8.43. Square 253614: stone assemblage composition by frequency and proportion. Artefacts <10 mm excluded here.

Assemblage reduction

Gabbro and volcaniclastic siltstone complete flakes both exhibit low SDI values (Table 8.44), indicating that both local and less locally available materials were similarly non-intensively reduced. No flakes have flaked or faceted platforms. Cortex is absent from all but two flakes. However, nearly half (n = 16, 48.5%) of the

complete flakes recorded at 253614 exhibit overhang removal. Overhang removal is presumed to indicate that core platforms were strengthened for more precise and successful flake removals. No marked changes in the reduction intensity of flakes occur through time.

MATERIAL	N	μ	SD
RI gabbro	9	1.23	0.49
Volcaniclastic siltstone	24	1.08	0.42

Table 8.44. Square 253614: Scar Density Index (SDI) for complete flakes (excluding flakes <10 mm).

Despite having slightly higher average SDI values, the nine gabbro flakes are substantially larger in mass and surface area than the volcaniclastic siltstone flakes (Table 8.45). In this context, flake size appears to relate

to original nodule size rather than reduction intensity. Most flakes here are 'square' in shape (Table 8.46): only two elongated flakes were recorded.

MATERIAL	WEIGHT (G)			SURFACE AREA (MM ²)	
	N	μ	SD	μ	SD
RI gabbro	9	7.0	11.0	823.2	1,080.2
RI Volcaniclastic siltstone	24	3.2	3.7	486.8	408.1

Table 8.45. Square 253614: weight and surface area for complete flakes (excluding flakes <10 mm).

MATERIAL	N	μ	SD
RI gabbro	9	1.1	0.3
RI Volcaniclastic siltstone	24	1.2	0.5

Table 8.46. Square 253614: elongation ratio for complete flakes (excluding flakes <10 mm).

The volcaniclastic siltstone core fragment (XU02-LA043) measures 50.5 mm x 31.1 mm x 20.3 mm. Two flake scars were removed from a single platform before

it was discarded. The core has a clear break, which may explain why it was discarded at this stage of reduction.

Tool selection and use

The two silicified tools found at 253614 (artefacts XU03-LA054 and XU03-LA058) are made on longitudinally broken flakes and have macroscopic and microscopic evidence for use along their edges. Although broken, these flakes are markedly larger (weight 9.13 g

and 4.59 g, surface area 1,062 mm² and 626.9 mm²) than the general flake assemblage (Table 8.45). This indicates that larger silicified flakes were preferentially selected for tool use.

Usewear and residue analysis

The two silicified artefacts from XU3 (AU2) were analysed for usewear and residue.

Usewear analysis of artefact XU03-LA054 revealed many shallow edge scars along the left dorsal and right

ventral margin and the ventral termination (n = 20; Figure 8.55). Directional polish was also located along the dorsal platform, parallel to the platform margin.

Residues were taken from the left dorsal margin and

ventral termination. Analysis detected a small number of plant fibres that were too scattered and broken to be diagnostic. However, a small cluster of tracheid cells and an unidentified fibre were recovered from the left dorsal margin. Tracheids are a type of cell which occur only in tracheophytes: ferns, gymnosperms and flowering plants (Crang et al. 2019). Of these clades, the only tracheophyte that grows on Rosemary Island and is known to have documented ethnographic use is the Kurrajong – *Brachychiton acuminatus* (Florabase 1989; Vicki Long, pers. comm. 2020). Kurrajong trees grow on the rocky slopes around Murujuga and provided Aboriginal people with seeds for making flour (Low 1988: 183; Clarke 2007: 91), bark for twine, gum for hafting, boughs for watercraft, and tuberous water-storing roots (Turner 1994; Clarke 2007: 80–81, 120).

The microscopic edge scarring, negative termination types, and absence of polish, other than the deep

directional polish running parallel to the platform, may indicate that artefact XU03-LA054 was used for woodworking (Claud et al. 2019; see earlier comments about the need for material-based usewear experimentation). This interpretation is supported by the presence of tracheids that most likely originate from *Brachychiton acuminatus*.

Usewear analysis of artefact XU03-LA058 revealed a small number ($n = 9$) of shallow edge scars along the right ventral margin and a single scar on the termination (Figure 8.56). Six locations were sampled for residues but only soil-related residues, such as non-soluble minerals, were recovered. Since no residues were recovered and the usewear evidence is limited, it is unclear whether the shallow edge scarring is related to very brief use or post-depositional processes. The artefact tested negative for blood.

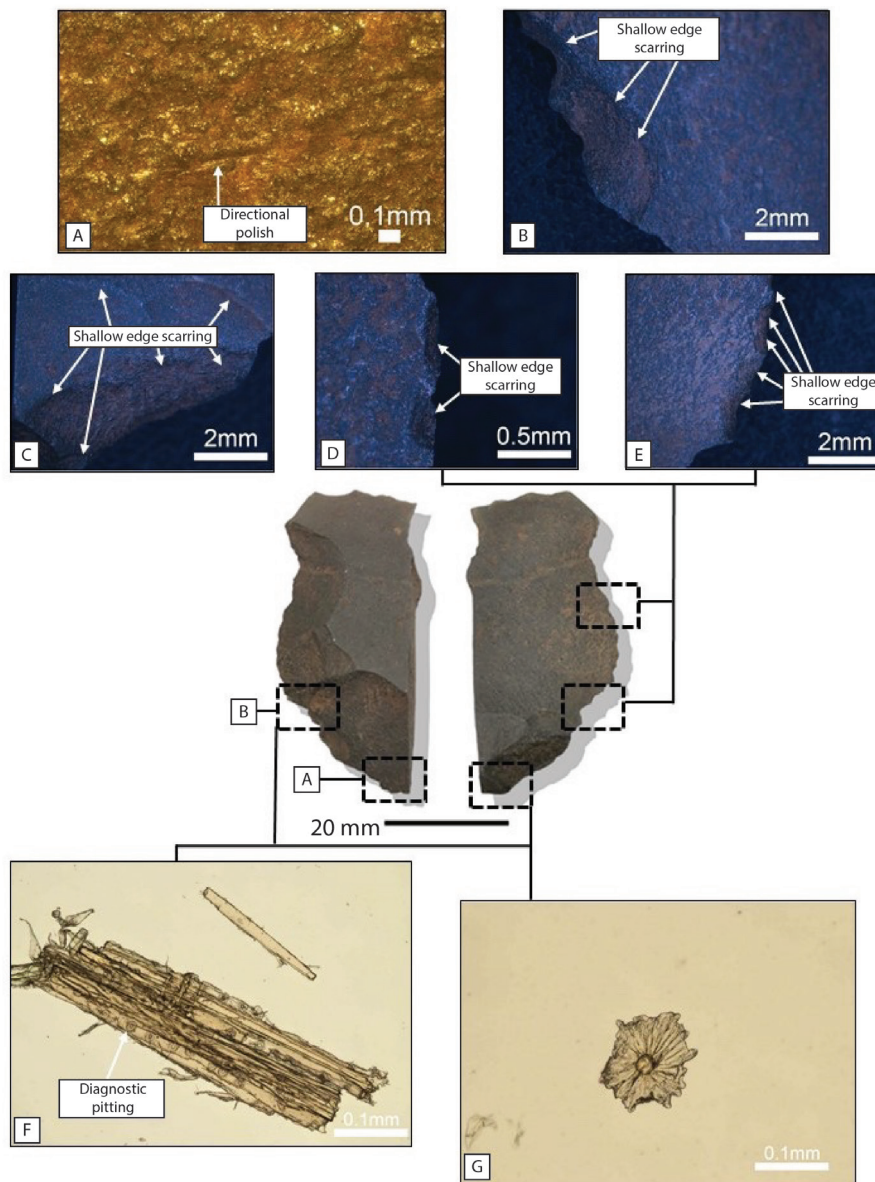


Figure 8.55. Artefact 253614-XU03-LA054 showing (A) directional polish parallel to the platform, (B-E) the large number of shallow edge scars on the artefact, (F) tracheid with diagnostic pitting and (G) an unidentified plant fibre. Scale is 20 mm.

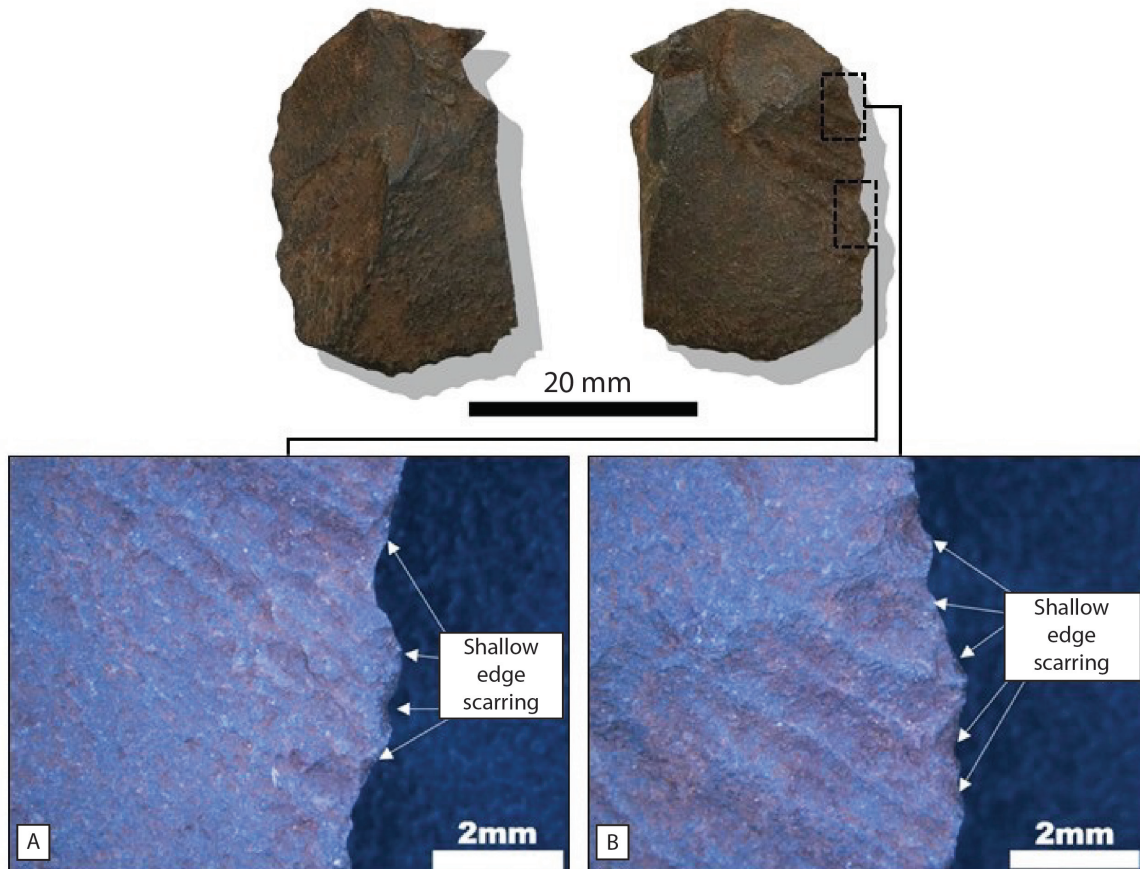


Figure 8.56. Artefact 253614-XU03-LA058. Shallow edge scarring focalised along the right ventral margin. Scale is 20 mm.

Discussion

The three artefacts in the earliest analytical unit demonstrates only very occasional stone tool manufacture by Aboriginal people at RIA-043 around c. 8,000 years ago. The main activity at this time was the consumption of *Terebralia* shellfish. The low density 253614 stone assemblage was predominantly discarded during the terminal occupation at this location over a c. 400-year period between c. 7,412 and 7,268 cal. BP. People continued to consume *Terebralia* and a range of other shellfish species, although proportions of shellfish indicate slightly lower consumption rates than in the earliest occupation phase. Throughout this Early Holocene occupation, in the three episodic visits interpreted in this square, groups using the 253614 southern knoll non-intensively knapped (primarily) volcaniclastic siltstone nodules. Geological mapping places the source of this lithic material several kilometres to the east of this location, although an artefact found on nearby Rosemary 8 showing the geological contact zone in a single artefact suggests that closer sources may exist. Overhang removal scars on flakes indicate that care was taken by knappers to prepare core platforms for more successful flake removals. The high proportion

of very small debris (<1 cm) at the site indicates on-site knapping and possibly also tool manufacture and/or maintenance. Two non-intensively used tools demonstrate woodworking activities and/or plant processing. Larger fine-grained silicified flakes were clearly preferred for these manufacturing tasks.

Occupation in this square and that excavated at Rosemary 8 statistically overlap and indicate that people were likely using this broader landscape – which includes several domestic structures – contemporaneously during the Early Holocene.

The stratified Early Holocene phases of midden deposition on the knolls indicate that people first consumed mainly *Terebralia* by the waterhole, and that they carried lithic materials to the site from the various lithic sources. Their continued use of this area, for a range of activities, intensified over time. *Terebralia* consumption appears to have been declining in the terminal phases of this site complex's use, at which time there was a broadening of the species being collected from a slightly wider range of ecosystems. Stone tool manufacture increased in this phase generally, as did the use of these tools for plant processing.

Wadjuru Pool

Wadjuru Pool (DPLH 978) is located within a sand dune system near the south-western corner of Rosemary Island (Figure 8.40). The site is located around a low-lying domed gabbro outcrop with a small depression in its centre which holds water after rain. This rock outcrop has extensive evidence of grinding, and two engraved motifs. The surface of the dune around Wadjuru Pool is covered with deflated archaeological material, including shell (*Melo amphora* and *Tridacna* sp.), flaked stone artefacts and portable grindstones. Three stone features, including one standing stone, are located towards the south of the site. A gabbro boulder pile with 35 engraved motifs is located at the southern extent of the site. The site is named for the pool on the domed outcrop – and for the *Wadjuru* vine which grows abundantly on the nearby rocky outcrop (Bradshaw 1995).

This site was first excavated by Elizabeth Bradshaw (1995), when a 50 cm x 50 cm test square (named WPEB here) was excavated to the east of the pool (Figure 8.57). The current excavation was undertaken on 4–10 April 2014 by Jo McDonald and Leslie Zubieta. A single 1 m x 1 m square was excavated 50 m south-west of the domed outcrop. Grinding patches on this outcrop were recorded in detail and surface artefact recording was completed by the whole UWA team. This site's contents – including the assemblage excavated earlier by Elizabeth Bradshaw – were analysed by Meg Berry (2018). Her main results are summarised here. The lithic assemblage was re-analysed by Wendy Reynen to ensure comparability of lithic identification.

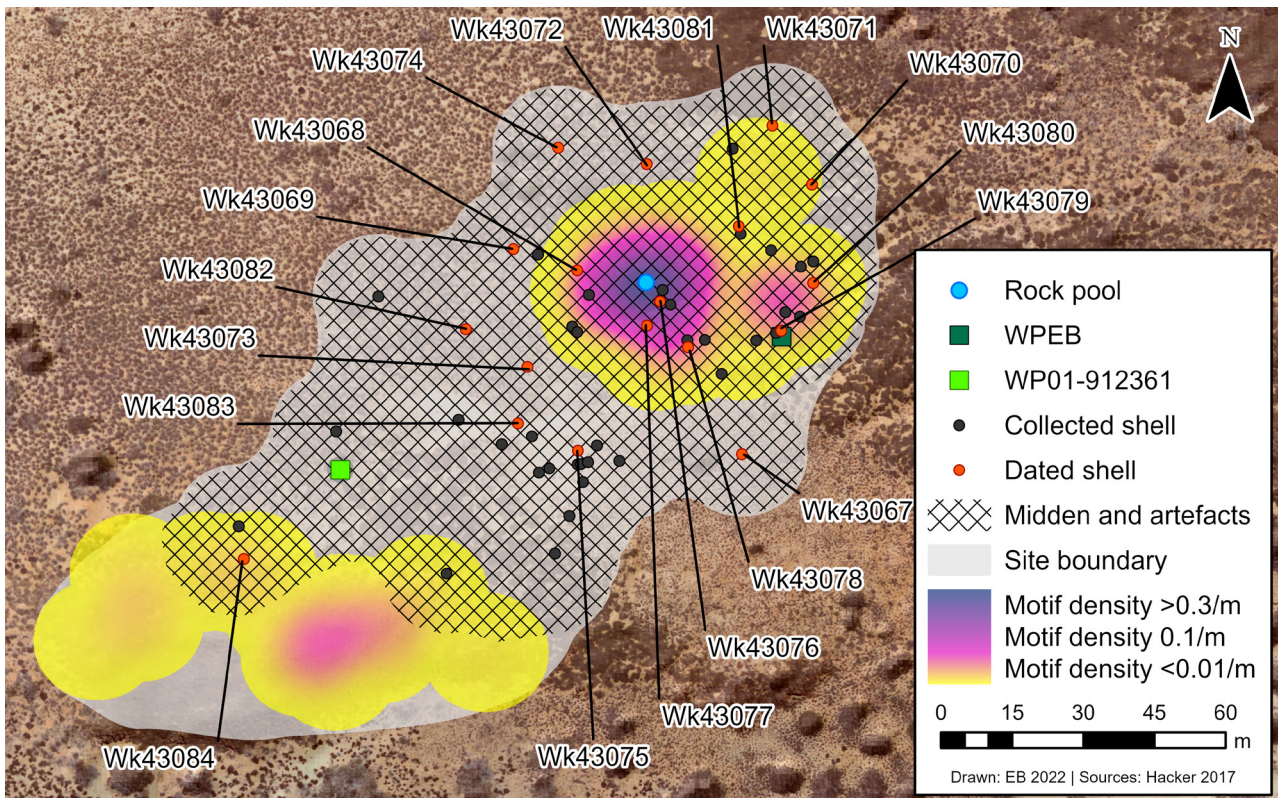


Figure 8.57. Wadjuru Pool showing location of current and previous excavations, the rock hole with grinding patches and the collected *Melo* samples (see Berry 2018 for analysis).

Square WP01-912361

The excavation here aimed to discover whether pre-Holocene occupation existed at Wadjuru Pool (Bradshaw 1995). The excavation square was located further away from the rock hole where it was hoped that a red Pleistocene dune may survive beneath the calcareous, paler dune surface. Square 912361 was

excavated in 5 cm excavation units or according to visible stratigraphic breaks, whichever was smaller. A 25 cm x 25 cm sondage was excavated in the north-west corner at c. 1.3 m depth. Excavation reached a depth of 1.53 m before hitting an impenetrable calcium carbonate base (Figure 8.58).

Stratigraphy and dating

Five stratigraphic units were identified in the field (Figure 8.59 and Figure 8.59). Within the profile, colour intensifies and becomes generally redder with depth, although no red Pleistocene dune was encountered. Compaction also increased with depth. Consolidated decomposing bedrock rubble encrusted in calcium carbonate was found at the base of the sequence immediately over volcanic bedrock.

Sediment analysis was conducted on bulk sediment samples collected from each XU. Analyses included

particle size analysis, mineralogy, bulk chemistry, pH and electro conductivity (see Berry 2018: Appendix II). Sediments were well sorted and predominantly composed of carbonate (90%), quartz (10%) and minor clay (1%). Rounded windblown grains derive from a now-drowned Abydos coastal plain. Grain size increases with depth, with increased frequencies of coarse and very coarse sands at the lowest levels (Berry 2018: Figure 9.25). Analysis indicates a high windblown content throughout the sequence.



Figure 8.58. Square 912361 near the base of the excavation.

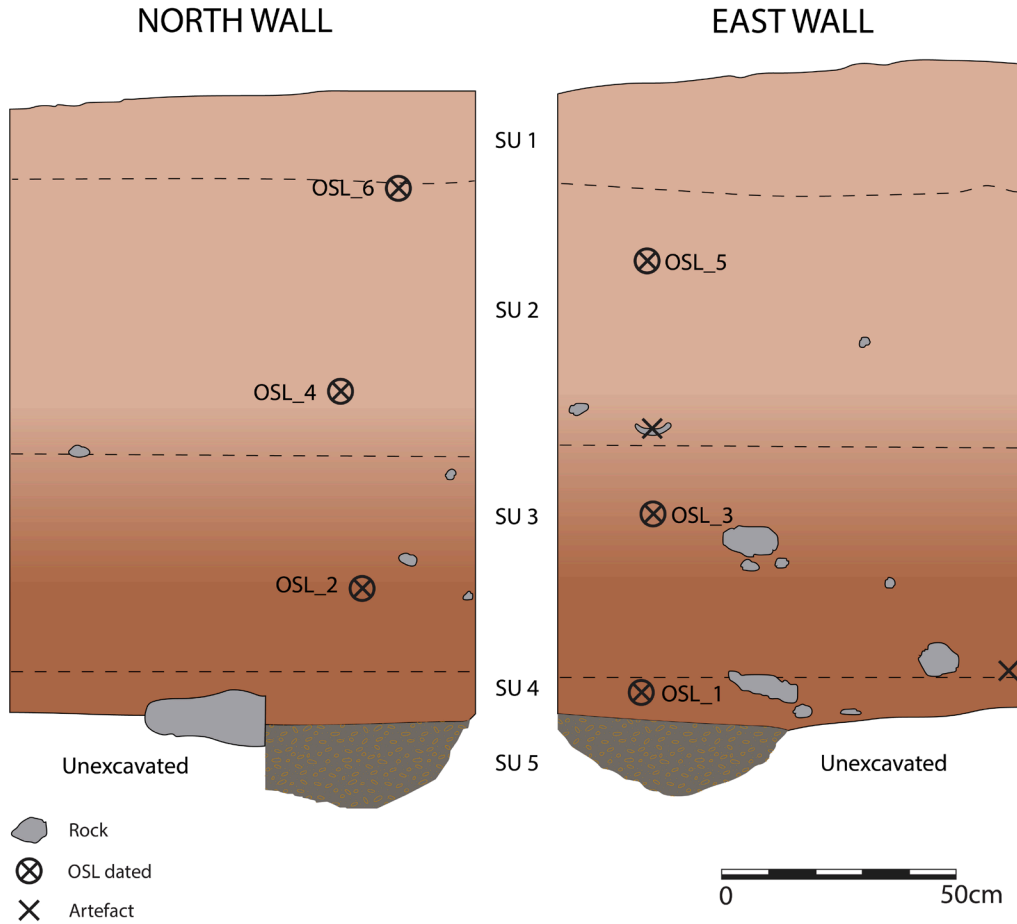


Figure 8.59. Stratigraphy from north and east profiles of 912361. Boundaries are transitional in colour and hardness (from Berry 2018: Figure 9.24).

UNIT	DEPTH BELOW SURFACE (CM)	EXCAVATED WEIGHT (KG)	DISCARDED ROCK (KG)	PH	MUNSELL
XU01	5.0	82.30	82.30	8	7.5YR 5/6
XU02	10.4	69.50	69.50		7.5YR 5/6
XU03	16.2	47.75	47.75		7.5YR 5/6
XU04	19.0	58.10	58.10		7.5YR 5/6
XU05	23.9	60.25	60.25	8	7.5YR 5/6
XU06	29.1	93.00	93.00	8	7.5YR 5/6
XU07	34.0	67.80	67.80	8	7.5YR 5/6
XU08	39.3	126.10	126.10		7.5YR 5/6
XU09	45.9	116.40	116.40		
XU10	51.2	86.75	86.75		7.5YR 5/6
XU11	56.9	110.25	110.25		7.5YR 5/6
XU12	64.1	78.80	78.80	8.5	7.5YR 5/6
XU13	69.9	103.60	103.60		
XU14	74.9	124.90	124.90		
XU15	80.3	65.25	65.25	8	5YR 5/4
XU16	85.9	96.50	96.50		
XU17	90.8	110.60	110.60		
XU18	95.9	72.00	72.00		5YR 5/4
XU19	100.9	95.75	95.75		
XU20	105.9	155.45	155.45		5YR 4/6
XU21	114.1	129.40	129.40		
XU22	119.8	70.50	70.50		
XU23	123.7	67.50	67.50		5YR 4/6
XU24	129.1	135.20	135.20		
XU25-30	152.9	70.40	70.40	8	5YR 4/6
Total		2,294.05	48.20		

Table 8.47. Square 912361 excavation weights for deposit and sediment characteristics.

Radiocarbon dating

In the absence of dateable charcoal and bone, 12 AMS radiocarbon dates were obtained from shells excavated from 912361 (Table 8.48). Most (nine) of these were obtained from *Terebralia* spp; two AMS dates were received from *Saccostrea* sp. and one AMS date was obtained on *Melo amphora*. All shells submitted for radiocarbon dating were located and recorded *in situ*. While reservoir effects of up to 600 years have been identified for radiocarbon dating *Terebralia* sp. (Petchey et al. 2006; due to terrestrial carbon uptake by the animal during its lifetime), this species is the most common in the site and therefore by necessity the material which was dated. The oyster dates derive from the middle of the sequence (XUs 14 and 15) and provide an age determination for what was observed to be an *in situ* dinnertime

camp (see field notes 6 April 2014; CRAR+M Database). Several oyster lids and bases were uncovered together in an undisturbed state. The *Melo* was found towards the top of the sequence in compact paler sand and was located in an undisturbed, i.e. flat, position.

The shell material revealed an Early to Mid-Holocene sequence (Table 8.48, Figure 8.60), with several reversals confirming the mobile sandy sediments at the site. These results likely reflect deflations, blowouts and re-deposition of materials associated with cyclonic events (see Przywolnik 2002: 139) as well as periods of more intensive occupation when there is bio-turbation of the surface material with older and contemporary occupation evidence.

Optically stimulated luminescence (OSL)

Six single-grain OSL samples were collected from the northern and eastern walls of the square (Table 8.48). These were dated by the Prescott Environmental Luminescence Laboratory, University of Adelaide (Spooner and Questiaux 2016; see Berry 2018: Appendix III). Well-bleached dispersed grains in all six samples throughout the sequence indicate significant post-depositional mixing. This is apparent in the spread of grain-age distributions, and higher water content in some samples. The Adelaide laboratory employed the Finite Mixture Model (FMM) for interpreting the OSL results, which reduces the potential for several depositional events or processes contributing to the age determination (Spooner and Questiaux 2016: 5; in Berry 2018). The OSL

results confirm an initial Early Holocene occupation with a date of 9.6 ± 0.3 ka at the base of the profile. There is a significant jump to the Mid-Holocene (4.6 ± 0.2 ka) at 110 cm BS, with the uppermost OSL date revealing a recent age of around 300 years ago (0.29 ± 0.02 ka).

The combined OSL and radiocarbon dates confirm the problems with the reversals in WP01-912361 (Table 8.48). The OSL dates suggest a relatively slow and steady accumulation of deposit in the earlier phases of site use, with an accelerated deposition sequence in the last 3,500 years. There is a good fit between the earliest OSL and *Terebralia* dates. All *Terebralia* dates fall between 9,374 and 6,409 calibrated years – regardless of their depth within the sequence (Table 8.48).

LAB CODE	SAMPLE TYPE	SU	XU	DEPTH (CM)	AU	AGE	ERROR
OZR813	<i>Terebralia</i> sp.	1	XU3	7	1	8,660	35
OZR814	<i>Terebralia</i> sp.	1	XU5	14	1	6,060	30
AD14089	Quartz	2	-	22	1	290	20
OZR815	<i>Melo amphora</i>	2	XU8	28	1	3,420	25
AD14088	Quartz	2	-	44	1	780	20
Wk43066	<i>Saccostrea</i> sp.	2	XU14	64	1	4,339	20
AD14087	Quartz	2	-	68	1	2,800	100
Wk43064	<i>Saccostrea</i> sp.	2	XU15	72	1	4,364	20
OZR816	<i>Terebralia</i> sp.	2	XU15	72	1	8,735	30
OZR817	<i>Terebralia</i> sp.	2	XU19	91	2	8,420	40
Wk43063	<i>Terebralia</i> sp.	2	XU20	98	2	6,269	20
AD14086	Quartz	2	-	98	2	3,400	100
OZR818	<i>Terebralia</i> sp.	2	XU21	100	2	6,415	30
AD14085	Quartz	3	-	110	3	4,600	200
OZR819	<i>Terebralia</i> sp.	3	XU24	121	3	7,390	30
Wk43062	<i>Terebralia</i> sp.	3	XU24	122	3	7,190	22
AD14084	Quartz	4	-	135	3	9,600	300
Wk43061	<i>Terebralia</i> sp.	4	XU26	138	3	8,768	24

Table 8.48. Radiocarbon and OSL determinations from Square 912361 at Wadjuru Pool.

Bayesian analysis

A series of Bayesian sequence depositional models, based on the analytical and stratigraphic units, were used to understand the chronology within 912361 (Bronk Ramsey 2008, 2009a). Using multiple models to establish the most robust chronology is especially important for Wadjuru Pool given the number of inversions (Table 8.48). The models for analytical and stratigraphic models follow the same structure and parameters described previously (see chapter 2 and above). The analytical units were established based on archaeological assemblage

patterning (Berry 2018) while the stratigraphic model follows Figure 8.60. Given that most of the dates for Wadjuru Pool individually overlap with other dates in the sequence, there is evidence for continuous occupation. As such, both the stratigraphic and analytical models follow continuous designs (see Bronk Ramsey 2009a). Calibrations and reporting conventions follow previous models (see above; Heaton et al. 2020; Stuiver and Polach 1977; Veth et al. 2017).

Analytical units model

The initial results for the analytical unit model show some clear outliers (Table 8.49). In AU1, OZR813 and OZR816 have extremely low A-index values (5.5 each) and do not even register outlier probabilities (i.e. these dates are

highly likely to be outliers). Interestingly, OZR814, with a similar age as OZR813 and OZR816, is not registered as an outlier.

NAME	68.2%		95.4%		SUM. STATISTICS			INDICES	
	FROM	TO	FROM	TO	μ	σ	M	AI	OP
Boundary: Deposit Surface	100	30	100	0	50	30	50	100	
Phase: AU1									
OZR813	6,380	3,400	6,460	1,120	4,560	1,470	4,950	5.5	
OZR814	6,270	6,060	6,400	2,400	5,810	1,030	6,150	90.4	86
AD14089	310	270	330	250	290	30	290	103.4	98.7
OZR815	3,060	2,870	3,190	2,760	3,030	330	2,980	100.6	95.8
AD14088	800	760	840	110	730	160	780	95.1	90.3
Wk43066	4,240	4,030	5,330	3,830	4,150	320	4,140	98.6	93.8
AD14087	2,900	2,690	3,040	2,550	2,800	200	2,800	101	96.1
OZR816	6,370	3,170	6,430	150	4,110	1,740	4,540	5.5	
Wk43064	4,270	4,080	4,380	3,970	4,170	150	4,170	102.4	97.4
Boundary AU2/AU1	6,460	6,210	6,610	4,380	6,230	370	6,320		
Phase: AU2									
OZR817	6,670	6,320	7,200	6,120	6,520	260	6,500	5.5	
AD14086	6,650	6,300	7,240	5,530	6,460	330	6,480	5.5	
Wk43063	6,490	6,340	6,590	6,280	6,430	80	6,420	98.6	98.6
OZR818	6,610	6,430	6,700	6,360	6,520	90	6,520	102.6	98.9
Boundary AU3/AU2	6,890	6,430	7,320	6,400	6,760	260	6,700		
Phase: AU3									
AD14085	8,200	6,570	9,710	6,480	7,800	960	7,550	5.5	
OZR819	7,640	7,500	7,720	7,410	7,570	110	7,570	102.7	97.7
Wk43062	7,460	7,320	7,550	7,240	7,390	120	7,390	102.7	97.7
AD14084	9,770	9,150	10,160	8,790	9,430	400	9,450	96.2	95.1
Wk43061	9,210	9,020	9,350	8,920	9,110	180	9,120	101.3	96.2
Boundary: Deposit Base	10,460	9,260	12,040	9,050	10,180	820	9,980		

Table 8.49. Initial Bayesian results for Wadjuru Pool using analytical units.

In AU2, both OZR817 and AD14086 are registered as outliers. Again, these have exceptionally low A-index values (5.5 each) and do not return outlier probabilities. On face value, this may seem strange since they have similar modelled ages to Wk43063 and OZR818. However, this is because their modelled ages substantially differ from their unmodelled ages of $8,420 \pm 40$ and $3,400 \pm 100$ respectively. The model has essentially forced OZR817

and AD14086 towards 'more probable' ages. Finally, for AU3, only AD14085 is an outlier, with a 5.5 A-index and no outlier probability too. Its modelled date (8,197–6,569 cal. BP) also differs from its unmodelled date ($4,600 \pm 200$ cal. BP). OSL dates should not differ substantially from their original ages since they do not require calibration. The initial analytical model also returns very low overall A-index results ($A_{\text{model}} = 4.4$; $A_{\text{overall}} = 4.2$).

NAME	68.2%		95.4%		SUM. STATISTICS			INDICES	
	FROM	TO	FROM	TO	μ	σ	M	AI	OP
Boundary: Deposit Surface	99	31	99	1	51	29	52	100	
Phase: AU1									
OZR814	6,260	6,090	6,300	5,980	6,150	90	6,160	99.6	96
AD14089	310	270	330	250	290	20	290	101.2	96.3
OZR815	3,060	2,880	3,150	2,800	2,970	90	2,970	101.1	96.1
AD14088	800	760	820	740	780	20	780	101.4	96.5
Wk43066	4,240	4,050	4,340	3,950	4,130	110	4,140	100.7	95.6
AD14087	2,900	2,700	3,010	2,600	2,800	100	2,800	100.9	95.9
Wk43064	4,260	4,080	4,360	3,980	4,170	90	4,170	101.2	96.2
Boundary: AU2/AU1	6,440	6,220	6,530	6,100	6,320	110	6,320		
Phase: AU2									
Wk43063	6,490	6,340	6,580	6,280	6,420	80	6,420	96.9	96.1
OZR818	6,610	6,440	6,700	6,360	6,520	80	6,520	100	96.2
Boundary: AU3/AU2	6,910	6,440	7,330	6,400	6,780	260	6,710		
Phase: AU3									
OZR819	7,640	7,500	7,700	7,420	7,560	70	7,570	101.2	96.1
Wk43062	7,460	7,320	7,540	7,250	7,390	80	7,390	100.9	95.9
AD14084	9,780	9,170	10,100	8,910	9,480	310	9,480	97.6	95.3
Wk43061	9,210	9,020	9,300	8,960	9,130	90	9,120	100.9	95.9
Boundary: Deposit Base	10,660	9,280	12,730	9,060	10,400	1,070	10,100		

Table 8.50. Final Bayesian results for Wadjuru Pool using analytical units.

These five outlier dates were removed and the model re-run (see Figure 8.51). This model returned good results with no outliers, including OZR814. All dates have <5% chance of being outliers while all A-index values are above 60%. The model also returns good A-index results ($A_{\text{model}} = 104.4$; $A_{\text{overall}} = 101.1$). The analytical units

model estimates that occupation at Wadjuru Pool began at 10,458–9,264 cal. BP before transitioning to AU2 at 6,912–6,439 cal. BP. The span of AU2 is short since it transitioned to AU1 at 6,457–6,214 cal. BP. AU1 then continues until modern times.

Stratigraphic units model

The initial results for the stratigraphic model in Table 8.51 shows that OZR813 and OZR814 in SU1 are outliers, with very low A-index results (5.5) and no outlier probability registered. Since we know that the surface is essentially modern, and that only two dates in SU2 return ages <1,000 cal. BP, the model has heavily altered OZR813 and OZR814 (from $8,660 \pm 35$ and $6,060 \pm 30$ BP respectively) to the 'more probable' ages (see Table 8.51). OZR816 and OZR817 also are suggested to be outliers in SU2. Given that their unmodelled determinations were respectively $8,735 \pm 30$ and $8,420 \pm 40$ cal BP – 2,000

years older than the next oldest ages in SU2 – this is no surprise either. Finally, in SU3, with an A-index of 7.7 and a 97.2% chance of being an outlier, AD14085 can also be rejected.

As with the final analytical unit model (Table 8.52), the final stratigraphic model also returns strong results with all individual A-index results well above 60% and all dates having a <5% chance of being an outlier. The overall model A-index results are also strong ($A_{\text{model}} = 106.2$; $A_{\text{overall}} = 102.6$).

NAME	68.2%		95.4%		SUM. STATISTICS			INDICES	
	FROM	TO	FROM	TO	μ	σ	M	AI	OP
Boundary: Deposit Surface	70	0	100	0	50	30	50	100	
Phase: SU1									
OZR813	160	30	250	10	120	80	110	5.5	
OZR814	160	40	250	10	120	70	110	5.5	
Boundary: SU2/SU1	280	110	310	30	190	140	190		
Phase: SU2									
AD14089	310	270	340	240	320	200	290	101	96.3
OZR815	3,060	2,870	3,160	2,780	2,970	140	2,970	101.5	96.8
AD14088	800	760	830	730	780	150	780	101.9	97.1
Wk43066	4,240	4,040	4,370	3,910	4,150	150	4,140	100.7	95.7
AD14087	2,910	2,690	3,060	2,550	2,800	190	2,800	100.4	95.3
OZR816	7,400	5,820	7,500	2,110	5,980	1,410	6,510	5.5	
Wk43064	4,270	4,080	4,400	3,950	4,180	180	4,170	100.6	95.6
OZR817	7,380	5,860	7,480	3,900	6,190	1,060	6,540	5.5	
AD14086	3,500	3,290	3,630	3,170	3,400	150	3,400	101.4	96.3
Wk43063	6,470	6,300	6,670	4,020	6,280	530	6,380	97.2	92.1
OZR818	6,640	6,450	6,870	6,230	6,440	600	6,540	98.2	93.3
Boundary: SU3/SU2	7,480	6,980	7,550	6,480	7,050	520	7,190		
Phase: SU3									
AD14085	7,730	7,130	8,480	4,670	7,380	580	7,440	7.7	2.8
OZR819	7,620	7,470	7,710	7,400	7,550	100	7,550	100.3	97.4
Wk43062	7,480	7,330	7,550	7,260	7,410	80	7,400	100.1	97.6
Boundary: SU4/SU3	9,020	7,450	9,100	7,440	8,060	510	7,880		
Phase: SU4									
AD14084	9,770	9,150	10,120	8,880	9,480	320	9,470	97	95.7
Wk43061	9,210	9,020	9,330	8,940	9,130	130	9,130	101.4	96.6
Boundary: Deposit Base	10,680	9,180	13,840	9,050	10,400	1,000	10,110		

Table 8.51. Initial Bayesian results for Wadjuru Pool using stratigraphic units.

Final considerations from Bayesian analysis

Both the initial analytical and stratigraphic models register a similar set of dates as outliers so we can be confident that, based on the information we have, these are outliers. It is likely that OZR814 is also an outlier, and this is captured by the stratigraphic model. Both models provide equally strong results and either could be justifiably selected for analysis. The analytical model

may provide a better treatment of the upper units, incorporating potential mixing within AU1 while also managing to separate out AU2 and AU3 with good chronological resolution. Hence the original analytical units (Berry 2018) have been retained. The results for this analytical unit model are shown in Figure 8.60.

NAME	68.2%		95.4%		SUMMARY STATISTICS			INDICES	
	FROM	TO	FROM	TO	μ	σ	M	AI	OP
Boundary: SU2/SU1	280	90	280	0	150	80	160	100	
Phase: SU2									
AD14089	310	270	330	250	290	20	290	102.7	96.9
OZR815	3,060	2,880	3,150	2,800	2,970	90	2,970	101	96
AD14088	800	760	820	740	780	20	780	101.8	96.8
Wk43066	4,240	4,050	4,330	3,960	4,140	90	4,140	101.4	96.2
AD14087	2,900	2,700	3,000	2,590	2,800	100	2,800	101	96
Wk43064	4,260	4,080	4,360	3,980	4,170	90	4,170	101.3	96.2
AD14086	3,500	3,300	3,610	3,200	3,400	100	3,400	100.9	96
Wk43063	6,460	6,300	6,560	6,240	6,390	80	6,390	101.3	96.1
OZR818	6,639	6,460	6,720	6,380	6,540	90	6,540	101.3	96.2
Boundary: SU3/SU2	7,400	6,780	7,460	6,540	7,030	270	7,050		
Phase: SU3									
OZR819	7,630	7,480	7,700	7,410	7,560	70	7,560	100.1	96.1
Wk43062	7,470	7,320	7,540	7,260	7,400	70	7,400	100.1	96
Boundary: SU4/SU3	9,110	7,490	9,140	7,480	8,220	530	8,120		
Phase: SU4									
AD14084	9,750	9,150	10,090	8,930	9,480	300	9,470	95.9	95.6
Wk43061	9,210	9,030	9,310	8,970	9,130	90	9,130	100.8	96
Boundary: Deposit Base	10,780	9,130	15,230	9,020	10,530	1,250	10,130		

Table 8.52. Final Bayesian results for Wadjuru Pool using Square 912361 analytical units.

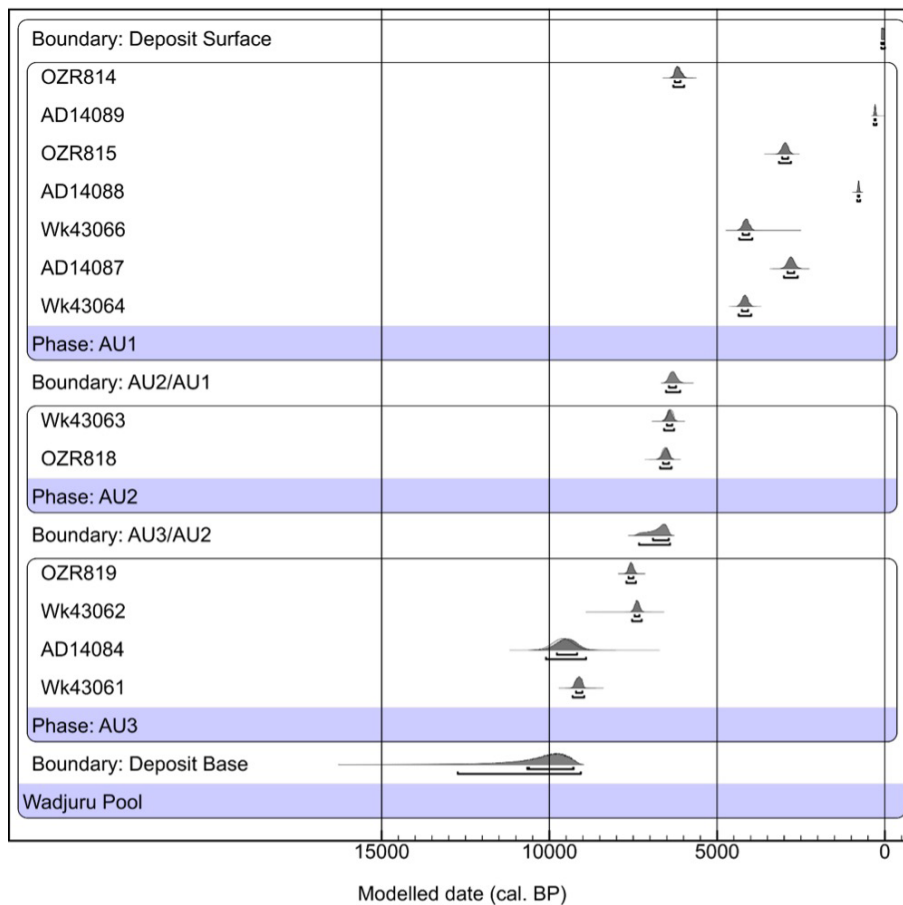


Figure 8.60. Final Bayesian model for 912361 Wadjuru Pool based on analytical units.

The surface assemblage

Extensive grinding activity has been documented across WP-001, with 141 grinding patches recorded on the rock pool's domed outcrop (Berry 2018: Figure 9.11). One grinding patch was also recorded on the engraved boulder pile to the south, amongst the engraved rock art

assemblage. The deflated surface scatter artefacts and shell around the central bedrock outcrop includes an extensive manuport/portable assemblage (Figure 8.62), some of which contains grinding usewear and residues (see Berry 2018: 252–258). The surface flaked artefact

assemblage has not been recorded.

The extensive surface scatter includes many complete and fragmentary *Melo amphora* shells. The assemblage includes 176 individual specimens (some fragments), which were recorded during fieldwork in

2014. Berry (2018) found that the average length (of the apex) of the *Melo amphora* fragments is 7.6 cm, although most shells are between 5 cm and 9 cm – smaller than a full adult size (Figure 8.61), likely reflecting preferred *Melo amphora* size selection by foragers in the past.

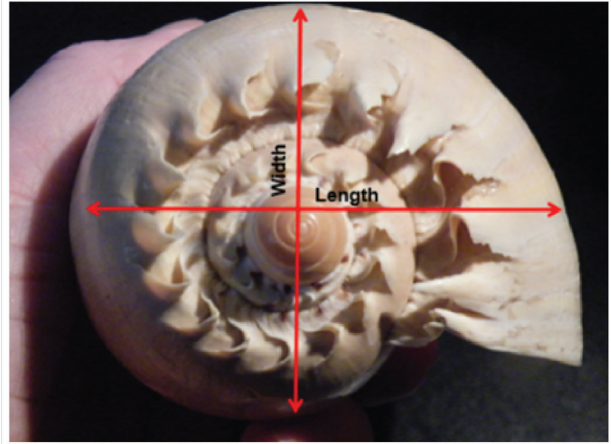
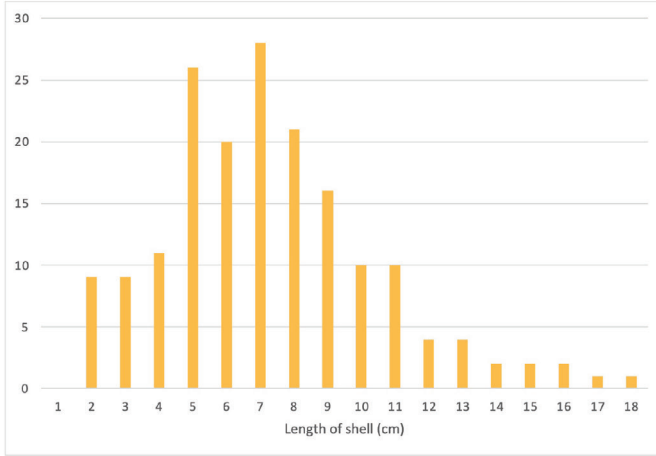


Figure 8.61. Size range of the surface *Melo amphora* assemblage (left; from Berry 2018: Figure 9.19) and (right) showing measurements (from Berry 2018: Figure 6.4).

A sample of 46 surface *Melo amphora* fragments were collected and a geographically dispersed (random) sample of 18 specimens were subsampled and sent to Waikato Radiocarbon Laboratory for AMS radiocarbon dating. This surface *Melo amphora* assemblage reveals a recent occupation signature at Wadjuru Pool. *Melo* shells reveal that groups visited Wadjuru Pool repeatedly during the last 2,500 years, with almost continuous occupation

between c. 1,500 and 500 years cal. BP (Table 8.53). The surface *Melo amphora* material confirms persistent use of the outer islands of the archipelago after sea level rise created this outermost island of the archipelago but suggest that this south-western corner of the island was not still being used when whalers arrived in the archipelago 300 years ago (Figure 8.63).

WP SAMPLE CODE	LAB CODE	AMS MEASUREMENT (YEARS BP)	13C CARB ‰	18OCARB ‰	% MODERN CARBON	CALIBRATED AGE RANGE (95.4%)
SS31	Wk43078	592 ± 20	2.19	-0.51	92.9 ± 0.2%	520-627
SS144	Wk43071	600 ± 20	1.99	-0.65	92.8 ± 0.2%	528-627
SS13	Wk43069	765 ± 20	2.12	-0.69	92.8 ± 0.2%	570-720
SS102	Wk43067	811 ± 20	2.11	-0.70	92.8 ± 0.2%	669-726
SS43	Wk43081	823 ± 20	1.99	-0.48	90.3 ± 0.2%	671-730
SS34	Wk43079	845 ± 20	2.75	-0.55	90.0 ± 0.2%	673-740
SS148	Wk43072	991 ± 20	1.29	-0.38	88.4 ± 0.2%	798-921
SS37	Wk43080	1,107 ± 20	1.55	-0.60	87.1 ± 0.2%	926-1,048
SS79	Wk43082	1,122 ± 20	3.24	-0.28	87 ± 0.2%	929-1,054
SS88	Wk43084	1,168 ± 20	1.74	-0.46	86.5 ± 0.2%	962-1,060
SS25	Wk43076	1,235 ± 20	1.52	-0.58	85.7 ± 0.2%	1,058-1,179
SS142	Wk43070	1,252 ± 20	1.00	-0.48	92.8 ± 0.2%	1,066-1,177
SS17	Wk43073	1,376 ± 20	2.72	-0.46	84.3 ± 0.2%	1,177-1,299
SS180	Wk43074	1,460 ± 20	2.12	-0.95	83.4 ± 0.2%	1,291-1,355
SS8	Wk43083	1,519 ± 20	1.62	-0.29	82.8 ± 0.2%	1,311-1,406
SS11	Wk43068	1,673 ± 20	2.77	-0.78	92.8 ± 0.2%	1,428-1,584
SS28	Wk43077	2,330 ± 20	2.15	-0.69	74.8 ± 0.2%	2,151-2,351
SS24	Wk43075	2,490 ± 20	1.32	-0.73	73.4 ± 0.2%	2,360-2,705

Table 8.53. Wadjuru Pool surface *Melo amphora* assemblage showing the seriated AMS radiocarbon determinations.

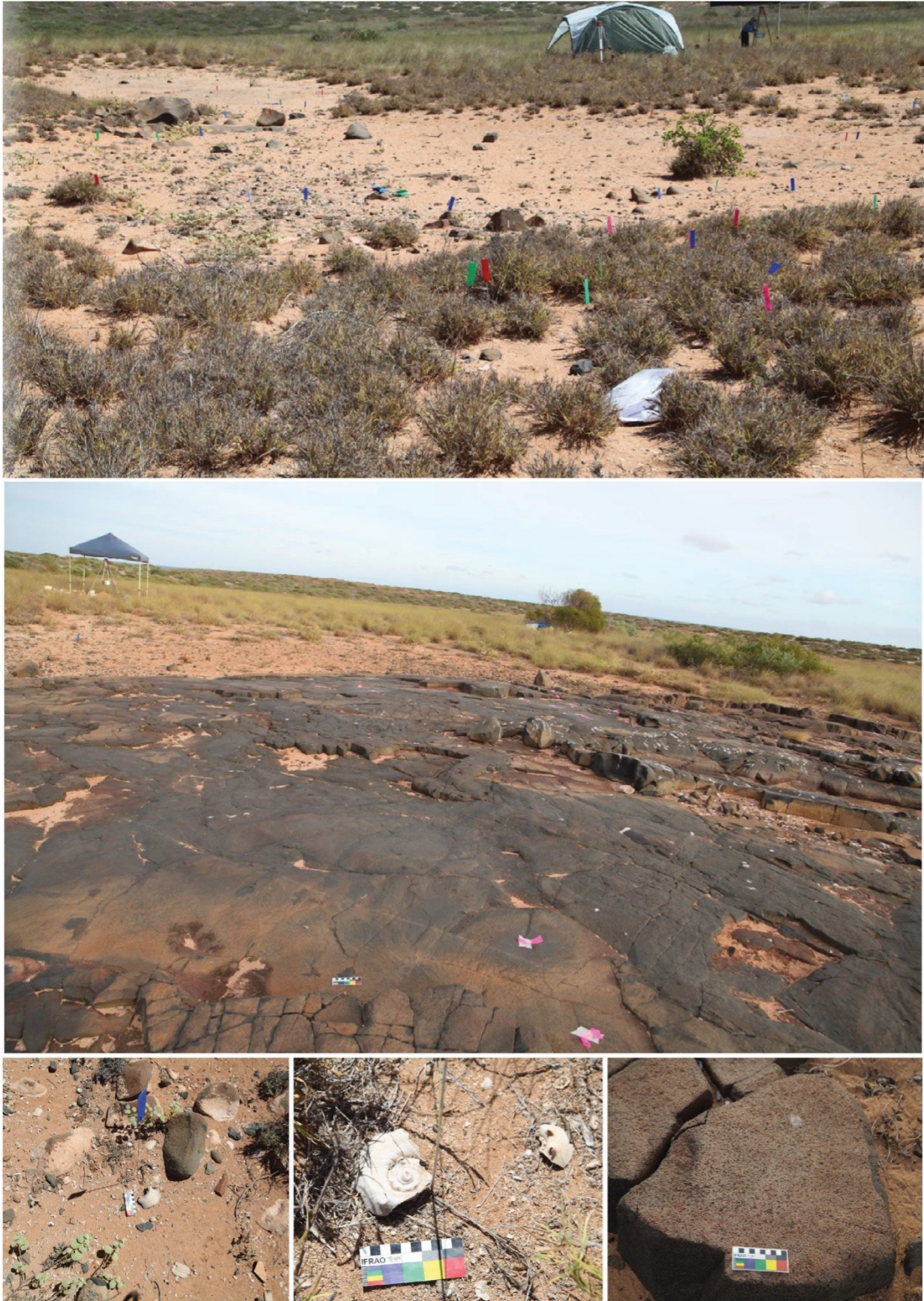


Figure 8.62. Surface collections across MLP WP001 with examples of the surface *Melo* and grinding evidence. Excavation (domed shelter) and sieving station (square pagoda) in background.

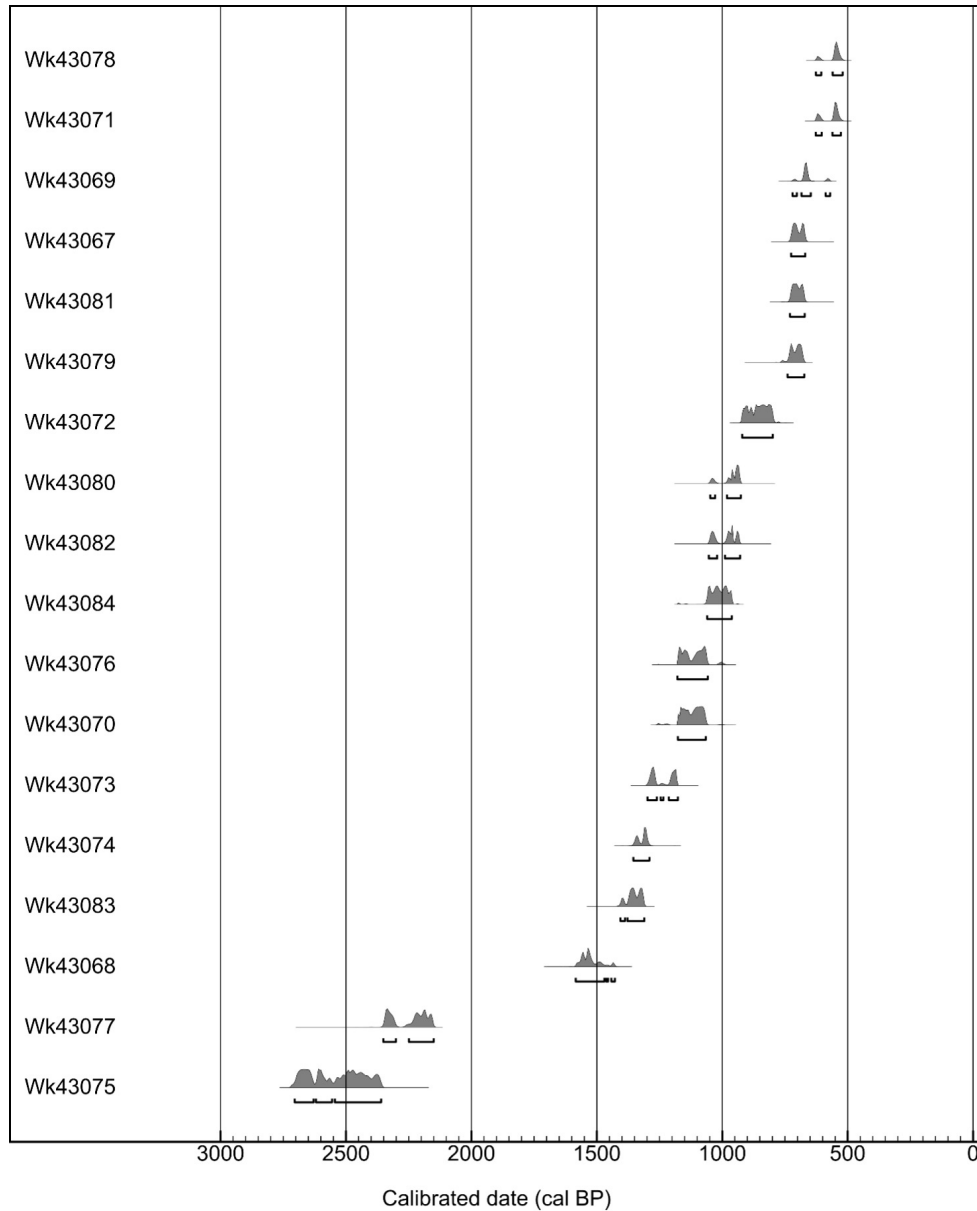


Figure 8.63. The 18 surface *Melo amphora* dates calibrated using Marine20 (Heaton et al. 2020) with a 109 ± 25 marine reservoir value for shell (Veth et al. 2017).

The excavated assemblage

Over 7.6 kilograms of cultural material was analysed from 912361. Peak accumulation of deposit is found at the base of the sequence in XUs 23–24 (Table 8.54). Shellfish remains (6.3 kg) contribute significantly to the assemblage (Figure 8.64 and Table 8.54). Flaked stone artefacts (945.2 g) are the next most common

component. Ground stone material (338.4 g) was found only in XU2, in keeping with the widespread distribution of this material across the contemporary land surface. Poorly preserved faunal remains, mostly fish bone (18.6 g in total), are present throughout the assemblage in low frequencies.

UNIT	AU	FLAKED ARTEFACTS	GROUND STONE ARTEFACTS	SHELL	BONE	ORGANICS	TOTAL WEIGHT
XU01	1	9.3		51.2	0.6	30.8	91.9
XU02	1	11.6	338.4	88.9	3.8	2.9	445.6
XU03	1	7.9		28.1	0	2.1	38.1
XU04	1	1.8		22.8	1.4	4.2	30.2
XU05	1	22.8		41.5	0	0	64.3
XU06	1	1.3		42.9	0.8	0.1	45.1
XU07	1	33.4		31.7	0.2	0	65.3
XU08	1	36.0		95.2	0.6	4.7	136.5
XU09	1	2.2		60.1	0	2.5	64.8
XU10	1	26.1		171	0	0	197.1
XU11	1	150.6		124	0	0	274.6
XU12	1	66.1		29.8	0	0.7	96.6
XU13	1	2.6		69.6	0.2	0	72.4
XU14	1	10.0		163.7	0.7	0	174.4
XU15	1	0.5		79	0.9	0.1	80.5
XU16	2	3.2		117.6	2.3	0.03	123.13
XU17	2	3.1		128.4	0.4	0.01	131.91
XU18	2	14.6		135.1	0	0	149.7
XU19	2	171		152.8	0.6	0	170.5
XU20	2	29.3		359.8	2.7	0	391.8
XU21	2	52.1		331	0.6	0	383.7
XU22	3	1.8		155.9	0	0	157.7
XU23	3	119.0		306.6	0.3	0.6	426.5
XU24	3	310.2		3,282.9	0.3	0.4	3,593.8
XU25-30	3	12.8		255	2.1	6.0	275.9
<i>Total</i>		<i>945.2</i>	<i>338.4</i>	<i>6,324.7</i>	<i>18.6</i>	<i>55.7</i>	<i>7,682.6</i>

Table 8.54. Weights of cultural material in 912361 (in grams).

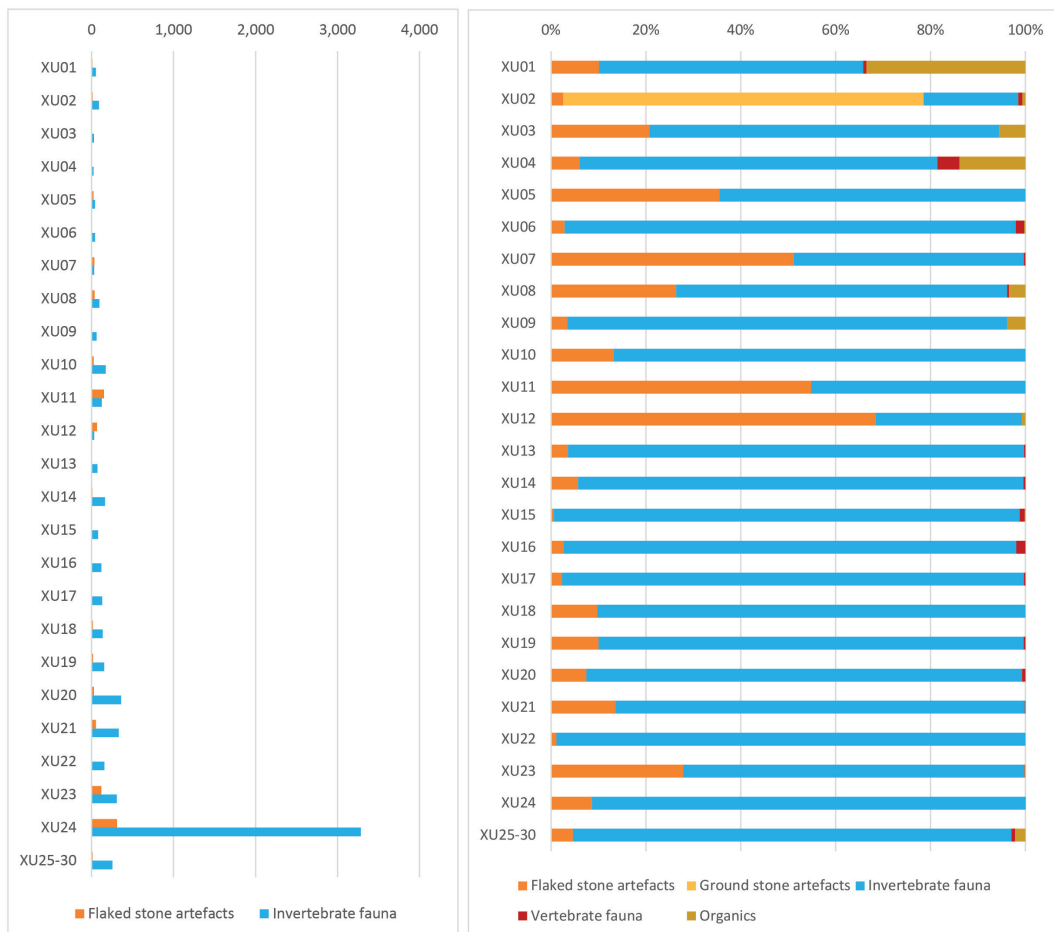


Figure 8.64. Square 912361: (left) weight of dominant archaeological material per XU, and (right) proportions of cultural remains in each XU.

Shellfish remains

Shellfish remains dominate the assemblage (Table 8.55). *Terebralia* sp. is the most common species followed by chiton (*Acanthopleura* sp.). *Melo amphora*, *Saccostrea* sp., *Lunella cinereus*, *Monodonta labio* and *Patella* sp. are also found throughout the sequence, although these are most common in the uppermost units. *Telescopium* is restricted to the basal unit (AU3). Tusk shell (*Dentalium* sp.) was found only in the uppermost layer. The shell remains reflect a changing focus in habitat throughout

occupation of the site. The earliest occupation (AU3) reveals an intensive focus on mangrove forests during the Early Holocene. The expansion of the fringing reef systems by c. 7,000–6,000 years cal. BP is reflected by the increased presence of shellfish from these types of habitats in AU2 and AU1. There is an increased predation of sandy intertidal species after 6,000 cal. BP with less intense, although continuous pulses of occupation visible at the site.

HABITAT	SPECIES	AU1 (XU1-15)	AU2 (XU16-21)	AU3 (XU22-30)	TOTAL (G)
Mangrove mudflats	<i>Telescopium telescopium</i>		2.8	16.5	19.3
Mangrove mudflats	<i>Terebralia</i> sp.	151.1	650.3	4,109.6	4,911.0
Rocky	<i>Acanthopleura gemmata</i>	596.3	248.14	5.2	849.6
Rocky	<i>Chicoreus</i> sp.	3.0			3.0
Rocky	<i>Cypraea</i> sp.	1.4			1.4
Rocky	<i>Lunella (Turbo) cinereus</i>	40.1	87.5	13.5	141.2
Rocky	<i>Monodonta labio</i>	8.5	48.4	5.9	62.7
Rocky	<i>Patella</i> sp.	14	36.4	3.3	53.7
Rocky	<i>Saccostrea</i> sp.	170.3	57	6	233.3
Rocky	<i>Trochus hanleyanua</i>	11.3	64.6	1.6	77.5
Sandy/rocky	<i>Vexillum crocatum</i>	0.3	12.6		12.9
Sandy	<i>Dentalium</i> sp.	1.5			1.5
Sandy	<i>Melo amphora</i>	75.5	13.7	18	107.1
Sandy	<i>Syrinx aruanus</i>	26.5	1.9		28.4
Sandy/mudflats	<i>Acrosterigma</i> sp.	0.4		0.2	0.7

Table 8.55. Square 912361: shell weights (in grams) in the analytical units (from 5 mm sieve).

The artefacts and shellfish from the original test square (Bradshaw 1995) were re-analysed, and this square (with fewer dates) shows much clearer patterning. Bradshaw's original interpretation was reinforced: her earliest occupation period was Early Holocene, with a strong focus on the *Terebralia* species with the largest amount of stone artefacts also present in this earliest occupation (Figure 8.60 and 8.61). The coastline was, at this time, still some distance to Wadjuru Pool. The most intense deposition of shellfish and stone artefacts occurred around 9,000 cal. BP. The next main phase of occupation was just pre-islandisation, where habitats for shellfish species changed to rocky and reef intertidal, showing the development of large reef systems around Rosemary after 7,500 years cal. BP. *Saccostrea* sp. becomes more dominant in the assemblage during this time. A significant reduction in stone tool manufacture also occurs. The upper level was undated but is assumed to represent a tailing off in the use of this landscape after it became an island. A shift to sandy intertidal shellfish species would have resulted from continually rising sea levels, with a decline in mangrove forests and the establishment of sandy beaches, which are now the focus for Hawksbill and Leatherback turtle rookeries.

While having several dating inconsistencies, the 912361 sequence shows this same general trend,

although the sandy intertidal species are more intensively exploited after 6,300 cal. BP (Figure 8.65). Notably absent from this assemblage is *Anadara granosa*, the sandy intertidal bivalve, which dominates shell middens on Murujuga itself during the Late Holocene (Clune 2002; Clune and Harrison 2009; see Chapter 15). The presence of higher ranked sandy intertidal species such as *Melo amphora* and *Syrinx aruanus* (Wells and Bryce 1986: 86, 116) throughout the sequence in relatively small proportions in the Early and Mid-Holocene indicates the collection of this shell material for water carrying and storage (i.e. as a non-economic species). Widely distributed baler across the deflated surface of the site dates to between 2,500 and 500 years ago. This indicates the persistent use of this place after Rosemary Island formed, when potable water was only present after rain.

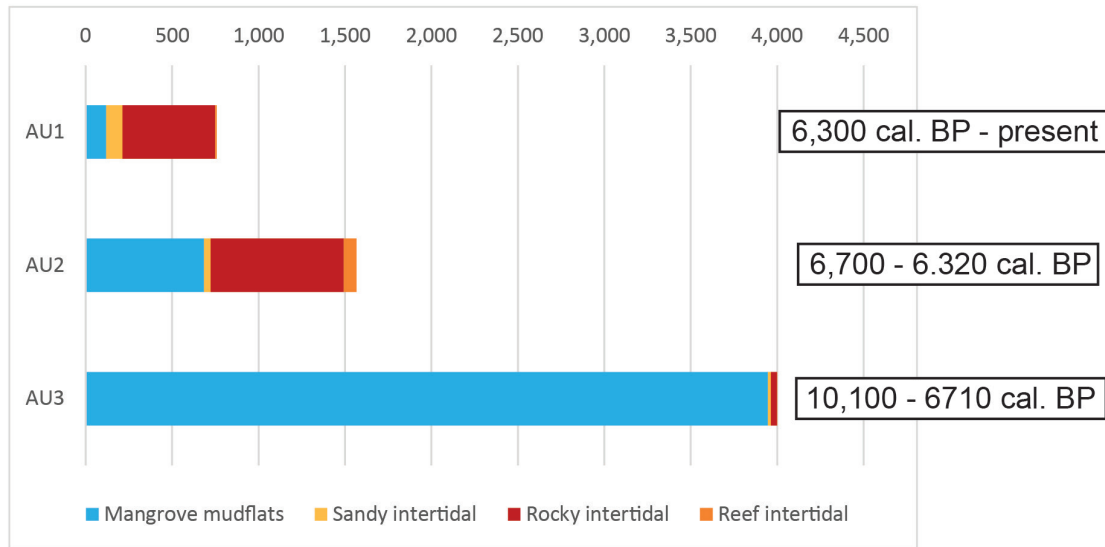


Figure 8.65. Square 912361: shellfish assemblage weights per AU (in grams) coded for habitat and Bayesian modelled phases.

Tusk shell beads (*Dentalium* sp.)

Two pieces of tusk shell (*Dentalium* sp.) were found in XU2 and XU8. These measured 7.6 mm x 3.9 mm and 14.1 mm x 2.2 mm. The *Dentalium* sp. piece from XU2 was analysed for trace residue and surface modification (see Stephenson 2016, in Berry 2018). The edge of this shell was found to have polished edges around the rim (Figure 8.66). The sediments within this shell were examined by Stephenson. Plant residues including trichomes (plant hairs), phytoliths and individual and clustered starches of grasses commonly associated with the spinifex (*Panicoides* sp. family) were collected. Several of the plant fibres were frayed, indicating rolling of the material, possibly into string.

This individual *Dentalium* is interpreted, based on the use-polish and residues, as a bead that had been strung on a grass fibre. Given its location in XU2, it is likely that the bead was lost from a string of *Dentalium* (necklace or bracelet) worn on-site relatively recently, i.e. in the Late Holocene. Direct dating of the bead would be destructive and was not undertaken. This bead adds to the growing evidence for the wearing of personal adornments around the archipelago, with intensive bead manufacture documented on Enderby Island around 1,000 years ago (see Goldwyer 2018). The presence of beads is documented on Barrow Island from the Terminal Pleistocene (see Veth et al. 2017) and is known to have occurred on the north-west coast even earlier (Balme and Morse 2006).

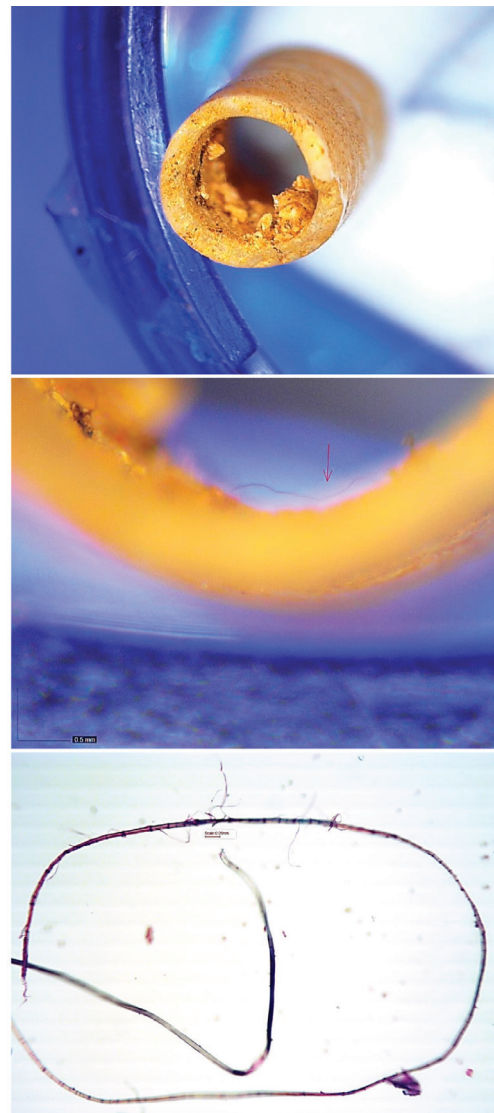


Figure 8.66. *Dentalium* bead from XU2, showing location of polish on outer rim (top). Fibrous material was identified from within the shell (middle, from Berry 2018: Appendix IV by Stephenson). Note the concave breaks (top) identified by Goldwyer (2018) as a common characteristic of local bead manufacturing, and fibre (spinifex?) observed in the bead's interior.

Sea urchin

Sea urchin (*Echinodae* sp.) spines were found in all analytical units with an increase in the more recent layers. Sea urchins inhabit the rocky intertidal zone, and this evidence for exploitation by groups during low tide

Faunal remains

Bone fragmentation and weathering in 912361 has prevented comprehensive species identification. The high porosity and bone structure irregularity indicates that most of this material is marine fauna (Dr Tiina Manne (University of Queensland), pers. comm., 2016). Parrotfish grinding apparatus (tooth and upper

pharyngeal) were identified in AUs 1 and 3 (Figure 8.67). Parrotfish is a large species that inhabits reefs (Allen 1997). They have been found in other archaeological assemblages from Cape Range (Morse 1993; Przywolnik 2002) and from the Montebello Islands (Veth et al. 2007).

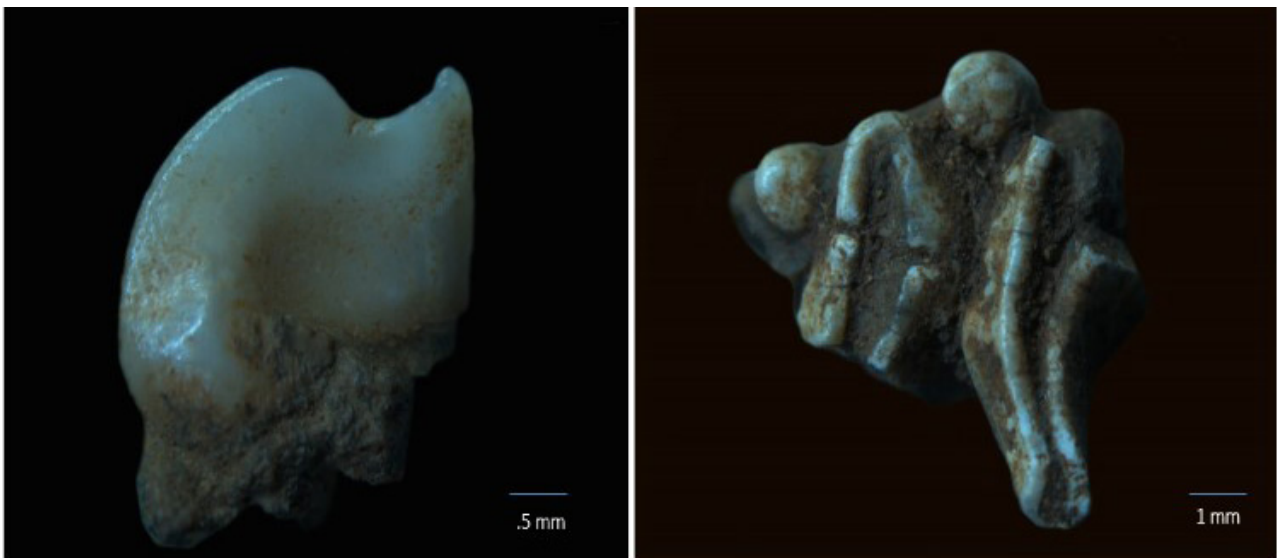


Figure 8.67. Square 912361 Parrotfish: (left) upper pharyngeal tooth and (right) upper grinding apparatus (from Berry 2018: Figure 9.31).

Stone artefacts

The 912361 stone artefact assemblage comprises 845 flaked stone artefacts. Most of these (587) are microdebitage (<1 cm maximum dimension). Artefact

Assemblage composition

Lithic material identifications at 912361 were determined through pXRF analysis of 23 representative stone artefacts (Figure 8.68). Artefacts were made on six different raw materials (Table 8.56). Gabbro is the most common lithology. Marked variation in grain size and colour occurs within this category (5). For example, nearly one-quarter of the gabbro artefacts are medium-coarse grained ($n = 30$, 23.4%), 25 (19.5%) are fine-grained and 16 (12.5%) are medium-grained. The fourth category of gabbro categorised here is 'very fine-grained' ($n = 57$, 44.5%) – and was clearly a preferred variety of gabbro for tool-stone knapping. This is differentiated from other gabbro types recorded here due to its very fine-grained characteristics, being chemically very similar to basalt with the only difference being in their texture i.e. grain

density (i.e. per 1 m x 1 m x 1 m) square is 521 artefact/m³. The stone assemblage was characterised within the three analytical units (AUs) outlined above.

size / crystal forms. However, basalt occurs specifically within volcanic extrusive settings, while gabbro is found in intrusive settings such as on the Dampier Archipelago. In this site context, unless otherwise stated, the term 'RI gabbro' refers to all gabbro varieties excluding the very fine-grained variety.

Gabbro, including the very fine-grained material, occurs locally on Rosemary Island. Indeed, most materials found at 912361 have local sources on Rosemary Island. All gabbro varieties occur along the western side of the island, and volcanoclastic siltstone is widely distributed across the eastern side of the island. The source of the silicified material is currently unknown. A small quartz outcrop is located on the north-eastern tip of the island, and quartzite occurs geologically on the easternmost

part of Rosemary Island. Chert, comprising a very small proportion of the assemblage, has no known sources on the island. The chert found at WP001 appears to be poor

quality, exhibiting multiple internal inclusions and heat-cracked surfaces (Figure 8.69).

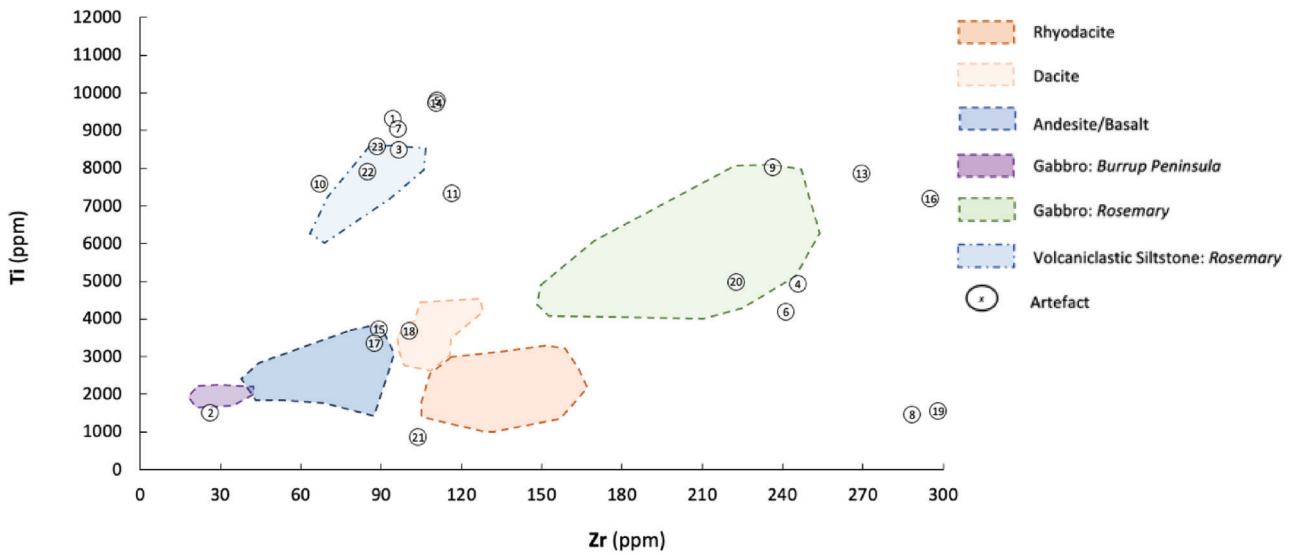


Figure 8.68. Square 912361: artefacts overlaid on the regional mapping of the different raw materials sampled from across the Dampier Archipelago (see Chapter 2).



Figure 8.69. Square 912361: (left) observed variation in RI gabbro grain size and colour: medium-coarse gabbro (912361-XU24-LA130) and fine-grained gabbro (912361-XU20-LA031); and (right) chert artefact (912361-XU08-LA323). Scale is 10 mm.

Most artefacts were discarded here during the earliest and most recent occupation phases (AU1 and AU3), with artefact density highest during the Early Holocene (Figure 8.70). Raw material proportions change through time. The most obvious shift is in the decreasing use of very fine-grained gabbro through time, while artefact discard of other varieties of gabbro increases proportionally from the earliest to the most recent occupation. The high proportion of very fine-grained gabbro in AU3 is partly due to a very high number of <1 mm flakes, indicating intensive *in-situ* reduction of this material during this earliest occupation

phase. In contrast, the remaining AU3 gabbro microdebitage component (n = 24) is proportionally smaller than the gabbro flaked component (n = 44), indicating less intensive on-site reduction. More silicified artefacts are discarded during AU2, when use of quartz and quartzite decreases. Chert, the only non-local material, occurs in very small quantities throughout the sequence. Visitors to WP001 were mostly using locally sourced tool-stone throughout the site's use; but, as with the shellfish resources being consumed on-site, there is evidence of a changing focus for the way the site was occupied.

MATERIAL	VERY FINE-GRAINED GABBRO	%F	CHERT	%F	QUARTZ	%F	QUARTZITE	%F	RI GABBRO	%F	VOLCANICLASTIC SILTSTONE	%F	SILICIFIED	%F
AU														
AU1	96	27.7	4	1.2	48	13.8	8	2.3	123	35.4	48	13.8	20	5.8
AU2	36	31.3	1	0.9	4	3.5	0	0.0	25	21.7	27	23.5	22	19.1
AU3	170	44.4	11	2.9	32	8.4	1	0.3	68	17.8	67	17.5	34	8.9
Total	302	35.7	16	1.9	84	9.9	9	1.1	216	25.6	142	16.8	76	9.0

Table 8.56. Square 912361: stone artefact assemblage showing material frequency by AU.

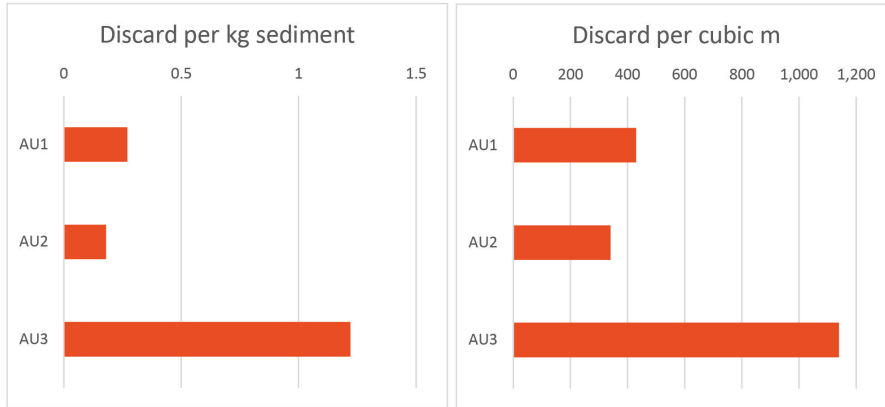


Figure 8.70. Square 912361: artefact density per kilogram sediment and per cubic metre for each AU.

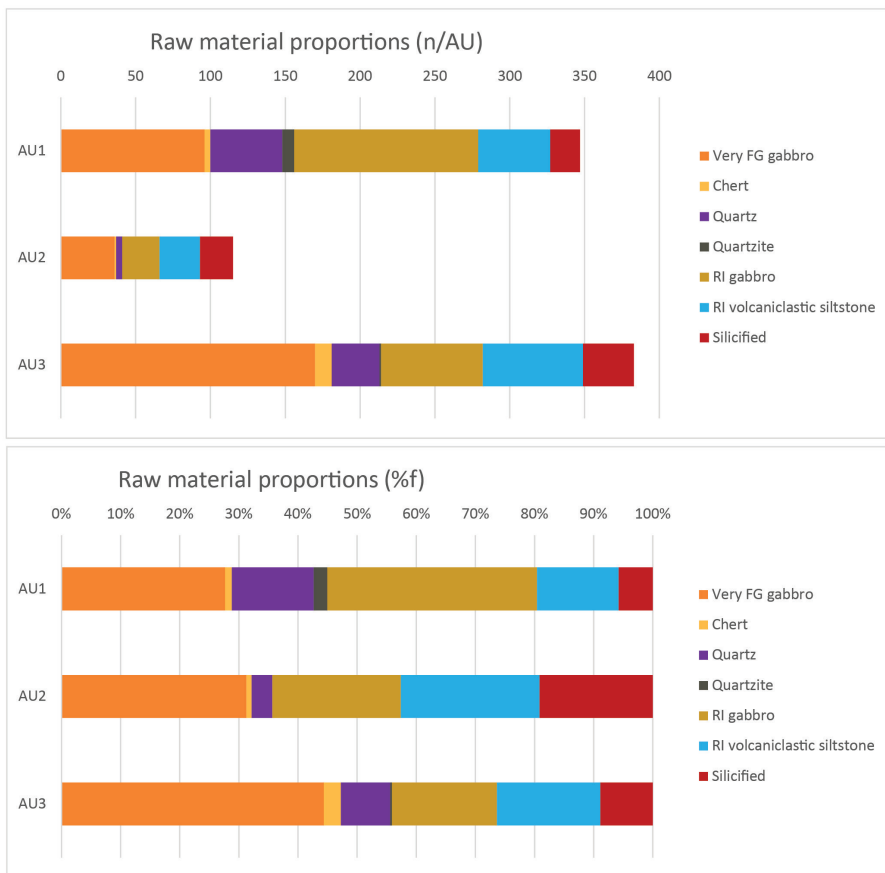


Figure 8.71. Square 912361: proportions of raw materials for each AU.

Longitudinally and transversely broken flakes dominate the WP01-912361 assemblage (Table 8.57). A higher frequency of broken flakes to complete flakes occurs within each occupation phase and could reflect several factors, such as manufacturing error or natural or cultural post-depositional breakage. Given the low artefact density at this site, however, it is unlikely that the high flake breakage rate (NAS to MNA ratio, Table 8.57) is due to human trampling, which may have indicated intensive site use. As found in Square 619706 (from the north of the island), cores comprise a very low proportion of this assemblage: only two silicified cores were recovered from AU1 (n = 1) and AU2 (n = 1) from the

assemblage. A single silicified tool was identified within the site's earliest assemblage.

The substantial microdebitage component of the WP01-912361 assemblage comprises complete and broken flakes made on materials typically found in the 4 mm assemblage (gabbro varieties, volcaniclastic sediment and silicified material), except for chert and quartz. Few chert (n = 8) and quartz (n = 8) larger artefacts were recovered, but chert (n = 14) and quartz (n = 76) microdebitage are proportionally more dominant throughout all AUs. This may indicate that chert and quartz artefacts were knapped on-site and then removed. Overall, microdebitage is proportionally more common

during the most recent phase of occupation AU1 (2 mm: 81%, 4 mm: 19%) and least common during the earliest occupation phase AU3 (2 mm: 59%, 4 mm: 41%).

ARTEFACT TYPE MATERIAL	BROKEN FLAKE		COMPLETE FLAKE		CORE/CORE FRAGMENT		TOOL		TOTAL		NAS: MNA RATIO
	N	%	N	%	N	%	N	%	N	%	%
Andesitic basalt	34	59.6	23	40.4					57	22.1	1.7
Chert	1	50	1	50					2	0.8	2
Quartz	6	75	2	25	-	-	-	-	8	3.1	4
Quartzite	7	87.5	1	12.5	-	-	-	-	8	3.1	2.7
RI gabbro	42	59.2	29	40.8	-	-	-	-	71	27.5	1.7
Volcaniclastic siltstone	58	65.9	30	34.1	-	-	-	-	88	34.1	1.8
Silicified	15	62.5	6	25	2	8.3	1	4.2	24	9.3	2.1
<i>Total</i>	<i>163</i>	<i>63.2</i>	<i>92</i>	<i>35.7</i>	<i>2</i>	<i>0.8</i>	<i>1</i>	<i>0.4</i>	<i>258</i>	<i>100</i>	

Table 8.57. Square 912361: stone assemblage composition by frequency and proportion. Flakes <10 mm excluded here.

Assemblage reduction

Flakes from 912361 were discarded at different stages of reduction intensity (Table 8.58). The complete chert flake (912361-XU08-LA323) has the highest SDI value, which, along with multiple flake scar directionality and an absence of cortex, indicates that this flake was removed from an intensively reduced nodule. This result is not surprising as chert must have been transported to the island rather than sourced directly from nearby outcrops and was probably conserved as a rarer tool-stone resource. The comparatively lower SDI values for gabbro are also not surprising given the medium-coarse grained nature of this rock and its ubiquitous distribution on this western side of the island. Fine-grained gabbro nodules appear to have been relatively more intensively reduced ($n = 10$, $\mu 1.07 \pm 0.35$) than medium-coarse grained gabbro nodules ($n = 19$, $\mu 0.9 \pm 0.4$) but overlapping standard deviations indicate no marked distinction in reduction intensity. Volcaniclastic siltstone flakes, sourced from the eastern side

of Rosemary Island, have a slightly higher average SDI value than gabbro. Again, fine-grained flakes made on this material have somewhat higher average SDI values ($n = 24$, $\mu 1.3 \pm 0.69$) than medium-grained volcaniclastic siltstone flakes ($n = 5$, $\mu 0.94 \pm 0.28$). Fine-grained varieties of the local materials were preferred for relatively more intensive knapping.

Only 14 flakes (15.2%) have remnant cortex on their dorsal surfaces or platforms. Two volcaniclastic siltstone flakes and a gabbro flake were entirely cortical, indicating that they had been removed at an early stage of nodule reduction, although the source of siltstone on the opposite side of the island from this site indicates an unexpected result. Local procurement and decortication is the expected finding with locally abundant materials on the island. The remaining 12 flakes with some cortex are of very fine-grained gabbro ($n = 6$), gabbro ($n = 3$), volcaniclastic siltstone ($n = 1$) and silicified ($n = 1$).

MATERIAL	N	μ	SD
Very fine-grained gabbro	23	1.09	0.35
Chert	1	2.42	-
Quartz	2	1.33	0.21
Quartzite	1	0.48	-
RI gabbro	29	0.96	0.39
Volcaniclastic siltstone	30	1.22	0.64
Silicified	7	1.31	0.47

Table 8.58. Square 912361: Scar Density Index (SDI) for complete flakes (excluding flakes <10 mm).

Much like the reduction indices, flake size varies widely within and between material types, as indicated through the range of mean and standard deviation values for weight and surface area (Table 8.59). Overall, flakes made on locally available and abundant gabbro varieties and volcaniclastic siltstone are, on average, much larger than the few flakes made on chert, quartz and quartzite. Medium and coarse-grained gabbro and volcaniclastic siltstone flakes are generally larger than their fine-grained varieties. Artefacts made on all materials typically have

similar percussion length and width values: elongated flakes are uncommon (Table 8.59).

The non-local chert flake is small (11.6 mm maximum dimension). This combined with reduction attributes indicates that this flake was removed from a core in an advanced stage of reduction. Indeed, other broken chert flakes are all very small (<13 mm). Quartz artefacts discarded at WP1 are all under 10 mm in dimension ($n = 76$, 90.5%). This could reflect a low availability of quartz on Rosemary Island, the nature/characteristics

of the source location, or quartz quality and knapping behaviours. A quartz flake from AU1 (912361-XU05-LA301) exhibits crushing on its platform and distal ends, indicating that it was removed from a nodule using bipolar percussion. Quartz tends to shatter when struck,

creating many small fragments, accounting for the high proportions of quartz debris in the assemblage (see Hiscock 1986). No noticeable patterns or changes in flake size or reduction intensity between flake assemblages occur through time.

MATERIAL	WEIGHT (G)			SURFACE AREA (MM ²)	
	N	μ	SD	μ	SD
Very fine-grained gabbro	23	2.0	2.4	346.8	287.7
Chert	1	0.3	–	116.0	–
Quartz	2	1.4	1.6	220.0	160.9
Quartzite	1	0.3	–	127.0	–
RI gabbro	29	5.3	7.6	641.3	712.8
RI volcaniclastic siltstone	30	6.0	14.9	603.7	766.1
Silicified	7	0.4	0.3	142.4	43.9

Table 8.59. Square 912361: weight and surface area for complete flakes (excluding flakes <10 mm).

MATERIAL	N	μ	SD
Very fine-grained gabbro	23	1.0	0.5
Chert	1	0.8	–
Quartz	2	1.4	0.2
Quartzite	1	0.9	–
RI gabbro	29	1.0	0.3
Volcaniclastic siltstone	30	1.2	0.6
Silicified	7	1.0	0.2

Table 8.60. Square 912361: elongation ratio for complete flakes (excluding flakes <10 mm).

The two cores discarded in 912361 are made on very fine-grained silicified material. The smaller of the cores (XU24-LA273, Figure 8.72), found amongst the evidence for the initial occupation of the site, has a high SDI value (2.43) and was intensively reduced at the point of discard, with further flakes unable to be easily removed. Although the larger core (XU21-LA274) does not have

extensive flake scars relative to its surface area (SDI: 1.32), both cores are small (weight: 6.67 g and 28.28 g), exhibit evidence for platform preparation, and were rotated to remove flakes. These cores were probably discarded at the site because they had little remaining use-life, having been brought here from elsewhere, potentially some distance away.



Figure 8.72. Square 912361: small, silicified core (XU24-LA273) discarded during AU3. Scale is 10 mm.

Usewear and residue analysis

A single tool discarded at WP1 (XU26-LA267) has macroscopic and microscopic evidence for usewear along its edges. The mottled dark-coloured silicified artefact was visually identified with potential macroscopic usewear and residue (Figure 8.73). Microscopic usewear analysis revealed shallow edge scarring along the ventral and dorsal sides of both lateral margins and the ventral

termination. A small amount of polish and edge rounding is also present on the dorsal ridge of the platform.

Residues extracted from the right dorsal and left ventral margin tested negative for blood. Several small, non-diagnostic plant fibres, a raphide and an unidentified plant fibre were recovered. Raphides are calcium oxalate crystals which occur in the bioforine cells of more than

3,750 species of plant and are thus difficult to attribute to a single species (Christenhusz and Byng 2016: 203; Crang et al. 2019: 463–464). While the recovered raphide is consistent with those of *Dioscorea* sp., which includes Australia's native yams (Raman et al. 2014), the usewear documented on the artefact is not diagnostic of tuber

processing (Berehowyj 2013) and is more consistent with the processing of harder materials (Claud et al. 2019). Raphides are also present in groups of up to 36 per bioforine cell (Crang et al. 2019: 463–464), and the presence of a single raphide is therefore unlikely related to use.

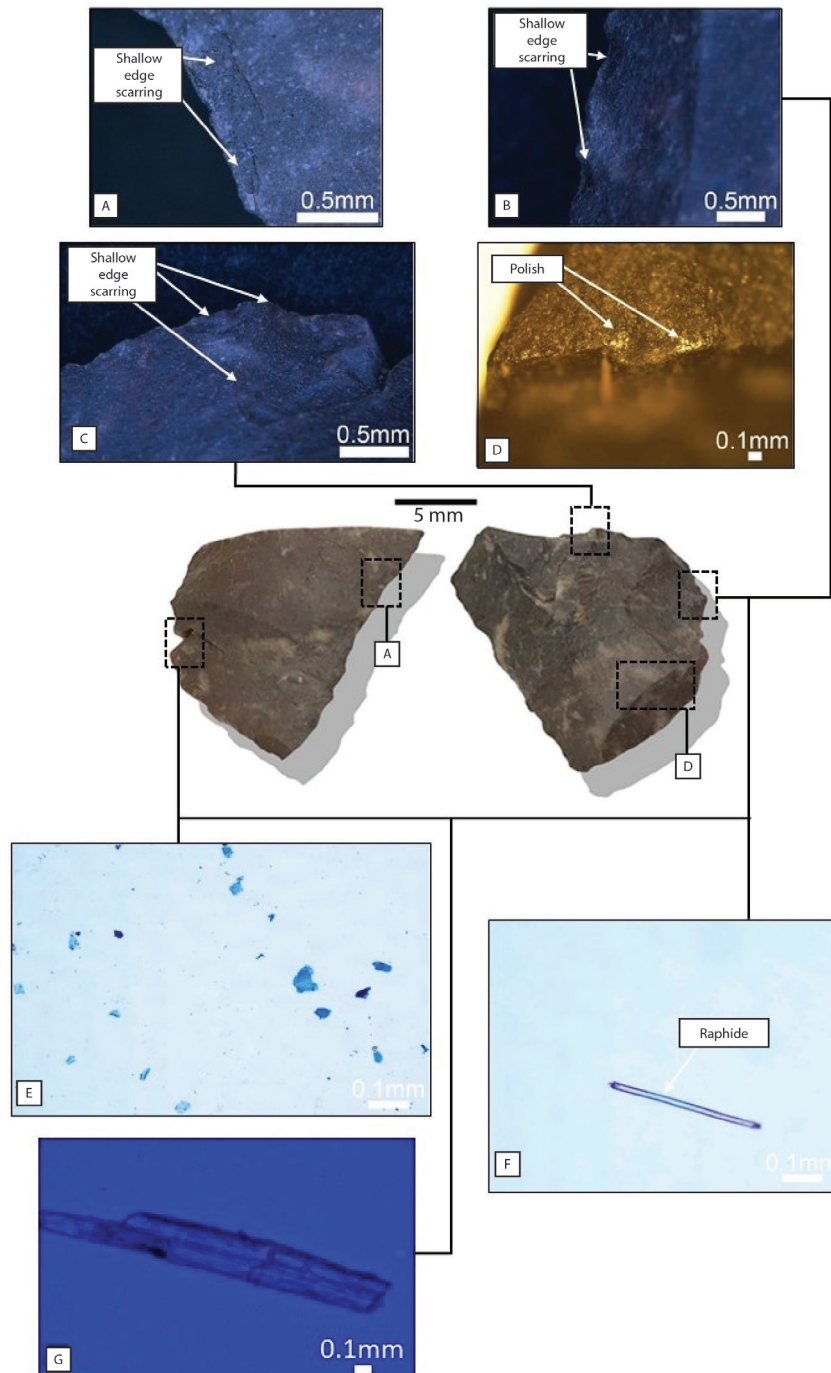


Figure 8.73. Artefact XU26-LA267, (A–C) showing shallow edge scarring and (D) polish usewear, (E) a typical scatter of small plant fibres, (F) a raphide and (G) an unidentified plant fibre. Scale is 5 mm.

Discussion

The excavated assemblage at Wadjuru Pool indicates an initial occupation by a highly mobile group of hunter-gatherer-collectors from before 10,000 years ago,

with peak activity being documented between 9,000 and 8,000 years ago. At this time, people were exploiting the extensive mangrove forests which had established along

the ever-encroaching shorelines and estuaries. People were also processing plant materials, with multiple plants being processed at this time.

After 7,000 years ago, when Rosemary Island was established through further sea level rise, there is evidence of an occupation shift by smaller populations occupying the site in a more episodic manner and focusing on reef and rocky intertidal shellfish species for their food. During the last 6,000 years episodic visits to Wadjuru Pool include the oyster dinnertime camp dated to 4,100 cal. BP. The surface *Melo amphora* specimens across the surface of the site provide evidence for Wadjuru Pool being a continued focus in the Late Holocene with occupation in evidence throughout the last 1,200 years. This was likely seasonally based, after rain when Wadjuru Pool would have contained water for a short time, possibly during turtle nesting or hatching. This continuing use of this landscape post-landisolation alters the earlier interpretation based on Bradshaw's (1995) excavation, i.e. that site occupation did not continue after Rosemary Island was formed by rising sea levels.

Changing shellfish exploitation through time illustrates highly adaptable economic strategies in the context of rapidly changing environments (Berry 2018; McDonald and Berry 2016; Manne and Veth 2015; Veth et al. 2014). The repeated use of Wadjuru Pool during the last millennium confirms that people were accessing the island well before the European contact period. Early explorers' accounts provide evidence of island use into the historic period (campfires, occupation sites and food remains), with Aboriginal people observed moving through the archipelago on mangrove log canoes (Dampier 1699; King 1818).

Wadjuru Pool's lithic assemblage demonstrates that people also accessed other parts of Rosemary Ranges/ Island to source tool-stone in different ways through time. We must reiterate these conclusions are based on a single metre test sample from a cultural landscape covering hectares. The assemblage is composed entirely of locally available materials, although some more fine-grained components may not be from the immediate vicinity of Wadjuru Pool. Rarer materials include chert, providing insights into people arriving at this place with mobile toolkits procured from elsewhere. Veth (1982: 66–68) documented a disproportionately high occurrence of non-local materials in major habitation sites in the Dampier Archipelago, with more expedient and locally derived sources used at task-specific sites. This suggests WP1 was a major habitation site in the Early Holocene but that during the Mid to Late Holocene this use changed to an episodically visited 'task-specific site'.

Local material preferences clearly varied through time. The factors driving raw material selection may have included individual or group preferences for source locations, material aesthetics, flaking properties or cultural reasons. Through time, flake attributes suggest that nodules were typically not intensively reduced at the point of flake removal, and that no marked shifts in knapping practices occurred. Given this, the higher proportion of debris in the most recent occupation phase (AU1) compared to the earliest site visits (AU3) may relate to a number of factors, such as post-depositional movement, the removal of more intensively reduced flakes and cores from this location after on-site knapping or may in fact be an artefact of sampling. In contrast to the flake assemblage, the two cores in the Wadjuru Pool assemblage were more intensively reduced and were discarded towards the end of their use-life. This, together with the very low proportion of cores in this sampled assemblage, could indicate the transport of nodules away from the area after some on-site knapping.

Lithic analyses suggest that highly mobile groups visited Wadjuru Pool during its initial Early Holocene occupation. At this time, they likely produced much of the rock art documented on the rock pile to the south of the domed waterhole. While none of this rock art has been dated, the contrast state information shows that more art was produced earlier in the sequence than was produced in the more recent past (Berry 2018).

The change in shellfish species from mangrove forest environments towards open sand / mudflat / reef marine resources is reflected in Wadjuru Pool's engraved corpus. The small rock art assemblage on the rock pile is dominated by anthropomorphic and zoomorphic figures and (CS4) motifs from the Early to Mid-Holocene stylistic phases (see Chapter 7; also see McDonald 2015; Mulvaney 2015). Berry (2018) argued for two phases of low-intensity rock art production at Wadjuru Pool. She argued that the first phase was associated with Early Holocene site use after 10,000 years ago, while the more recent art reflected an emergent marine landscape. This engraving corpus is argued to correlate with the second phase of site use, at or around the time of insolation (c. 6,900 years cal. BP to c. 6,700 cal. years BP), characterised by a resource focus on the emergent rocky and reef intertidal shellfish species.

After 2,500 years ago, and particularly between 2,000 and 500 cal. BP, site use persisted and people repeatedly visited Wadjuru Pool. In the absence of a permanent water source here, this visitation must have been seasonal: after rain, and coinciding with periods of turtle egg laying and/or hatching. It seems likely that the extensive grinding activity on the domed surface of the Wadjuru waterhole took place during this time given the

absence of grinding furniture in the earlier layers of the excavated squares and the extensive deflated surface scatter of this type of material. The *Dentalium* sp. shell beads and an incised ochre fragment (Berry 2018) found amongst the recent assemblage and on the surface provide insights into additional symbolic behaviours during the Late Holocene. The surface ochre material

may be indicative of body painting or the decoration of wooden/shell implements. Shell beads have now been found across the archipelago in many of our excavations, indicating that personal ornamentation was widespread amongst these coastal hunter-gatherer-fisher peoples throughout the Late Holocene.

References

- Allen, G. 1997. *Marine fishes of tropical Australia and south-east Asia*. Perth: Western Australian Museum.
- Balme, J. and K. Morse. 2006. Shell beads and social behaviour in Pleistocene Australia. *Antiquity* 80(310): 799–811. <https://doi.org/10.1017/S0003598X00094436>
- Berehowyj, L. 2013. Can use-wear be used to identify tuber processing on siliceous stone? An experimental study from Australia. *Australian Archaeology* 77: 9–19. <https://doi.org/10.1080/03122417.2013.11681975>
- Berry, M. 2018. Murujuga Desert, Tide, and Dreaming: Understanding Early Rock Art Production and Lifeways in Northwest Australia. Unpublished PhD thesis, University of Western Australia.
- Blunt, Zane. 2019. Sea Level Rise and Islandisation: How did the Reconfiguration of Murujuga's Holocene Landscape Influence Indigenous People's Occupation and Resource Exploitation on Enderby and Rosemary Islands? Unpublished BA (Hons) thesis, Archaeology and Centre for Rock Art Research + Management, University of Western Australia.
- Bradshaw, E. 1995. Dates from archaeological excavations on the Pilbara coastline and islands of the Dampier Archipelago, Western Australia. *Australian Archaeology* (41): 37–38. <https://doi.org/10.1080/03122417.1995.11681559>
- Bronk Ramsey, C. 1998. Probability and dating. *Radiocarbon* 40: 461–474. <https://doi.org/10.1017/S0033822200018348>
- Bronk Ramsey, C. 2008. Deposition models for chronological records. *Quaternary Science Reviews* 27: 42–60. <https://doi.org/10.1016/j.quascirev.2007.01.019>
- Bronk Ramsey, C. 2009a. Bayesian analysis of radiocarbon dates. *Radiocarbon* 51: 337–360. <https://doi.org/10.1017/S0033822200033865>
- Bronk Ramsey C. 2009b. Dealing with outliers and offsets in radiocarbon dating. *Radiocarbon* 51: 1023–1045. <https://doi.org/10.1017/S0033822200034093>
- Christenhusz, M. and J. Byng. 2016. The Number of known plant species in the world and its annual increase. *Phytotaxa* 261(3): 201–217. <https://doi.org/10.11646/PHYTOTAXA.261.3.1>
- Clarke, P. 2007. *Aboriginal People and their Plants*. Kenthurst, NSW: Rosenberg Publishing.
- Claud, E., C. Thiebaut, M. Deschamps, A. Coudenneau, C. Lemorini, V. Mourre and F. Venditti. 2019. The use-wear studies on the lithic industries. *Palethnologie* 10. <https://doi.org/10.4000/palethnologie.4137>
- Clune, G. 2002. Abydos, An Archaeological Investigation of Holocene Adaptations on the Pilbara Coast, Northwestern Australia. Unpublished PhD thesis, University of Western Australia.
- Clune, G. and Harrison, R. 2009. Coastal shell middens of the Abydos coastal plain, Western Australia. *Archaeology in Oceania* 44(S1): 70–80. <https://doi.org/10.1002/j.1834-4453.2009.tb00069.x>
- Crang, R., S. Lyons-Sobaski and R. Wise. 2019. *Plant Anatomy: A Concept-Based Approach to the Structure of Seed Plants*. Cham: Springer Nature Switzerland.
- Dampier, W. 1699. *A New Voyage Round the World*. London: J. Knapton.
- Florabase. 1989. *Brachychiton acuminatus* Guymer. Perth: Department of Biodiversity, Conservation and Attractions. <https://florabase.dpaw.wa.gov.au/browse/profile/12716>.
- Fairweather, J. 2019. Geological and Geochemical Characterisation of the Archean Fortescue Group, Rosemary Island, and Associated Archaeological Material from the Dampier Archipelago, Western Australia. Unpublished Geology Honours thesis, University of Western Australia.
- Gallant, J. C., N. Wilson, T. I. Dowling, A. M. Read and C. Inskeep. 2011. *SRTM-derived 1 Second Digital Elevation Models Version 1.0*. Canberra: Geoscience Australia. <https://ecat.ga.gov.au/geonetwork/srv/eng/catalog.search#/metadata/72759>.
- Hacker, J. 2017. *Orthomosaic and Lidar Data from Deep History of Sea Country Project*. Adelaide: Flinders University. Goldwyer, W. 2018. An Archaeological Investigation of Late Holocene Shell Bead Manufacture, Dampier Archipelago, Northwestern Australia. Unpublished BA (Hons) thesis, Centre for Rock Art Research + Management, University of Western Australia.
- Hayes, E., R. Fullagar, C. Clarkson and S. O'Connor. 2014. Usewear on the Platform: 'Use-flakes' and 'Retouch-flakes' from Northern Australia and Timor. In *An Integration of the Use-Wear and Residue Analysis for the Identification of the Function of Archaeological Stone Tools*, Proceedings of the International Workshop, eds C. Lemorini and S. Nunziante Cesaro, pp. 77–90. Oxford: Archaeopress.
- Haynes, J. R. 2017. Significance and role of Si in crop production. In *Advances in Agronomy*, ed. D. Sparks, pp. 83–166, vol. 146. <https://doi.org/10.1016/bs.agron.2017.06.001>
- Heaton, T., P. Köhler, M. Butzin, E. Bard, R. Reimer, W. Austin, C. Bronk Ramsey, P. M. Grootes, K. A. Hughen, B. Kromer, P. J. Reimer, J. Adkins, A. Burke, M. S. Cook, J. Olsen and L. C. Skinner. 2020. Marine20 – the marine radiocarbon age calibration curve (0–55,000 cal BP). *Radiocarbon* 62: 779–820. <https://doi.org/10.1017/RDC.2020.68>
- Hiscock, P. 1986. Technological change in the Hunter River valley and the interpretation of late Holocene change in Australia. *Archaeology in Oceania* 21: 40–50. <https://www.jstor.org/stable/40386710>
- King, Phillip Parker. 1818. *Remark Book. King Family Papers*. MLMSS 5277 microfilm reel CY2565, items 1–3. Mitchell Library, Sydney.
- Lourandos, H. 1993. Hunter-gatherer cultural dynamics: long- and short-term trends in Australian prehistory. *Journal of Archaeological Research* 1(1): 67–88.
- Low, T. 1988. *Wild Food Plants of Australia*. Sydney: HarperCollins Publishers.
- McDonald, J. 2015. I must go down to the seas again: Or, what happens when the sea comes to you? Murujuga rock art as an environmental indicator for Australia's north-west. *Quaternary International* 385: 124–135. <https://doi.org/10.1016/j.quaint.2014.10.056>
- McDonald, J.J. and M. Berry. 2016. Murujuga, Northwestern Australia: when arid hunter-gatherers became coastal foragers. *Journal of Island and Coastal Archaeology* 12: 24–43. <https://doi.org/10.1080/15564894.2015.1125971>
- Manne, T. and P. Veth. 2015. Late Pleistocene and early Holocene exploitation of estuarine communities in northwestern Australia. *Quaternary International* 385: 112–123. <https://doi.org/10.1016/j.quaint.2014.12.049>
- Morse, K. 1993. West Side Story: Towards a Prehistory of the Cape Range Peninsula, Western Australia. Unpublished PhD thesis, University of Western Australia.

- Mulvaney, K. 2015. *Murujuga Marni: Rock Art of the Macropod Hunters and Mollusc Harvesters*. Perth: UWA Publishing.
- O'Connor, S. 1999. *30,000 years of Aboriginal Occupation: Kimberley, North West Australia*. Terra Australis 14. Canberra: ANU Pacific Institute. <http://hdl.handle.net/1885/127429>
- Petchey, F. and S. Ulm. 2012. Marine reservoir variation in the Bismarck region: an evaluation of spatial and temporal change in ΔR and R over the last 3000 years. *Radiocarbon* 54(1): 45–58. https://doi.org/10.2458/azu_js_rc.v54i1.13050
- Przywolnik, K. 2002. Coastal sites and severe weather in Cape Range peninsula, northwest Australia. *Archaeology in Oceania* 37(3): 137–152. <https://doi.org/10.1002/j.1834-4453.2002.tb00515.x>
- Raman, V., H. Horner and I. Khan. 2014. New and unusual forms of calcium oxalate raphide crystals in the plant kingdom. *Journal of Plant Research* 127(6): 721–730. <https://link.springer.com/article/10.1007/s10265-014-0654-y>
- Semeniuk, V. (1993). The Pilbara Coast: a riverine coastal plain in a tropical arid setting, northwestern Australia. *Sedimentary Geology* 83(3–4): 235–256. [https://doi.org/10.1016/0037-0738\(93\)90015-W](https://doi.org/10.1016/0037-0738(93)90015-W)
- Shakoor, S., M. Bhat and S. Mir. 2014. Phytoliths in plants: a review. *Journal of Botanical Sciences* (3): 10–24.
- Spooner, N. and D. Questiaux. 2016. Report on results from Optically Stimulated Luminescence (OSL) of six sediment samples from Rosemary Island. Unpublished report to the Centre for Rock Art Research and Management, University of Western Australia, in Berry (2018): Appendix IV.
- Stuiver, M. and H. A. Polach. 1977. Discussion reporting of 14C data. *Radiocarbon* 19: 355–363. <https://doi.org/10.1017/S0033822200003672>
- Stephenson, B. 2016. Investigation of a shell bead, 'WP1 912361 XU2', Wadjuru Pool, Rosemary Island, Western Australia. Unpublished report to the Centre for Rock Art Research + Management, University of Western Australia.
- Turner, M. 1994. *Arrernte Foods: Food from Central Australia*. Alice Springs: Institute for Aboriginal Development Press.
- Veth, P. 1982. Testing the Behavioural Model: The Use of Open Site Data. Unpublished Honours thesis, University of Western Australia.
- Veth, P., K. Ditchfield and F. Hook. 2014. Maritime deserts of the Australian northwest. *Australian Archaeology* 79: 156–166. <https://doi.org/10.1080/03122417.2014.11682032>
- Veth, P., K. Aplin, L. Wallis, T. Manne, T. Pulsford, E. White and A. Chappell. 2007. *The Archaeology of Montebello Islands, North-West Australia: Late Quaternary Foragers on an Arid Coastline*. Oxford: Archaeopress.
- Veth, P., I. Ward, T. Manne, S. Ulm, K. Ditchfield, J. Dortch, F. Hook, F. Petchey, A. Hogg, D. Questiaux, M. Demuro, L. Arnold, N. Spooner, V. Levchenko, J. Skippington, C. Byrne, M. Basgall, D. Zeanah, D. Belton, P. Helmholtz, S. Bajkan, R. Bailey, C. Placzek and P. Kendrick. 2017. Early human occupation of a maritime desert, Barrow Island, North-West Australia. *Quaternary Science Reviews* 168: 19–29. <https://doi.org/10.1016/j.quascirev.2017.05.002>
- Ward, I., P. Larcombe, K. Mulvaney and C. Fandry. 2013. The potential for discovery of new submerged archaeological sites near the Dampier Archipelago, Western Australia. *Quaternary International* 308: 216–229. <https://doi.org/10.1016/j.quaint.2013.03.032>
- Wells, F. and C. Bryce. 1986. *Seashells of Western Australia*. Perth: Western Australian Museum.
- Williams, A. N., S. Ulm, C. S. M. Turney, D. Rohde and G. White. 2015a. Holocene demographic changes and the emergence of complex societies in prehistoric Australia. *PLoS ONE* 10(6): 1–17. <https://doi.org/10.1371/journal.pone.0128661>

First published in 2022 by
UWA Publishing
Crawley, Western Australia 6009
www.uwap.uwa.edu.au
UWAP is an imprint of UWA Publishing,
a division of The University of Western Australia.



THE UNIVERSITY OF
**WESTERN
AUSTRALIA**



Centre for
Rock Art Research
+ Management

This book is copyright. Apart from any fair dealing for the purpose of private study, research, criticism or review, as permitted under the Copyright Act 1968, no part may be reproduced by any process without written permission. Enquiries should be made to the publisher.

Copyright © 2023

The moral right of the author/s has been asserted and the Indigenous Cultural and Intellectual Property rights of the Murujuga Aboriginal Corporation, as representatives of the Ngarda ngarli are acknowledged.

ISBN: 978-1-76080-242-4
Design by Upside Creative.